CHAPTER I

INTRODUCTION

1.1 GENERAL

Induction motor (IM) is the most frequently used and commonly encountered machine in industries due to its simple construction, simple design, less maintenance, low cost, self starting property, wide range of power ratings from few horsepower to hundreds of horsepower, low torque ripples and no brushes. Besides these advantages, the IM also has some inherent drawbacks due to nonlinear and coupled relationship among flux and current, the possibility of cracking the rotor conductors due to hot spots at plugging and reversal, poor power factor and lower efficiency. Advanced control techniques used in AC machine and its variants, pooled with the advances in both digital signal processing and power electronic devices have led to the better use of AC machines in superior performance adjustable speed applications. The control of the asynchronous machine, however, is difficult because the dynamics of the machine are multivariable, highly coupled and non-linear. Despite of these limitations induction motor account for 70% of electric energy used in the industries and it makes strong motivation to explore different methods to improve efficiency of the IM. Efficient use of IM is desired especially when operating in variable speed applications. The variable speed operation of the IM under different loading conditions for high performance, efficient drive have been the main focus of this thesis

1.2 INDUCTION MOTOR

The induction motors (IM) are the main types of AC motors being used at present worldwide. These are also called asynchronous motors. These motors may be classified as three phase and single phase induction motors. Three phase induction motors are used for heavy load and industrial applications, while single phase induction motors are most commonly used for light load and domestic applications. These motors are known as induction motors because in these motors, emf is induced by means of electromagnetic induction. This induced emf depends on the mechanical design of the stator and rotor. The material used and the geometry of the rotor decides the dynamic performance of the motor.

1.2.1 Losses in Induction Motor

An induction motor consists of mainly fixed losses and variable losses. The fixed losses are independent of current drawn and composed of iron losses and friction and windage losses. The variable losses consist of resistive losses in stator and rotor circuit. Motors of standard ratings are used for domestic and industrial small load applications. If the application does not match with the standard ratings of motor then motor becomes underutilized. For the premium motors where, the rating of induction motor matches with the application then about 94 percent efficiency can be achieved for load between 75 percent to full load. The remaining total 6 percent losses comprises of about 3 percent copper losses, 1.5 percent iron losses, 1 percent windage and friction losses and 0.5 percent stray losses as shown in the Fig. 1.1. These proportions of losses depend upon the design aspects of the motor. For an induction motor windage and friction losses, Stray losses and at rated voltage the iron losses are constant. The copper losses depend on the current drawn by the induction motor and vary according to the load.

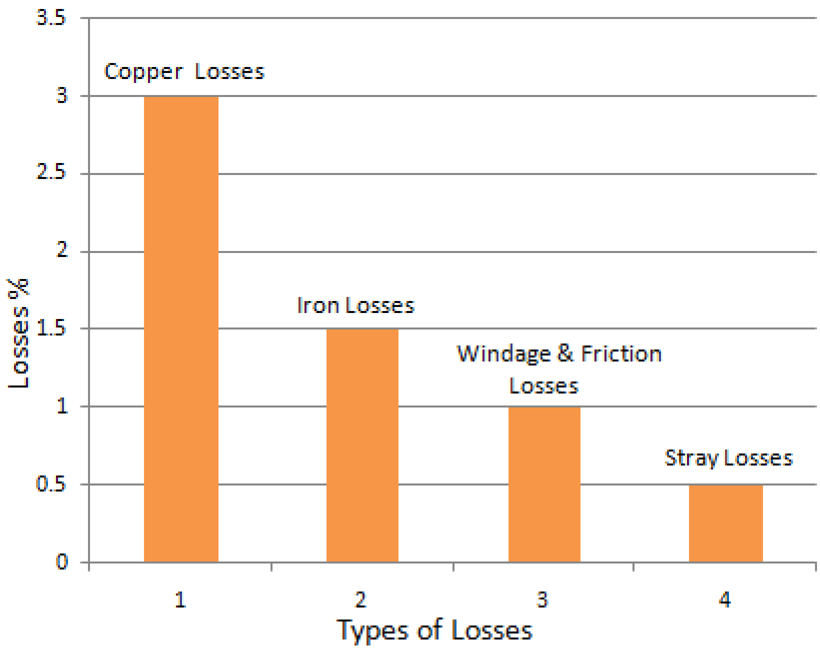

Fig. 1.1 Premium induction motor losses

1.2.2 Ways to Improve Efficiency of IM Operation

A large number of motors operate at less than 50 percent of its capacity for its entire life span. These motors exhibit low efficiency and utilize much more electrical power than they really require. Besides extra power consumption due to underutilized, it generates more heat in the motor which results sound and vibrations in the system and decreases the life of motor. For these types of operations and for variable speed applications in order to improve the efficiency and durability variable frequency drives (VFD) are introduced. In VFDs optimal voltage is used for the drive system when load is reduced which results in the reduction of consumption of electrical power.

By using digital technology some intelligent units are available in the market which recommends various functions for power saving and minimization of stresses to the motor. Life of drive system components like contactors etc. increases and requires less maintenance with the use of soft starting function. Controlled stopping function decreases the shock and prolongs the life of the drive system. Automatically switch off function of the power supply when motor draws more current than the prescribed value protect the motor from fault. Programming these types of functions in the starting panel, life of the drive components, motor and switchgear can be increased along with the saving of power by decreasing the current drawn and temperature of the motor.

The efficiency of the motor is affected largely with the variation of winding temperature. The winding temperature can be controlled with the use of internal and external cooling methods to get the higher efficiency. Temperature has a considerable effect on the efficiency of the motor due to the positive temperature coefficient of the material used in the winding. With the increase of the motor temperature motor losses increases and efficiency decreases. At loads higher than the rated value efficiency reduces speedily with temperature as compared to the normal load as shown in Fig. 1.2. It implies that motor require additional cooling when operated at excess load and efficiency of motor can be improved by using low temperature coefficient materials for its construction [184].

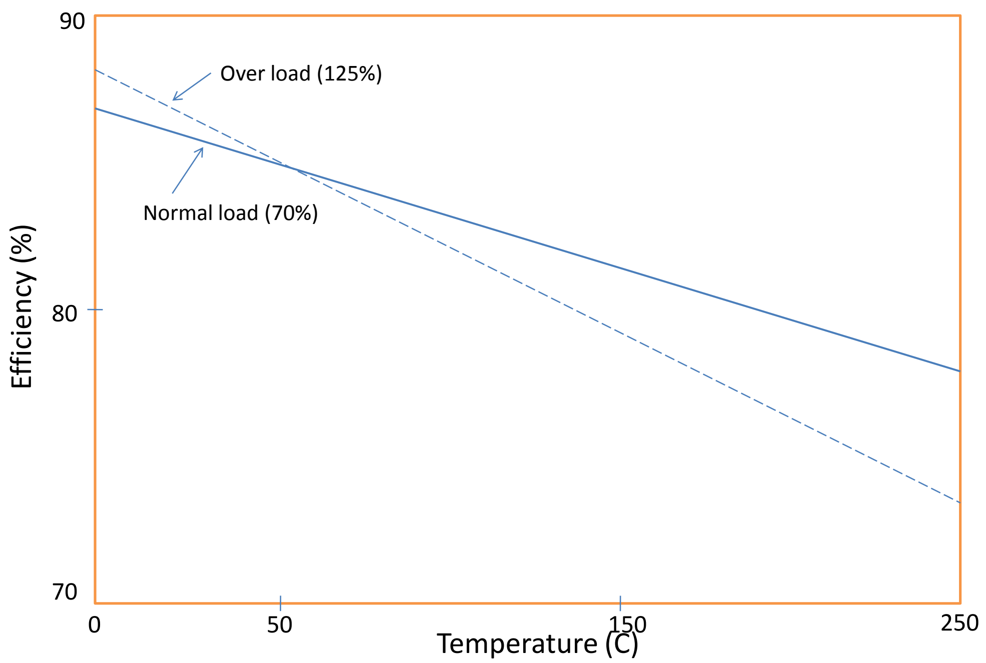

Fig. 1.2 Efficiency with temperature

The motor winding temperature is load dependent and increases more rapidly at overload operation as shown in Fig. 1.3. The motor exhibit good efficiency in the range of 60 percent to 110 percent load and efficiency decreases very fast beyond this range of load as shown in Fig. 1.4

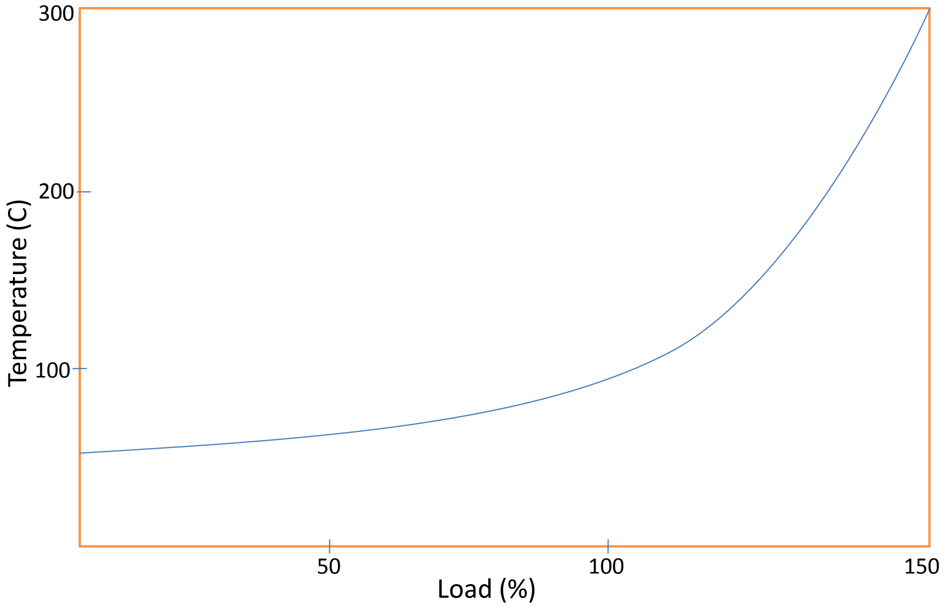

Fig. 1.3 Winding temperature variation with load

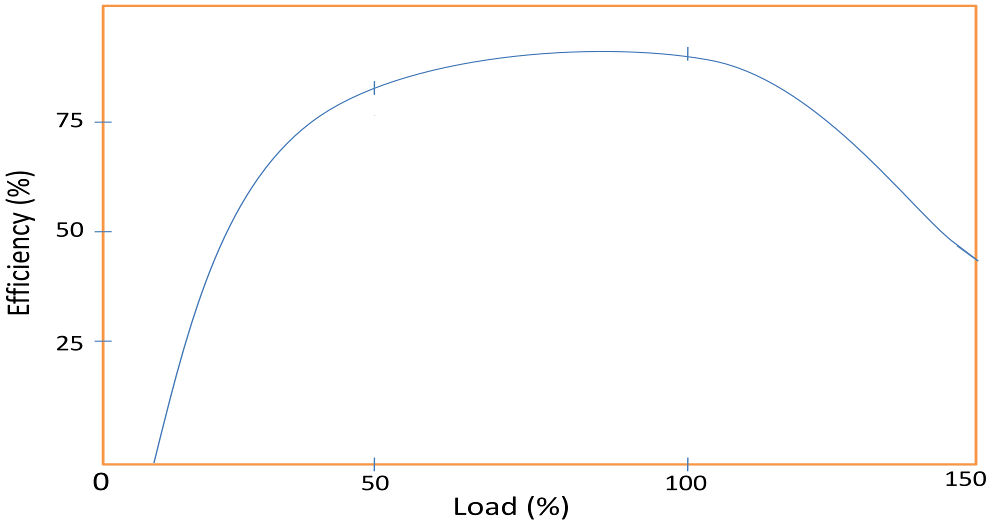

Fig. 1.4 Efficiency variations with load

1.3 ELECTRIC DRIVES

1.3.1 AC Drives

The system that is used to control the motion is called drive and if an electric motor is employed to control the motion then it is called an electric drives. These electric drives are basically classified into AC drive and DC drive systems. The AC drives are further classified into scalar and vector controlled drives. Scalar control is easy and simple to implement control method where, magnitude of control variable is altered to change the speed of motor. It generates poor dynamic response but good steady state performance. These methods are basically slow due to coupling effect of flux and torque. When precise control of speed is not required, it can be used. In this scheme the air gap flux is always maintained at the required value at the steady state. Vector control offers more accurate control of ac motors compared to scalar control. It allows, by means of co-ordinate transformation, to decouple the torque current from the rotor flux due to which transient response is fast, and hence induction motor behaves like a DC motor. They are thus used in high performance drive applications where oscillations in air gap flux linkages are unbearable. It allows speed control in all the four quadrants without any other control elements. It automatically limits operations to the stable region. Vector control scheme can be classified into direct and indirect vector control. Unit vector signals are used to ensure correct orientation of the current components responsible for production of flux and torque. Electric drive provides the essential voltage/current and frequency to the motor from main supply to get the required mechanical output. The electric drives can also be classified depending on application as constant speed or variable speed drives. The electric drive system is mainly used for variable speed applications.

1.3.2 Classification of AC Drives

Nowadays the variable frequency drives (VFD) become popular for high performance applications and can be classified as presented in Fig. 1.5.

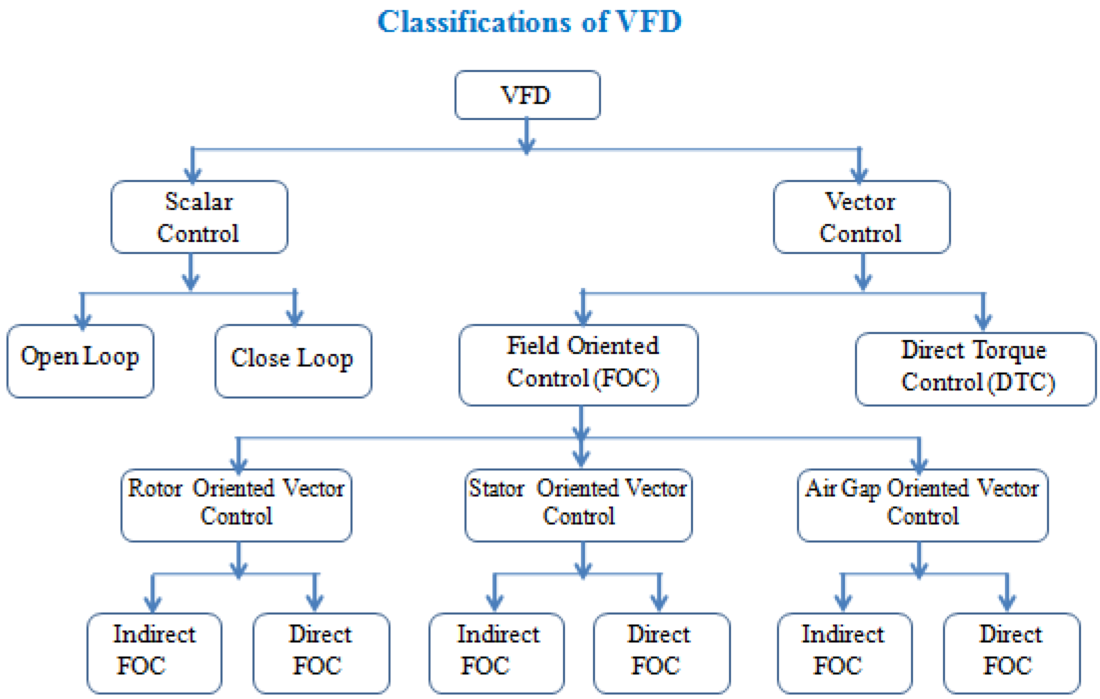

Fig. 1.5 Classifications of variable frequency drive system

AC drive system as compared to the basic conventional electric drive system for variable speed application is small in size, less expensive, more flexible, more efficient, requires low maintenance and can have control on high speed. But there is coupling between flux and torque current component. Earlier dc drive system was used for variable speed applications and ac drive system was used for constant speed applications. However with the advent of semiconductor devices and improvement in the speed control system, AC drive system becomes more popular for variable speed applications. But it was restricted for medium performance applications due to coupling between torque and flux current component. After introduction of field oriented control drive system and with the decreasing cost of semiconductor devices modern AC electric drive system as shown in Fig. 1.6 become favorable than DC drive for high performance applications.

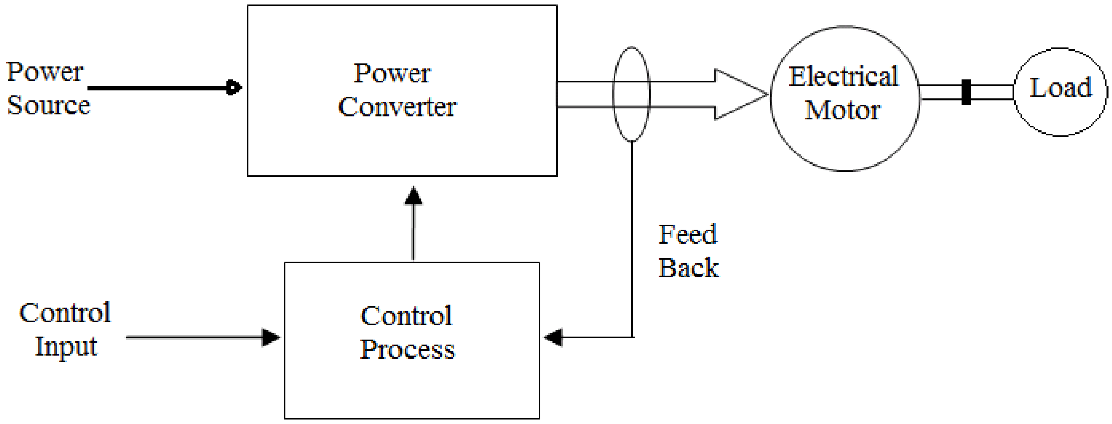

Fig. 1.6 The modern AC electric drive system for variable speed

Following are the fundamental components of modern AC electric drive system:

1.3.2.1 Power source

The requirement of the power source to the power converter is provided by this component. For providing dc source, batteries, photovoltaic and fuel cells of appropriate capacity is employed. Three phase or single phase ac supplies are common AC power sources in electric drives.

1.3.2.2 Power converter

This unit is used to provide the required regulated power to the electrical motor. Different types of control algorithms are available in the literature to process the input electric power using power electronics converters. There exists many types of power converters like current source inverter (CSI), cyclo converter, voltage source inverter (VSI), multilevel bridge inverter etc and depending on the availability and limitations any of these can be chosen. These are flexible, compact and efficient and can be used to convert AC to DC, AC to AC, DC to AC and DC to DC.

1.3.2.3 Electrical motor

This is the main part of the drive and depending on the required application it may be named as dc motor, synchronous motor, three phase induction motor and single phase induction motor. The electric motor converts electrical energy into mechanical energy in terms of motion and this energy can be imparted to the load which is coupled to the shaft of the motor.

1.3.2.4 Sensing unit

This unit is generally employed for closed loop operation of electric drives. Different types of sensors depending on the application like current sensor, voltage sensor, temperature sensor, torque sensor, speed sensor can be employed for providing the feedback signal to the control unit. Information received from these sensors is used to compare the actual performance to the required performance and may be utilized to ensure the good performance of the drive system. Encoders can be installed to measure the position of the shaft and speed of the motor needed to implement the control algorithm.

1.3.2.5 Control process

The control algorithm of the drive system is executed in this unit. By utilizing the feedback signal and input command, this unit processes the control algorithm and provides the appropriate control signal to the power converter. This is a very complex unit and its complexity depends on the requirement of the application. This unit mainly consists of microcontroller/digital signal processor to perform fast and accurate operation.

1.3.3 Conventional Speed Control Methods of IM

Principally IM is made for constant speed applications and its speed can be controlled by compromising its efficiency. IM performance can be enhanced by improving the design aspect of the motor. The losses occurred in the motor depends on the types of materials used for its construction. The copper material can be used instead of aluminum for rotor bars.

Hysteresis losses can be reduced by using high silicon contents steel for making the core and eddy current losses can be reduced by laminating the core. The electrical control of speed in motor is simpler as compared to the mechanical and hydraulic systems. The performance of the motor depends on operating design conditions. If motors are operated below optimum operating conditions, they become less efficient. Though the stator and rotor resistance of IM are fixed by design but due to rise in temperature they changes during operation of the motor and affects the performance of the motor. By using the rated condition of speed and voltage/current of the motor these parameters can be measured and motor operation can be improved. Conventionally the speed of IM can be controlled in many ways depending on requirement and availability of the resources. According to the general equation of speed control of IM, the speed is inversely proportional to the number of poles and also directly proportional to the supply frequency. Therefore the speed of motor can be altered by changing the number of poles and/or by changing the frequency and these are called pole changing and supply frequency changing methods of speed control of IM. However these methods of speed control are not popular and are rarely used. The torque developed by IM is directly proportional to the square of the applied voltage. So the speed of the motor can be controlled by varying the supply voltage. This method is generally used for domestic and small sized single phase induction motors where the criteria of running cost are not important. This method is not suitable for three phase IM and industrial applications because it requires an additional voltage changing system which may be expensive and reduces the efficiency of the motor. Reduction in developed torque is more with the corresponding reduction in the supply voltage and hence motor is underutilized. Also the developed torque of IM is directly proportional to the square of the rotor resistance and hence the speed of the motor can be controlled by varying the rotor resistance. This is called variable rotor resistance method of speed control. But it can be applied to the phase wound rotor IM only, where an external resistance can be added to the rotor circuit using slip rings. This method is used for applications where high starting torque is required. So the external resistance is used in the circuit at starting only and remains out of the circuit throughout the operation of the motor.

The V/f control and vector control methods are popular and used for control of modern AC drive systems. The constant V/f control method keeps the magnetic flux constant up to the rated speed as shown in Fig. 1.7. The magnetic flux depends upon stator voltage and frequency and hence the motor can be controlled by controlling voltage and frequency. For base speed, V/f ratio is kept constant to keep stator flux constant. If frequency is raised above rated value to increase the speed, flux will decrease as voltage cannot be increased above rated value. This region of operation is called as field weakening region. If the frequency is reduced to decrease the speed at rated voltage then flux will saturate causing excess of stator current which might harm the motor permanently.

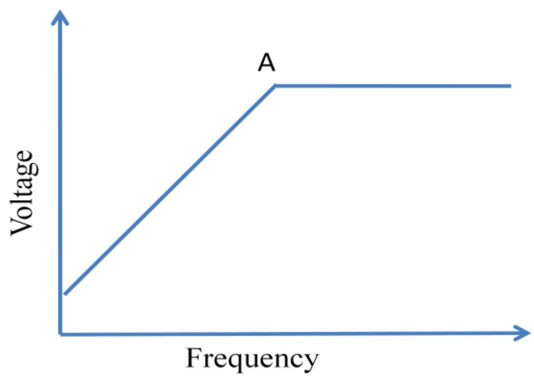

Fig. 1.7 Constant (V/f) method

There are many advanced algorithms available for controlling motor performances. In vector control method flux and torque can be controlled separately. The torque and voltage equations of an IM that explain the dynamic behavior are time dependent and because of continuously varying of the coefficient of coupling between rotor and stator windings, the dynamic control of an induction motor is non linear and complex. The complexity of the IM can be decreased by converting the three phase rotor and stator quantities to a set of two phase variable called d-q transformation theory.

1.3.4 Transformation Theory

There are two well known transformation methods i.e. Clarke transformation and Park transformation. The performance of three phase motors is generally depicted by their voltage and current equations. The coefficients of these equations that explains their performances are time varying except for the stationary rotor condition. For such type of system, the mathematical modeling tends to be complex as the induced currents, voltages and flux linkages change continuously. In order to analyze such a complex electrical machines, mathematical transformations are generally utilized to solve the time varying equations and decouple the variables. This is achieved by transforming all motor variables to a common frame of reference.

1.3.4.1 Clarke transformation

It is a three phase to two phase orthogonal stationary transformation. For a balanced three phase induction motor the three phase stationary frame of reference variables (v_{as}, v_{bs}, v_{cs}) and two phase stationary frame of reference variables (v_{qs}^{s}, v_{ds}^{s}) is shown in Fig. 1.8

Two phase stationary reference frame can be resolved into three phase components which can be written in matrix form as shown in equation (1.1):

$$\begin{bmatrix} v_{as} \\ v_{bs} \\ v_{cs} \end{bmatrix} = \begin{bmatrix} cos\theta & sin\theta & 1 \\ cos(\theta - \frac{2\pi}{3}) & sin(\theta - \frac{2\pi}{3}) & 1 \\ cos(\theta + \frac{2\pi}{3}) & sin(\theta + \frac{2\pi}{3}) & 1 \end{bmatrix} \begin{bmatrix} v_{qs}^{s} \\ v_{ds}^{s} \\ v_{0s}^{s} \end{bmatrix} \tag{1.1}$$

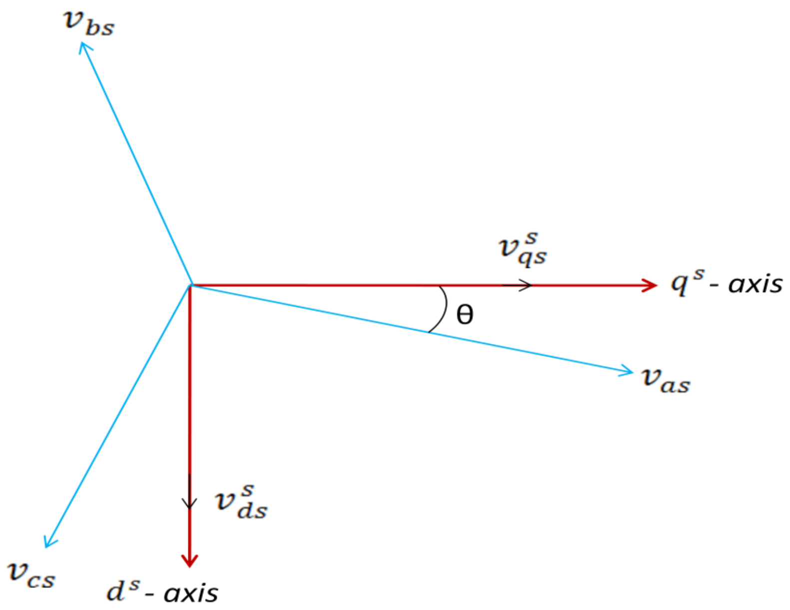

Fig. 1.8 Three phase and two phase stationary frame

Similarly three phase components can be resolved into stationary frame of reference which can be represented in matrix form as:

$$\begin{bmatrix} v_{qs}^{s} \\ v_{ds}^{s} \\ v_{0s}^{s} \end{bmatrix} = \frac{2}{3}\begin{bmatrix} cos\theta & cos(\theta-\frac{2\pi}{3}) & cos(\theta+\frac{2\pi}{3}) \\ sin\theta & sin(\theta-\frac{2\pi}{3}) & sin(\theta+\frac{2\pi}{3}) \\ 0.5 & 0.5 & 0.5 \end{bmatrix}\begin{bmatrix} v_{as} \\ v_{bs} \\ v_{cs} \end{bmatrix} \tag{1.2}$$

For simplicity make $\theta = 0$ in order to align v_{as} axis with v_{qs}^{s} axis such that

$$v_{as} = v_{qs}^{s} \tag{1.3}$$

$$v_{bs} = -\frac{1}{2}v_{qs}^{s} - \frac{\sqrt{3}}{2}\, v_{ds}^{s} \tag{1.4}$$

$$v_{cs} = -\frac{1}{2}v_{qs}^{s} + \frac{\sqrt{3}}{2}\, v_{ds}^{s} \tag{1.5}$$

Similarly following equations can also be written as:

$$v_{qs}^{s} = v_{as} \tag{1.6}$$

$$v_{ds}^{s} = -\frac{1}{\sqrt{3}}v_{bs} + \frac{1}{\sqrt{3}}v_{cs} \tag{1.7}$$

1.3.4.2 Park transformation

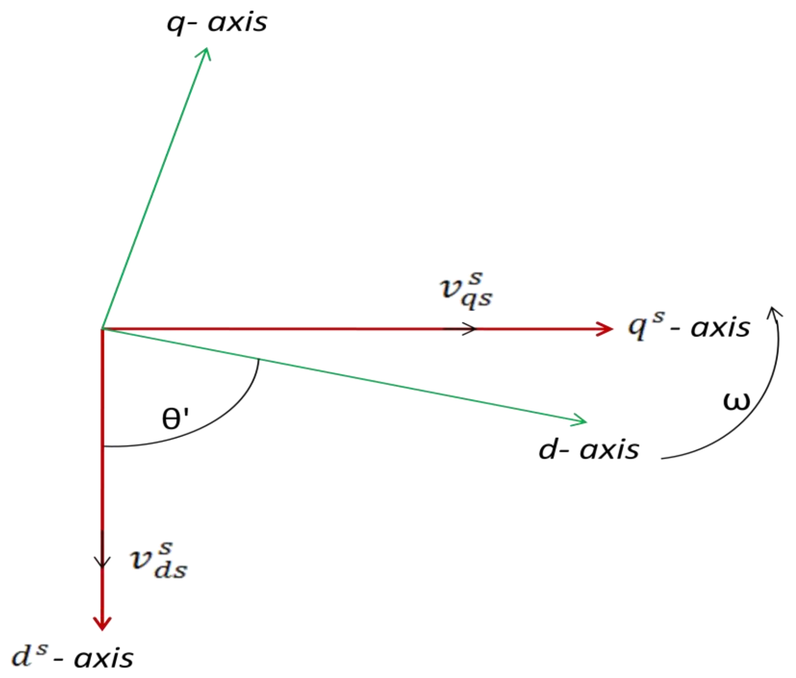

Fig. 1.9 Stationary to synchronously rotating frame

It is a two phase stationary frame to synchronously rotating reference frame transformation. By considering the vector diagram of Fig. 1.9, where d-q axis is rotating with synchronous speed of ω with respect to stationary axis, the voltage equations in dq axis can be written as:

$$v_{ds} = v_{qs}^s \sin\theta' + v_{ds}^s cos\theta' \quad (1.8)$$

$$v_{qs} = v_{qs}^s cos\theta' - v_{ds}^s sin\theta' \quad (1.9)$$

Resolving synchronously rotating reference frame into stationary frame

$$v_{ds}^s = v_{ds} \cos\theta' - v_{qs} \sin\theta' \quad (1.10)$$

$$v_{qs}^s = v_{ds} \sin\theta' + v_{qs} cos\theta' \quad (1.11)$$

Stator three phase balanced sinusoidal voltages can be written as:

$$v_{as} = v_m cos(\omega t + \phi) \quad (1.12)$$

$$v_{bs} = v_m cos(\omega t - \frac{2\pi}{3} + \phi) \quad (1.13)$$

$$v_{cs} = v_m cos(\omega t + \frac{2\pi}{3} + \phi) \quad (1.14)$$

Putting these three phase equations into (1.9) and (1.10)

$$v_{qs}^{s} = v_m cos(\omega t + \phi) \tag{1.15}$$

$$v_{ds}^{s} = -v_m sin(\omega t + \phi) \tag{1.16}$$

Using above equations in (1.11) and (1.12) we get:

$$v_{ds} = -v_m sin\phi \tag{1.17}$$

$$v_{qs} = v_m \cos\phi \tag{1.18}$$

Hence it is clear from these equations that the sinusoidal stator voltages which are in reference frame of stationary converted into DC like voltages in synchronously rotating frame.

1.3.5 d-q Reference Frame of the IM for Decoupled Control

Vector diagrams of an induction motor (IM) in synchronously rotating frame of reference are shown in Fig. 1.10 and in Fig. 1.11 for change in torque current component and for change in flux current component respectively. From the phasor diagram of Fig. 1.10, it is clear that with the increase of the torque current component, it does not affect the flux current component. It is also observed from Fig. 1.11, that with the increase of the flux current component, it does not affect the torque producing current component. The IM characteristic can behave like a dc motor, if the flux producing current component aligns in the direction of the rotor flux and torque producing current component is perpendicular to it. Hence flux and torque of an induction motor can be controlled independently provided the orientation of flux and torque current component maintained at orthogonal for all operating conditions.

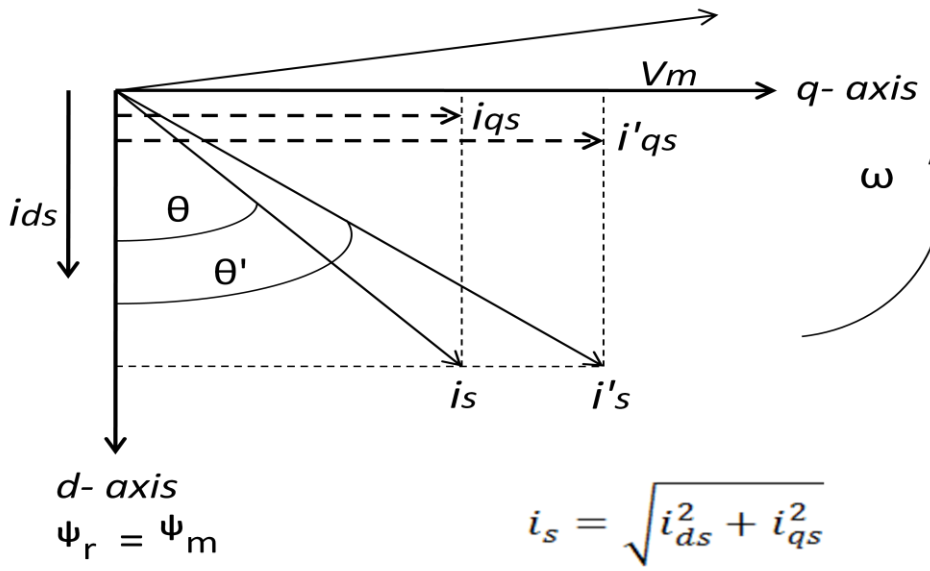

Fig. 1.10 Vector controlled of IM with an increase of torque current component

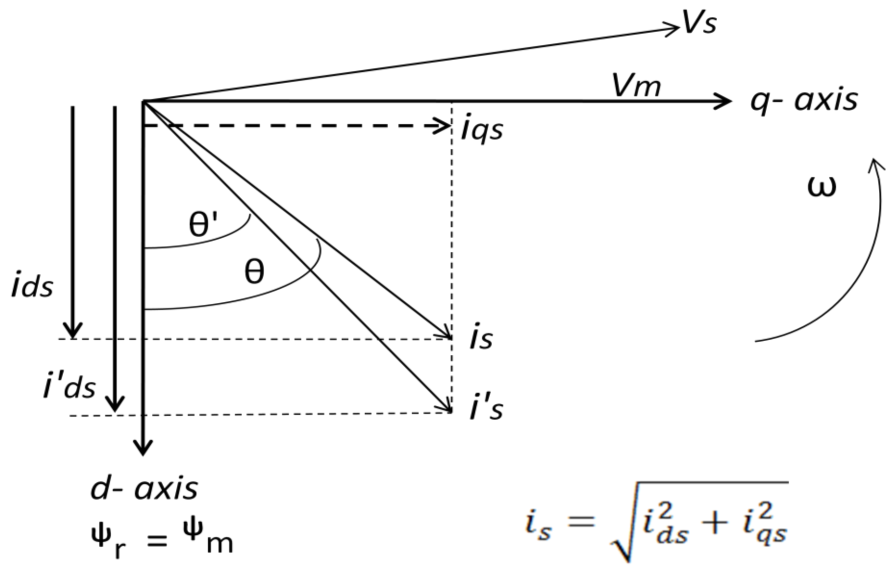

Fig. 1.11 Vector controlled of IM with an increase of flux current component

1.4 EFFICIENCY OF INDUCTION MOTOR

The extensive use of IM has brought the intention to improve efficiency and performance of drives for energy saving. The progress in the area of digital signal processing and semiconductor devices has made the implementation of IM drives cost effective in high performance control applications. In this work the efficiency improvement of variable speed

IM drives has been presented by optimal control of the flux producing current using loss model and search control methods. A loss model control of a fuzzy logic controller and PI controller based efficiency optimization scheme for a vector controlled IM drive is described. A new technique called deep valley search algorithm based on search control for efficiency optimization of vector controlled IM drive is also presented to reduce the core losses. Efficiency in the IM operation is discussed by selecting the appropriate rating of electric motor according to the requirement, by improvement in power quality to the motor and by use of an appropriate optimal control method.

Operation of motor at rated load is highly efficient, but at light load operation it has increased iron losses and less efficiency. Under such circumstances, it becomes impossible to improve the efficiency of motor by selection of motor rating and design or by input power quality improvement. However an appropriate control algorithm which minimizes the induction motor losses is needed to minimize iron losses of the IM by the optimum choice of the flux level. There are many optimal control methods available in the literature. Some of these optimal control methods to optimize AC drive system are based on to account either minimum stator current or maximum efficiency or maximum power factor or to have minimum total losses.

Minimum loss control schemes are more popular for efficiency optimization of IM and are broadly classified into two main categories i.e. search control (SC) and loss model control (LMC). SC measures the power input of the system and searches the optimal value of excitation. In SC there are oscillations in air gap flux and disturbances in torque but measurement of power is more accurate and easy due to small harmonics in source voltage and current waveform as compared to motor waveform. It is insensitive to parameters changes and reduces total energy consumption. Loss model control measures the stator current and speed and losses are computed using the machine loss model to determine the optimal air gap flux which minimizes the core losses. It is machine parameters dependent but dynamic response of the drive system is fast and it is suitable in field oriented control.

1.5 OBJECTIVES OF THE PRESENT WORK

The present research work objectives are to optimize induction motor efficiency at light load condition by minimizing the input power and losses etc. The proposed loss control methods limit the flux level as per the load conditions on the IM to maximize performance of the motor for different operating conditions.

The main research objectives are listed as follows:

I. Control of Induction Motor Drive using Full Spectrum Simulator (FSS)

A detailed analysis of the behavior and performance characteristics of the IM under constant V/f and indirect field oriented control (IFOC) of induction motor drive is presented. Modeling and simulation for both V/f as well as indirect field oriented control have been carried out by utilizing MATLAB/ Simulink and full spectrum simulator (FSS) to understand the dynamic behavior of induction motor drives. These IFOC and constant V/f models have been simulated offline and validated by real time simulation for different load and speed condition. Results of simulation obtained from both FSS offline and MATLAB simulator matches with the FSS online simulator.

II. Sensitivity Analysis of Induction Motor Performance

The parametric variations effect on an induction motor has been analyzed. A nonlinear equation of the IM is developed and solved for finding the slip under different load conditions. Sensitivity analysis of motor performance is discussed for the steady state equivalent circuit of the IM to predict the performance under parameter variations using analytically as well as computational methods.

III. Speed and Stator Resistance Estimation in Sensorless IM Drive

Model reference adaptive control based motor speed and stator resistance estimation methods in a sensorless control of the IM drive are presented. The stator resistance estimation involves the adaptive mechanism build up using adaptive neuro-fuzzy inference system and the estimated stator resistance is applied for making the rotor speed estimation independent of stator resistance. The projected algorithm is simulated in the environment of MATLAB and the results obtained are analyzed under different operating conditions. Moreover, the stability analysis of the drive using frequency response analysis method i.e. bode plot is carried out over a wide range of stator resistance variation.

IV. Efficiency Optimization in IFOC IM Drive Based on Loss Model Control

A simple and easily realizable technique for execution of a PI controller and fuzzy logic controller based efficiency optimization scheme for a vector controlled IM drive is presented. A new approach for efficiency optimization for an optimal control of iron losses only is demonstrated and it is compared with the optimal control of the total losses. The developed technique is tested under different operating conditions.

V. Efficiency Optimization in IFOC IM Drive Based on Search Control

A novel algorithm of searching the flux current component for optimization of efficiency of induction motor (IM) drives is presented. This new algorithm is called “deep valley search algorithm” and can be considered as an alternative to the search control problems. The online efficiency optimization of vector controlled induction motor drives through optimal control of search control (SC) approach is presented. The proposed drive system is simulated in a MATLAB environment and the improvement in the efficiency of the drive system is observed.

1.6 ORGANIZATION OF THESIS

The content of the thesis have been divided into following chapters:

Chapter 1 presents a brief introduction about AC drive system along with its historical background. Different control approaches used and their applications for Induction motor drive along with optimal efficiency techniques are also discussed.

Chapter 2 presents an extensive literature review on the IM drives with major focus on scalar control, vector control, parameter identification of induction motor, loss minimization, search control and loss model efficiency optimization techniques. Different control methods used and their variants were also discussed.

Chapter 3 presents the performance study of constant Volts-Hertz (V/f) and indirect field oriented control (IFOC) of IM drive. Off-line and real-time simulation using full spectrum simulator (FSS) is introduced. Modeling and simulations for the proposed algorithms have been presented using MATLAB/ Simulink and FSS to understand the dynamic behavior of induction motor. These IFOC and constant V/f models have been simulated under different load and speed conditions. Results of simulation obtained from both FSS offline and MATLAB simulator are found in agreement with the online FSS simulator.

Chapter 4 presents sensitivity functions and analytical methods to find out the sensitivity of the motor performance under parameter variations. The performances of motor have been presented in terms of motor parameters. The analysis is carried out by using the equivalent circuit of the induction motor with and without core loss resistance. The stability analysis is also carried out using state equations of the system.

Chapter 5 presents speed estimation technique based on X-MRAS model where instantaneous value and the steady state value of fictitious quantity of the stator current and voltage are used in the reference and in the adaptive model respectively. Adaptive mechanism for stator resistance estimation utilized ANFIS controller. The small signal stability analysis is described by linearizing the motor equations around the stable operating point. The transfer function obtained from the linearized model is then utilized to find out the stability of the IM drive system using Bode diagram.

Chapter 6 presents efficiency optimization of IM drive through the optimal control of d-axis current component using a loss model control method. The developed algorithm minimizes iron losses and the total motor losses to optimize the efficiency of the IM drive. The scheme has been implemented and compared using both fuzzy logic controller and PI controller. Performance analysis of the IM drive is carried out for sudden change in load torque and speed.

Chapter 7 presents on line efficiency optimization through a novel search algorithm called deep valley search algorithm of indirect vector control of IM drive system. The proposed algorithm optimizes the flux producing current component by using the dc link power as the controlled variable. Simulation results for sudden change in load torque and sudden change in speed of IM drive was carried out. The algorithm can be applied to any conditions and showed good performance at light load and low speed operations. The algorithm is applied successfully for transient conditions.

Chapter 8 presents the main conclusions of the research work and scope for the future work in the area of the IM drive system.

1.7 CONCLUSION

This chapter describes the main objectives of this research work and also provides an outline of this thesis. The requirement and importance of AC drives along with efficiency aspects of the induction motor is discussed in brief. The chapter wise analysis of the thesis is summarized. Induction motor losses and ways to improve efficiency of the motor is described in details. Importance of induction motor in AC drives is discussed. Various aspects and classification of AC drives along with explanation of conventional and modern drives are presented. Different efficiency optimization techniques are also discussed.

CHAPTER II

LITERATURE REVIEW

2.1 GENERAL

Induction Motors (IM) are generally used for domestic as well as for industrial applications. IMs are designed and constructed with maximum efficiency for operation at rated load torque and rated speed. But for most of the applications, IMs are generally operated at loads less than the rated loads. It is therefore, essential to increase the efficiency of the IM drive system for optimizing the energy requirements under different operating conditions. IMs are popular due to its numerous advantages despite of its inherent disadvantages [1]. Control techniques used in AC machines have led to the increased use of the IM in advanced performance drive applications [2]. The IMs consume a major portion of the electric energy generated worldwide. Hence IM drives performance need to be optimized to increase the energy efficiency by reducing the losses [3]. Various methods have been proposed in the literature for efficiency optimization. Prior to the introduction of semiconductor devices (1950s) induction motors were used for fixed speed applications and DC motors were used for variable speed applications. With the advent of semiconductor devices the IM became popular for variable speed applications because of the availability of variable frequency sources but it was limited to average performance applications due to the coupling effect between torque and flux control. This inherent coupling effect was solved by Hasse and Blaschke in the beginning of the 1970s with introduction of the field oriented control called vector control. Performance characteristics akin to a DC drive can be obtained by decoupling the torque and flux producing current components in vector control for both asynchronous and synchronous motor drives [4]-[7]. In 1986 a new methods of torque control in IM i.e. direct torque and flux control technique (DTC) was also proposed by Takashi and Noguchi.

Initially the control of motor drives was complex and expensive but with the reduction of the cost of semiconductor devices and availability of advance microprocessors the IMs have become favourable alternative to the dc motors drives [8].

2.2 INDUCTION MOTOR DRIVE SYSTEMS

2.2.1 Conventional Methods

An IM is a highly efficient motor when working close to its rated speed and torque. However, in most of the applications IMs operates at light load conditions and its power factor is low. It is therefore, essential for these applications to increase the efficiency of the IM drive system under such operating conditions for reducing the running cost and energy savings. The easiest way to increase the efficiency of the IMs at light load is to reduce the input supply voltage of the motor. This can be achieved easily by using star connection of induction motor. When motor stator winding is connected in star then the voltage applied to the IM is decreased by the factor of 0.577. But it limits the motor operating torque range to keep above the 0.33 p.u. load. This method is unsuitable for higher load applications because it reduces the efficiency due to the increased current drawn by the motor. The motor torque is directly proportional to the square of the applied voltage so with the decrease of the voltage the developed torque decreases by the factor of three when started in star connected mode [9],[10]. At starting the motors are generally operating at rated flux for getting superior dynamic performance. The air gap flux is programmed as per the load condition and it must be kept above the 0.3 p.u. Lower value of flux creates disturbance in the developed torque and generates more motor losses [11]. Optimal efficiency can be obtained by varying the value of flux. In inverter fed IM the losses can be neglected for the drive systems up to the size of 10kW but its effect becomes significant for the higher size of the drive system for considering the inverter and harmonic losses and it must be included for maximizing the efficiency [12]-[14]. The performance analysis of the ac drive system mainly depends on the voltage, frequency, speed and parameters of the motors. The quality of power supply to the IM also affects the performance of the system [15]. Optimization techniques based on Hook Jeeves [16] and sequential minimization approach [17] are presented for design of induction motor.

2.2.2 Efficiency Improvement with Design Consideration

Depending on the operating condition the design consideration of IM plays an important role to optimize the drive system. An improvement in performance is observed with some conventional algorithms like efficiency improves when voltage supplied to the motor increases [18]. In [19] authors achieved improvement in minimizing the losses by decreasing the number of turns in stator winding and increasing the length of stator core. The manufacturing and operating cost were considered as an objective function for optimizing the IM design [20]. In [21] author proposed to reduce harmonic current, flux, stack length of core and to increase reactance, to increase core depth of stator and rotor in order to get less torque pulsation of voltage source inverter fed induction motor. Optimal motor parameters calculations by using Hooke-Jeeves method based on computer programming is proposed in [22]. The Constraint Rosenbrock method by utilizing the objective of production cost was used to optimize the efficiency of motor [23]. It is suggested that stator slot design has considerable effect on harmonic, copper and iron losses and it can be improved by proper selection of the slot [24]. By improving the motor manufacturing process like annealing of the core, using advanced material, changes in slots and core axial length etc. the overall cost can be reduced and the efficiency can be improved [25]. Performance improvement of IM in terms of cost, efficiency, time convergence etc. is achieved than conventional techniques by applying some nature inspired algorithms to motor design like simulated annealing (SA) [26], particle swarm optimization (PSO) [27]-[30], evolutionary algorithm [31] and genetic algorithms (GA) [32]-[34] etc. The hybrid of among these nature inspired algorithm techniques has been proposed for motor design to handle the environmental changes [35]. In squirrel cage IM due to nonlinearity in magnetic circuit harmonics are generated. By considering the distribution of rotor bar conductor position in space the effect on these harmonics is evaluated and effect on stator current has been analyzed [36].

2.3 CONTROL OF INDUCTION MOTOR DRIVE

2.3.1 Scalar Control Method

Induction motor speed control methods like variation in frequency, rotor resistance and stator voltage, slip recovery, pole changing, constant V/f etc., are based on the magnitude of the control variables. Among these methods, the constant V/f method is most frequently used. In this method, flux and torque remains unchanged during speed variation by keeping V/f ratio constant. Only magnitude of control variable is altered. Up to the rated speed, V/f ratio is kept fixed to keep flux constant. Above rated speed, voltage is kept constant and frequency alone is made to increase. When frequency is increased above rated value of voltage to increase the speed, flux will decrease as voltage cannot be increased above rated value. This region of operation is called as field weakening region. If the frequency is reduced to decrease the speed of motor, then flux will saturate causing excess of stator current which might harm the motor permanently. The V/f control method is easy to implement, cheap, has broad range of motor speed control, good steady state performance and low starting current requirement. The absence of feedback signal in open loop makes this method very simple but at the same time it makes the system prone to instability. An optimal constant V/f controller was designed for different load conditions to improve the performance of drive system [37],[38]. However, it has somewhat poorer dynamic performance in comparison to vector control. The motor speed cannot be controlled precisely because only the synchronous speed is controlled. It cannot rectify any disturbance in the system. Hence in applications where requirement of accuracy is higher, constant V/f control method is not used [39],[40]. Variable frequency drive based centrifugal pump optimization carried out to improve the efficiency [41]. The HVAC and CT applications include induction motor scalar control method [42].

2.3.2 Vector Control Method

For an induction motor (IM) the current of stator can be projected along the rotor flux linkages by knowing the position of the synchronously rotating rotor flux at any instant, and then the IM can be controlled in the same way as that of a separately excited dc motor. Cross product of the stator magnetic field and armature current provides motor torque and for getting the maximum torque these two components must align perpendicular to each other. Various methods have been projected in literature for the control of IM drives. Vector and scalar speed control methods are commonly used in industry, among which vector control method has become the most efficient for higher performance applications and it overcomes the limitations of scalar control method. In vector control scheme the torque and the flux current components can be controlled independently [43],[44]. The torque and voltage equations which explain the dynamic performance of an IM are time varying and due to continuously changing of the coefficient of coupling between stator and rotor windings, the control of an IM become complex and non linear. This complexity of the induction motor can be decreased by transferring the three phase rotor and stator variables to two phase variables called d-q transformation [45]. Decoupling in rotor flux and torque is achieved by using the magnetizing current component [46]. The control methods based on decoupling are direct torque control (DTC) and field oriented control (FOC), which are used for controlling speed and torque [47]. The rotor and stator flux ripples based torque ripples are used to influence the switching sequences of the pulse width modulation in a vector controlled phase wound IM drive for estimation and reduction of the torque ripples [48]. Conventional DTC and hybrid DTC were proposed by [49],[50] in order to decrease the flux and torque ripples. Field oriented control is the most useful vector control method which has lower operating cost, higher efficiency and lower power consumption. [51]-[58]. Harmonics in input supply voltage, flux saturation and skin effects are considered for efficiency improvement by using input voltage and frequency as a controlled variables [59]. A new MRAS based speed estimation of sensorless IM drive using dq circuit effective impedances is proposed where flux computation is not required. This speed estimator is stable in all four quadrants [60]. Model reference adaptive system for the estimation and decoupling of the rotor resistance and flux in an indirect field oriented IM drive system is presented [61].

2.3.3 Soft Computing Method

Advancements in Artificial Intelligence based control methods have led to the increased use of fuzzy logic controller (FLC) in lieu of PI controllers. Fuzzy logic controller independently or in hybrid with other controller improves and smoothen the motor torque ripples and currents. In [62]-[64] decoupling in rotor flux and torque is achieved for induction motors using FOC principle by utilizing the artificial neural networks (ANNs). Neural network trained in order to enhance the efficiency by optimizing the flux. In [65] the performance between field oriented control and direct torque control are compared for induction motor drive. In [66] the IM drive is optimized by using system-level based minimization technique and is found lower than the component-based techniques. In [67] sensor less control of induction motor drive is obtained by using MRAS. To achieve variable voltage and frequency from an inverter [68],[69] suggested that space vector pulse width modulation (SVPWM) has improved dc bus utilization in comparison to the other pulse width modulations. The numerical approach through Genetic Algorithm (GA) is discussed to find the effect of motor parameters in loss model control strategy [70]. Optimization of three-phase induction motor for manufacturing process has been designed by using GA. A non linear problem of motor is derived and various methods of its solution has been proposed [71]. Input supply power quality to the inverter improved by tuning PID controller properly using particle swarm optimization (PSO) [72]. A hybrid system based on combining effect of GA and PSO is discussed for LMC [73]. At starting of the drive system motor draws high current in order to develop the required torque, which led to the torque pulsation. This starting torque variation was taken care in [74] by using back to back triggering of thyristors for the motors requiring normal starting torque. Model reference adaptive system along with the fuzzy logic controller is used to estimate and tune the motor parameters for getting high performance in an induction motor drive [75].

2.4 PARAMETER IDENTIFICATION

Induction motor parameters differ considerably with operating conditions. For estimating the motor parameters many types of methods are available like conventional methods [76],[77], offline parameter identification [78], online parameter identification [79], observer based method [80], MRAS based method [81], soft computing methods which includes fuzzy system, ANN, genetic algorithm, PSO and hybrid of these etc. [82]-[84]. For speed sensor less IM control the parametric effect and model uncertainties become more significant. Therefore the performance of the drive deteriorates with parameter variations during operation of the IM. To identify the parameters that have considerable effect on motor performances, sensitivity analysis is proposed for an induction motor [85]. The parameters of induction motor received from manufacturer have uncertainty because it is defined for a similar size frame motor. Furthermore, these parameters may change with varying operating conditions in motor like magnetic saturation and change in temperature. In order to avoid such a condition, it is essential to provide the accurate values of parameter to the controller. These parameters have to be achieved somehow from measurements, during initialization of the drive. Several methods for induction machine offline and online parameter estimation have been developed for application in high performance drives. The most common method, to manually find induction motor parameters, is to test motor under blocked rotor and no-load conditions. The variation of parameters also implies a variation in the performance characteristics of the motor. Sensitivity analysis is discussed for an induction motor to find out the parameters which have maximum impact on performance variables of motor [86]. The drive's behavior in terms of machine parameters sensitivity and stability can be determined by evaluating the locations of the eigen values in the s-plane and by analyzing the parameters affect on the eigen values. If such parameters are identified, then compensation scheme can be adopted for the same to reduce the drive's complexity and to improve the reliability of the overall system [87]. The sensitivity with respect to the controller parameters based on eigen values have been evaluated and the dominant parameters of the controller were identified. This leads to the better performance of drive because there is no need to optimize all the controller parameters simultaneously [88].

In this way sensitivity analysis results provide a lot of significant information regarding motor parameters [89],[90]. A nonlinear equation of the IM is derived and solved for finding the slip value using computational methods for estimating the realistic value of slip at different load conditions of the induction motor [91]. State space model helps to develop and analyse different control strategies for induction motor. Parameter sensitivity analysis is required to design the different kinds of controller for controlling speed and torque of the motor [92].

Stator resistance and speed estimation schemes based on voltage/current model, steady state model of IM, back-emf, model reference adaptive system (MRAS) etc. are available in the literature [93]-[97]. For online estimation of stator resistance an adaptive method is used. Nowadays sensorless vector controlled drive is popular and commercially accessible, but the parameter variation creates problem for speed estimation accuracy [98],[99]. In the literature several speed estimation methods have been proposed. Among these the machine model-based techniques, voltage/current model, speed estimation using MRAS and adaptive observer are very attractive [100]-[103]. These techniques are less sensitive to parameters and operate well even at zero and low speed operation. The other types of speed estimation methods in literature include slip control, state equations, flux observer, artificial intelligence, EKF, slot harmonics, reactive power and neural adaptive system etc. [104],[105]

Artificial intelligence based methods like adaptive neuro-fuzzy inference system (ANFIS), artificial neural network (ANN) are widely used for estimation of speed. MRAS has drawn much attention in this field of parameter estimation because it is easy to implement, it requires less computation and has good stability. Various MRASs based on flux, torque, reactive power and back electromotive force are proposed in literatures for speed estimation and have shown satisfactory results [106]-[110]. Flux and Back-emf based MRAS speed estimator works efficiently but suffers from integrator and low back-emf related problems respectively at very low rotor speed operation. These problems can be overcome by reactive power based MRAS but it suffers from stability related problems in the regenerative mode, however, X-MRAS can be used, which utilizes the steady state and instantaneous values of the stator current and voltage vectors to overcome this stability linked problem [111]-[116].

2.5 EFFICIENCY OPTIMIZATION IN IM

Induction motors (IM) are designed and constructed with maximum efficiency for operation at rated speed and torque. However, for most of the period during routine operations, IMs are generally operated at loads less than the rated torque. It is therefore, essential to increase the efficiency of the IM drive under such operating conditions for saving the energy consumption and reducing the cost of operation and also minimize adverse effect on the environment [117]. Efficiency improvement and energy saving in recent years are one of the most important objectives and have been getting a lot of attention by the researchers to maximize the efficiency of electrical motors. Researchers are developing new loss minimization methods to reduce the motor losses and maximize the efficiency. Many algorithms have been developed to improve the motor efficiency at different load conditions. Optimal control strategies for efficiency optimization are of three types search control, simple state control and loss model control. In simple state control method one particular variable is measured for running the induction motor at predefined reference speed. Power factor and slip frequency are generally used as the control variables in simple state control method. Objective function based on power factor does not require any load torque or rotor speed information and provides fast convergence [118]. Simple state control was the first method in drive system for energy optimization. However with advancement in the power semiconductor devices and control algorithms, other methods are evolved. Therefore the approaches for efficiency improvement are mainly divided into two categories, namely search controller (SC) and loss-model controller (LMC).

2.5.1 Loss Model Control Method

A large number of approaches using different variables are proposed in the literature to minimize the induction motor losses. In LMC the machine model is used to compute the motor losses by choosing a flux level to minimize the core losses. The LMC is faster than the search control technique but with the variation in motor parameters its performance deteriorates. This method is dependent on machine parameters, but it gives fast response [119]-[122]. In [123] optimum value of voltage and frequency is reported for a particular operating condition using loss model scheme. Efficiency optimization based on rotor reference flux has eliminated the requirement of classical vector control strategy [124]. Nonlinearity of magnetic circuit affects the design of loss model for optimization. In order to analyse the loss model properly the effects of nonlinearity and harmonics in the power supply are also considered [125]. An improvement in efficiency is observed when stator current is used as a control variable by decomposing the stator resistance into two components. When stator current is used as a variable instead of input power in search control algorithms then better results are observed in terms of torque ripples and loss reduction. The optimal value of stator current can be easily obtained in comparison to the input power because input power is less sensitivity to the change of flux. Therefore an algorithm is required to set a flux step for search control. A big flux step reduces the convergence time where as the small step size of flux increases the convergence time but decreases the flux and torque ripples. Search control algorithm makes the drive response sluggish [126]-[130]. To improve the efficiency of motor at light loads, the flux component of the current must be reduced for obtaining a balance between copper and iron losses [131]-[134]. An improvement in efficiency is observed when power factor is used as a control variable [135]-[137] by measuring power factor. In [138] designing of an online monitoring system for calculating efficiency of induction motors is studied. The optimization method based on the behavior of nature has been focused in literature to solve the optimization problems [139],[140]. Scalar and vector control strategies are also commonly used in AC drives to achieve optimal performance [141]-[143].

Loss model controller (LMC) for searching the optimal value of flux component that minimizes the motor losses is described [144],[145]. Different loss minimization algorithms for efficiency optimization were discussed for permanent magnet synchronous motor drives [146]. The LMC is more suitable in vector control since optimal flux can be obtained in a short time but in SC the flux oscillates around the optimal value. Hybrid method of loss model control and flux control through search control by utilizing the good features is also used for fast convergence [147]-[149]. Fuzzy logic based efficiency optimization and speed control is demonstrated for induction motor drives [150],[151]. The flux level at the lowest point is calculated by using the quadratic interpolation method [152]. In [153] relationship between flux-producing current component and ohmic losses was formulated to get the optimal value. Input power minimization is investigated through loss model controller using particle swarm optimization (PSO) and search controller to improve the performance of the drive system [154]. Rotor and speed estimation in a sensorless induction motor drive is presented in [155]. An optimal efficiency is proposed in [156] by utilizing the slip control method. The motor is fed through current source inverter and the system follows the optimal slip algorithm. A high-performance low cost field- oriented speed sensorless drives is discussed on the basis of measurement of dc link voltage and current by reducing the drive components [157],[158)]. In d-q coordinate direct axis current component as a variable is used to optimize efficiency of permanent magnet synchronous motor and reluctance motor along with the effects of core saturation [159]. Induction motor equivalent circuit that includes core loss component is studied for finding the parametric effect in loss model control and improving the efficiency [160]. An optimal efficiency algorithm based on GA and FLC is presented for minimizing the motor losses by controlling the flux producing current component and compared with the conventional FOC algorithm [161]. The efficiency improvement at the time of acceleration and deceleration duration is carried out [162]. For high accuracy and fast response indirect vector control of the maximum torque per power losses (MTPPL) method is implemented, where for a given load torque power losses are minimum [163].

2.5.2 Search Control Method

Search control method (SC) is machine parameter independent and it does not require motor parameter information for optimization. The SC technique iteratively search for the optimal value of flux till the measured power input settles down to the smallest value for a particular operating condition. But torque ripples are always present in this method because of the air gap flux oscillations and are relatively slow due to the search process [164]-[167]. A robust speed control of IM drive against load disturbances for efficiency improvement by adjusting the rotor flux is presented. In this the real time result and simulation result are obtained for fast dynamic response of speed command and flux without any overshoot by rejecting the load disturbances [168].

Input power is generally measured from dc link or source terminal sides and hence is more correct than the motor side measurement because it has lower harmonic and switching effects. Torque ripples are always present in this method due to the air gap flux oscillations and the performance is relatively slow. Stator current minimization SC has lower torque ripples because of the lack of oscillations in the air gap flux [169],[170]. In [171] optimal flux level is searched through Rosenbrock method to determine the minimum input power by using fuzzy controller. Minimum of input power in field oriented control (FOC) of the IM is obtained and compared to traditional control by using minimization of the current vector. Efficiency improvement of IM is discussed through optimal control by using LMC and SC that includes artificial neural network, Genetic algorithm, fuzzy logic, differential evolution in optimization, expert systems and nature inspired algorithms [172]-[177]. In [178] ripple correlation control application discussed to minimize the input power of induction motor. For steady state condition efficiency was compared in vector control using different approaches [179]. In order to minimize the DC link power, three techniques based on the power-flux Gradient, reducing the flux current component in a smooth manner and hybrid method of Loss Model and Search control for the efficiency optimization of vector controlled IM drives are presented [180]. The optimal value of rotor flux based on golden section technique such that the input power of the drive system is minimum is also discussed. Torque ripples produced due to air gap flux were smoothed by using critically damped second order filter which opposes the sudden change of flux. The drive system starts with rated flux and after achieving steady state, the efficiency optimization approach is activated in order to get the better performance. Whenever there is variation in speed command the flux sets itself to rated value till the steady state condition is achieved [181]. Efficiency optimization based on the flux and torque estimation is implemented for vehicle drive system [182]. The shortcomings of LMC and SC were minimized by using the input power as a controlled variable for energy optimization in the drive [183]. The motor efficiency can be improved by adopting superior cooling system and advanced material [184].

2.6 RESEARCH GAPS IDENTIFIED

An extensive literature survey is carried out and the following research gaps are identified:

1. The effect of inverter losses for efficiency optimization in AC drive system to be implemented.
2. Dynamic performance of the IM drives can be improved by minimizing the effect of ripples in speed and torque during load transition.
3. Developing advanced loss minimization techniques to reduce the motor losses and maximize the efficiency to mitigate the environmental problems.
4. Stability analysis of IM drive system especially at low speed needs to be investigated.
5. Advance optimization and suitable control techniques to be implemented to handle complicated and non-linear characteristics of induction motor. Various approaches can be developed to improve the modern induction motor (IM) efficiency at light load conditions.
6. The induction motor (IM) parameters are very significant in high precision motor drive system for tuning the controllers. Therefore algorithms to be developed for the controller to have accurate value of the parameters.

2.7 CONCLUSION

An extensive literature survey carried out in the field of AC drives system with major focus on Scalar Control, Vector Control, Parameter Identification, Sensitivity Analysis and Efficiency Optimization. Different control methods used and their variants were also discussed. Some important research gaps are also identified for further investigations.

CHAPTER III

CONTROL OF INDUCTION MOTOR DRIVE USING FULL SPECTRUM SIMULATOR (FSS)

3.1 GENERAL

The poly phase induction motor has become the choice of industries for many applications. The performance analysis of IM drive using conventional methods of speed control such as constant volts-hertz (V/f) as well as indirect field oriented control (IFOC) methods has been extensively discussed in the literature. The constant V/f control method is used to keep the V/f ratio constant and the indirect field oriented control method is used to obtain fast dynamic performance of the drive by decoupling torque and flux producing components of stator current. Modeling and simulation for both constant V/f and vector control (IFOC) have been developed by using MATLAB/ Simulink and full spectrum simulator (FSS). In this chapter the IM is modeled with the help of MATLAB/Simulink and full spectrum simulator which allows us to analyze the drive performance under different load conditions. Full spectrum simulator has allowed us to do both offline and real time simulation with hardware in loop (HIL) facility. These constant V/f and indirect field oriented control models have been simulated offline and validated with real time simulation under different load and speed conditions. Results obtained from both MATLAB and FSS offline simulator are found in agreement with the FSS online simulator.

There are many control methods available for the efficient control of induction motor (IM). With development in power semiconductor devices, power electronics and new digital signal processors the induction motors are widely used in advanced performance drive applications. The conventional methods of motor speed control such as variation in frequency, change in rotor resistance and stator voltage, slip recovery, constant V/f and pole changing etc. are based on the variation in magnitude of the control variables. Among these methods, the constant V/f method is most suitable for normal performance applications. In this method, torque and flux kept constant during speed variation by keeping V/f ratio constant. The V/f control method is comparatively cheap, easy to implement, exhibits good steady state and dynamic performance, has wide range of speed control, low requirement of starting current and wider operating region. The V/f control method has somewhat poorer dynamic performance as compared to the vector control. Thus in applications where higher value of accuracy is not required, the constant V/f control method is used [39].

In the IM stator current can be resolved along the rotor flux linkage by knowing the position of the synchronously rotating rotor flux at any instant, and then the IM can be controlled in the same way as that of a separately excited dc motor and it is known as vector control methods. Various methods have been discussed in literature for the control of induction motor, among which vector control has become the most effective scheme for high performance applications. In vector control scheme the flux and the torque current components can be controlled independently [43]. The control techniques based on decoupling are direct torque control (DTC) as well as field oriented control (FOC), which are used for controlling speed and torque are the most accepted vector control scheme which has higher efficiency, lower energy consumption and lower operating cost. Decoupling in torque and rotor flux can be achieved by using the magnetizing current component as a control variable. Decoupling in torque and rotor flux is achieved by using the artificial neural networks (ANNs) for induction motors using FOC principle [62]. The performance between direct torque control and field oriented control are compared for IM drive [65]. In efficiency optimization of the induction motor drives, the motor losses are obtained from system-level based minimization technique and are found lower than the component-based techniques like motor loss model, dc-link power minimization and torque maximization etc. [66]. Space vector pulse width modulation has better dc bus utilization and easier digital realization as compared to the other pulse width modulations for obtaining the variable frequency and voltage from an inverter [68]. In this chapter V/f speed control and an indirect field oriented vector control of three phase squirrel cage induction motor using space vector modulation are analyzed by using MATLAB/Simulation model and full spectrum simulator mini-001 under different speed and load torque conditions.

3.2 FULL SPECTRUM SIMULATOR (FSS)

Simulation is very important tool for engineers to design and understand the complicated systems. Different types of offline simulator with standard software packages are available in market such as MATLAB etc. But, these software suffers from various disadvantages. There is no relationship between simulation and the physical time in case of an off-line simulator whereas, in real-time simulation, the simulation and the physical time domain are same and allows analysis of a physical system in real-time. FSS is very important and flexible simulation tool for analyzing power electronics and power systems related development activities. Hence, FSS is becoming popular in teaching as well as in research and development activities for analyzing the components and systems in a solver for circuit equations with user defined elements (SEQUEL) environment.

The simulator based on SEQUEL can be used for the simulation of circuits and is a general purpose, public domain package. It has been developed for an easy incorporation of new library elements. FSS is useful for offline and real-time simulation in the areas of testing, control system and development for different power system and power electronic applications. FSS can perform real-time and off-line simulation at a reasonable cost and is easily configurable for conventional applications. Block diagram of interfacing FSS with controller is shown in Fig. 3.1. FSS has three cards each having three processors so that nine processes can be done simultaneously. For developing the system there are various components available in element library of FSS, which can be utilized for simulation. Furthermore, the user can create their own components to develop the various applications for addition in element library. The experimental set up for FSS Mini real time simulation is shown in Fig. 3.2.

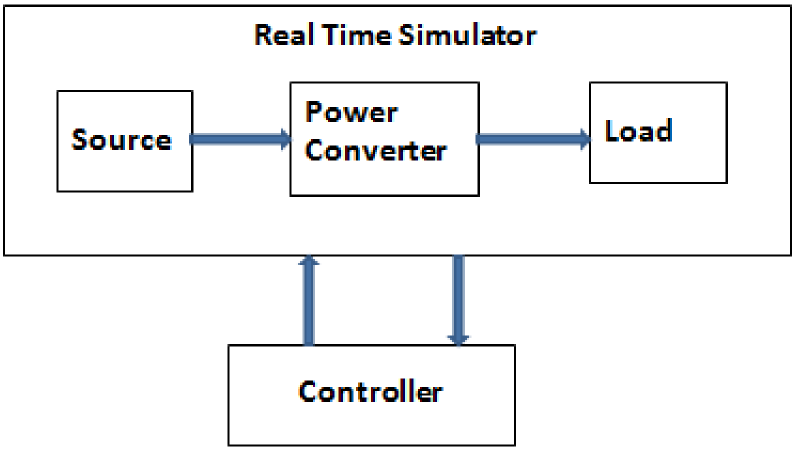

Fig. 3.1 Block diagram of interfacing controller with FSS

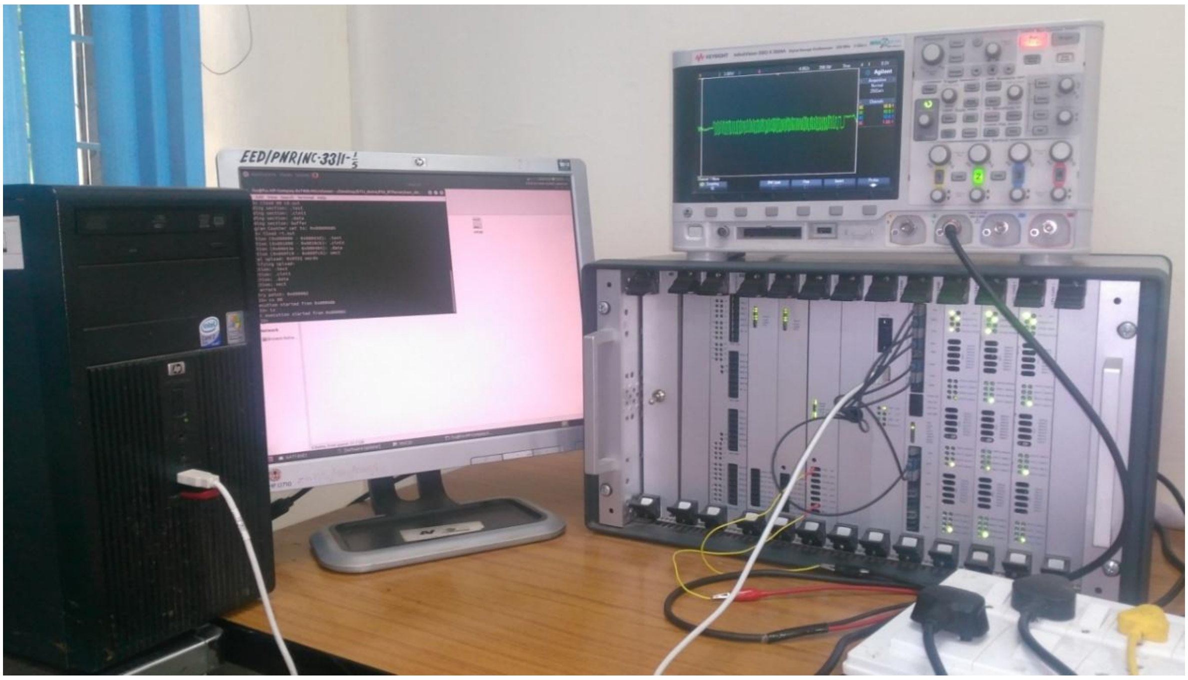

Fig. 3.2 Real time simulator set up

Windows operating system based computer is required for offline simulation and Linux based computer is required for real time simulation. So, two computers are needed for execution of the offline and real time simulation. On the other hand with the introduction of package of Linux based windows emulator, need of two computers can be eliminated. Pre processing in host computer execution and FSS hardware interfacing is shown in Fig. 3.3. The files which are to be executed in the FSS hardware for simulation are created in a number of steps in pre processing unit of host computer. The first step is to create the circuit file to start the process of simulation. The circuit file generally contains three sections.

I. Circuit section.
II. Solver section
III. Target section

The circuit section explains about the circuit elements which are taken from the general library. It describes about the inter connections of these circuit elements and how one element is connected to the other element of the library. It also defines the parameters of each element such as the magnitude and frequency of the voltage source element. The solver section explains about the start and stop time along with step size of the simulation. The solver section also defines the type of solver is used for simulation. The Target section defines about the offline simulation or real time simulation to be executed along with the generation of C code for the circuit. Next to the circuit file is the parser which is used to create the database for each element of the circuit file and generates the binary for downloading to the FSS hardware through USB link. These downloaded binary files are executed for getting the real time simulation result.

Linux based computer is required for real time simulation. The files which are to be executed in the FSS hardware for simulation are created in a number of steps in pre processing unit of host computer. The steps of pre-processing include circuit file creation and parsing of the circuit to create the database for each element of the circuit file. The hardware specific cross compiler is used to compile the generated code and for creating the downloadable binary files for the FSS hardware. These files are transferred to the FSS over a USB link for execution in real-time as shown in Fig. 3.3.

The motor/ inverter hardware need not to be used in the loop because for real time simulation FSS provide model based simulation. However, the simulation output can be observed in oscilloscope from the analog output card of the FSS.

The target section of the circuit file defines about the real time simulation or offline simulation to be executed along with the generation of C code for the circuit.

FSS has great flexibility in creating and modifying circuit elements. In order to check the operation of the modified circuit element/ circuit file created, offline simulation is needed. Moreover, the user can verify the functions of the real time libraries in offline environment.

The characteristics of various control algorithms are defined in the program written for the elements of the circuit file. The gains of PI controller along with the step sizes are also defined in the program.

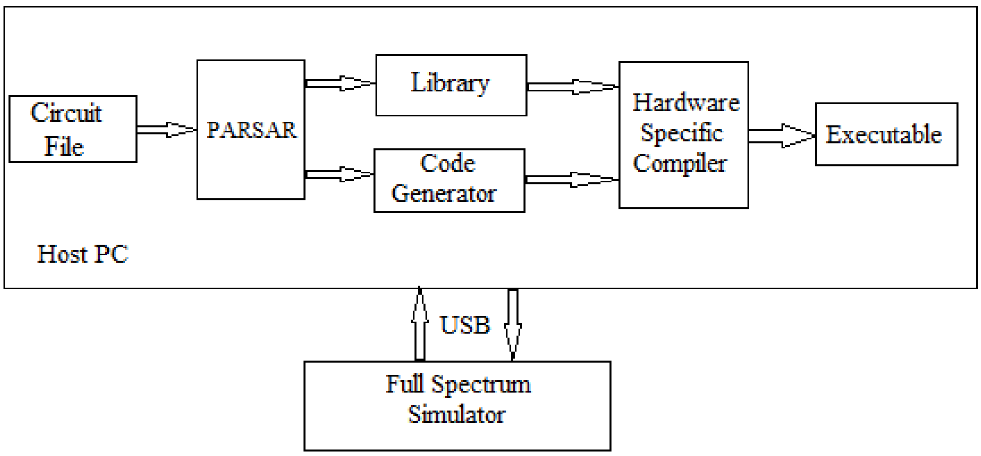

Fig. 3.3 Real time simulation in FSS

3.3 INDUCTION MOTOR MODEL

The torque and voltage equations that explain the dynamic analysis of an IM is time varying and due to continuously changing of the coupling coefficient between rotor and stator windings, the dynamic control of an IM becomes complex. The complexity of the IM can be reduced by changing the three phase stator and rotor variables to a set of two phase winding called d-q transformation [45]. In synchronously reference frame the d-q axis equivalent circuit of the IM is shown in Fig. 3.4.

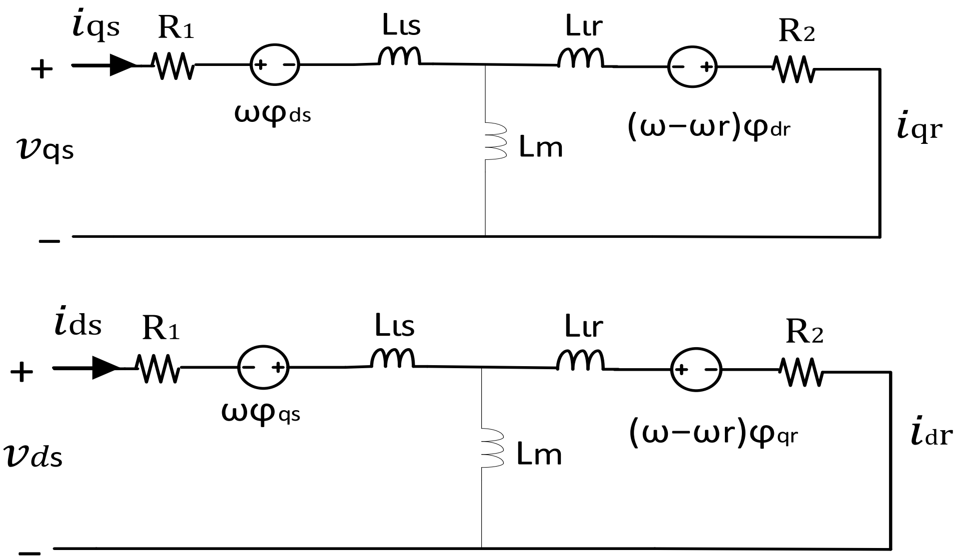

Fig. 3.4 d-q equivalent circuit

From *d-q* equivalent circuit, the voltage equations can be represented as:

$$v_{qs} = R_1 i_{qs} + \frac{\partial\varphi_{qs}}{\partial t} + \omega\varphi_{ds} \tag{3.1}$$

$$v_{ds} = R_1 i_{ds} + \frac{\partial\varphi_{ds}}{\partial t} - \omega\varphi_{qs} \tag{3.2}$$

$$v_{qr} = R_2 i_{qr} + \frac{\partial\varphi_{qr}}{\partial t} + (\omega - \omega_r)\varphi_{dr} = 0 \tag{3.3}$$

$$v_{dr} = R_2 i_{dr} + \frac{\partial\varphi_{dr}}{\partial t} - (\omega - \omega_r)\varphi_{qr} = 0 \tag{3.4}$$

The motor torque equation in terms of flux linkage and stator current components can be written as:

$$T_e = \frac{3P}{4}\frac{L_m}{L_r}(\varphi_{dr} i_{qs} - \varphi_{qr} i_{ds}) \tag{3.5}$$

Where v_{ds},v_{qs}, v_{dr},v_{qr} are the stator and rotor voltages in dq axis, φ_{ds}, φ_{qs} , φ_{dr}, φ_{qr} are the stator and rotor flux linkages in dq axis, i_{ds}, i_{qs}, i_{dr}, i_{qr} are the stator and rotor currents in dq axis, ω and ω_r are the angular speed of reference frame and rotor, R_1, R_2 are the stator and rotor resistances, L_m , L_r , L_s are the mutual, rotor and stator inductances.

The flux linkages equations can be represented as:

$$\varphi_{qs} = L_s i_{qs} + L_m i_{qr} \tag{3.6}$$

$$\varphi_{ds} = L_s i_{ds} + L_m i_{dr} \tag{3.7}$$

$$\varphi_{qr} = L_r i_{qr} + L_m i_{qs} \tag{3.8}$$

$$\varphi_{dr} = L_r i_{dr} + L_m i_{ds} \tag{3.9}$$

Further it can be shown that:

$$\varphi_{qs} = L_s \sigma i_{qs} + \frac{L_m}{L_r} \varphi_{qr} \tag{3.10}$$

$$\varphi_{ds} = L_s \sigma i_{ds} + \frac{L_m}{L_r} \varphi_{dr} \tag{3.11}$$

Where $\sigma = 1 - L_m^2 / L_s L_r$ is the leakage coefficient

Putting these values from (3.10) and (3.11) into (3.1) and (3.2) yields:

$$v_{qs} = (R_1 + \frac{\partial}{\partial t} L_s \sigma) i_{qs} + \omega (L_s \sigma i_{ds} + \frac{L_m}{L_r} \varphi_{dr}) \tag{3.12}$$

$$v_{ds} = (R_1 + \frac{\partial}{\partial t} L_s \sigma) i_{ds} - \omega L_s \sigma i_{qs} + \frac{L_m}{L_r} \frac{\partial}{\partial t} \varphi_{dr} \tag{3.13}$$

When d axis locked on the rotor flux vector then:

$$\varphi_{qr} = 0 \text{ and } \varphi_{dr} = \varphi_r \tag{3.14}$$

Putting these values in (3.3) and (3.5), yields:

$$(\omega - \omega_r) = \omega_{sl} = \frac{L_m}{L_r} \frac{R_2}{\varphi_{dr}} i_{qs} \tag{3.15}$$

$$T_e = \frac{3P}{4} \frac{L_m}{L_r} \varphi_{dr} i_{qs} \tag{3.16}$$

Where $i_{qr} = -\frac{L_m}{L_r} i_{qs}$ (3.17)

and ω_{sl} = slip frequency

For the steady state condition ($\varphi_{dr} = L_m i_{ds}$), the above expressions can be written as:

$$\omega_{sl} = \frac{R_2}{L_r}\frac{i_{qs}}{i_{ds}} \tag{3.18}$$

$$T_e = \frac{3P}{4}\frac{{L_m}^2}{L_r} i_{ds} i_{qs} \tag{3.19}$$

Hence rotor flux and torque of the IM can be controlled by d and q components of stator current.

3.4 SPEED CONTROL OF INDUCTION MOTOR

Motor speed can be changed by changing frequency of input signal, by changing number of poles and by changing slip. Changing the number of poles is normally not feasible once the motor design is completed and cost of motor also increases with increase in poles. Thus, generally frequency of motor is altered to increase or decrease the speed of motor and on the basis of this scalar and vector speed control techniques have been developed. Variable frequency drive (VFD) receives fixed voltage, fixed frequency sine wave input from power sources and it converts it into variable frequency, variable voltage, which is then used to control the speed of IM. A three phase, 4 pole, 2.2 kW, 430V, 50 Hz, 1430 rpm induction motor is used to carry out MATLAB simulation.

3.4.1 Constant Volts-Hertz (V/f) Method

In V/f method, motor develops constant torque, except at low speed or frequency and only the magnitude of control variables is controlled. There are open loop and closed loop scalar speed control methods available. The open loop volts/Hz control method of induction motor is very attractive due to its simplicity. Traditionally, induction motors were used for constant speed applications only. But with the use of various speed control methods available in literature it becomes possible to use induction motor for variable speed applications. Matlab simulink model is developed to analyze the open loop constant Volt/Hz method and to study the speed-torque characteristic. The power circuit consists of three phase power supply, rectifier, LC filter and PWM voltage fed inverter. The phase voltage V_s^* is generated from speed command by gain factor G which is calculated from rated voltage and frequency of motor so that the air gap flux remains constant. The boost voltage (V_o) is added for getting the rated motor flux and corresponding torque. The speed command is integrated to get angle θ and corresponding desired sinusoidal phase voltages (V_a^*, V_b^*, V_c^*) are generated as shown in the Fig. 3.5. These signals are fed to voltage source inverter which uses this signal to drive the three phase induction motor.

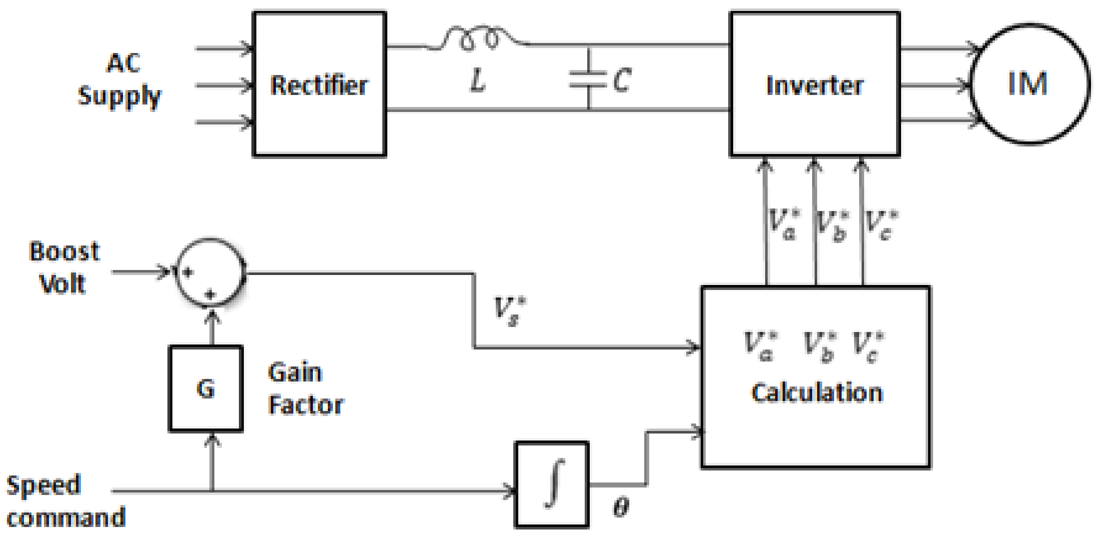

Fig. 3.5 MATLAB/ Simulink model for constant V/f

3.4.2 Indirect Field Oriented Control (IFOC) Method

In IFOC vector control method of induction motor the unit vector is generated in feed forward manner and the dynamics of motor is improved for practical applications, where the flux and torque currents are mutually decoupled so that the motor behaves similar to a separately excited dc motor. Matlab/Simulink model is used for simulation of three phase IM drive system. It consists of inverter, three-phase IM and PI controllers. For analyzing the system performance, all of these components were modeled. The torque command current

(i_{qs}^*) component is generated from the speed controller loop, whereas the current command (i_{ds}^*) is generated from the flux command. For executing the vector control approach, IM line currents are controlled with the help of current controller so as to track the reference voltage commands. The unit vector is generated by integrating the sum of the motor speed and slip frequency. The complete diagram of the drive system is shown in Fig. 3.6.

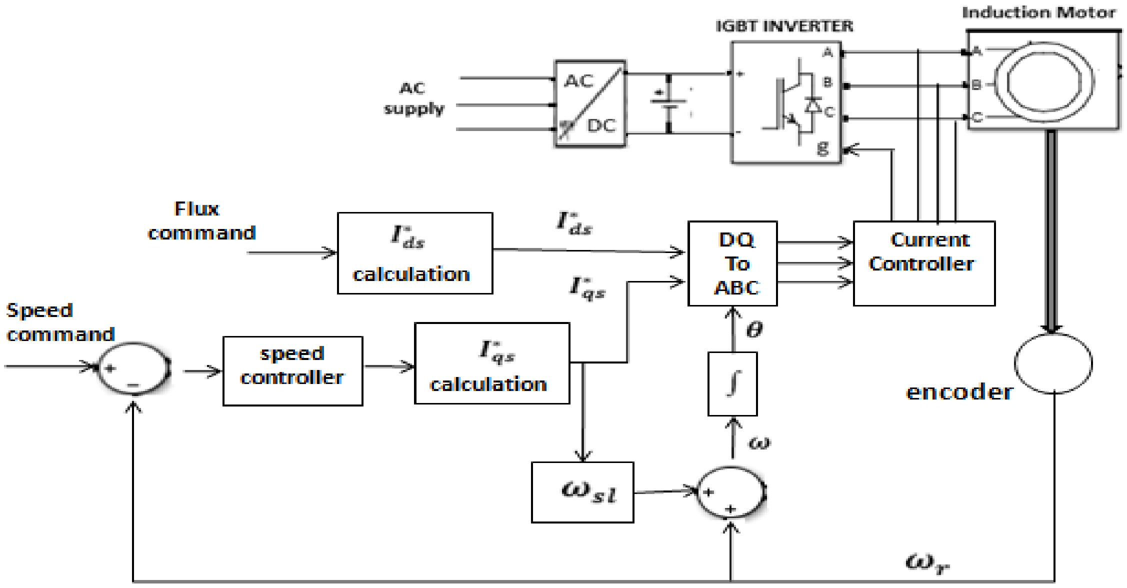

Fig. 3.6 MATLAB/ Simulink model for IFOC

3.5 RESULTS AND DISCUSSION

The simulation of constant V/f speed control and indirect vector control of three phase IM drive is carried out by using both MATLAB/ Simulink model and full spectrum simulator for sudden change in load torque and speed. FSS offline simulation of 50 micro second step sizes was used with simulation start time of zero second and simulation end time of 3 seconds (i.e. 0 to 60000 micro seconds).

3.5.1 Simulation Results of Constant Volts-Hertz (V/f) Method

Simulation of constant V/f IM drive system is carried out and analyzed for a sudden change in load torque and speed in MATLAB/ Simulink and FSS. Fig. 3.7 shows dynamic performance of constant V/f using MATLAB/ Simulink while Fig. 3.8 and Fig. 3.9 show dynamic performance by using FSS for offline and real time simulation respectively. Initially the motor is at rest and started with sudden speed command of 125 rad/sec at t = 0.5 sec and then again changed to zero rad/sec at t = 2 sec. Initially motor draws high starting current to build up the necessary starting torque as shown in the simulated result. But, when motor start tracking of the commanded speed, motor current starts decreasing with the increase of frequency.

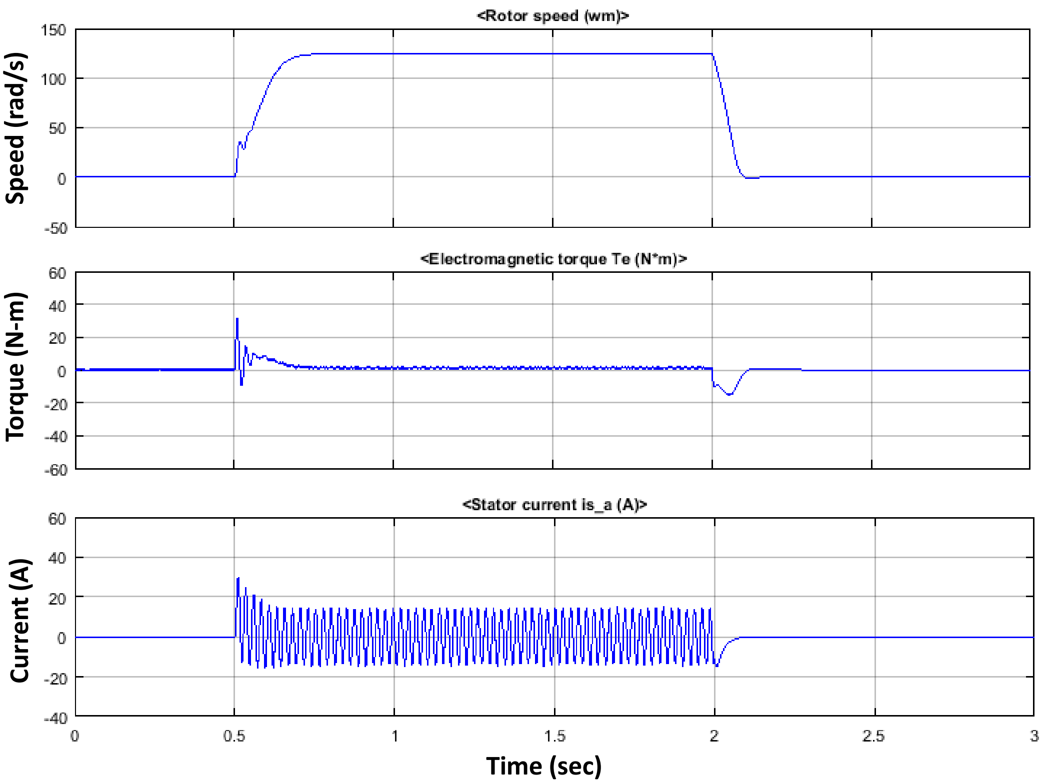

Fig. 3.7 Matlab simulation for speed, torque and current

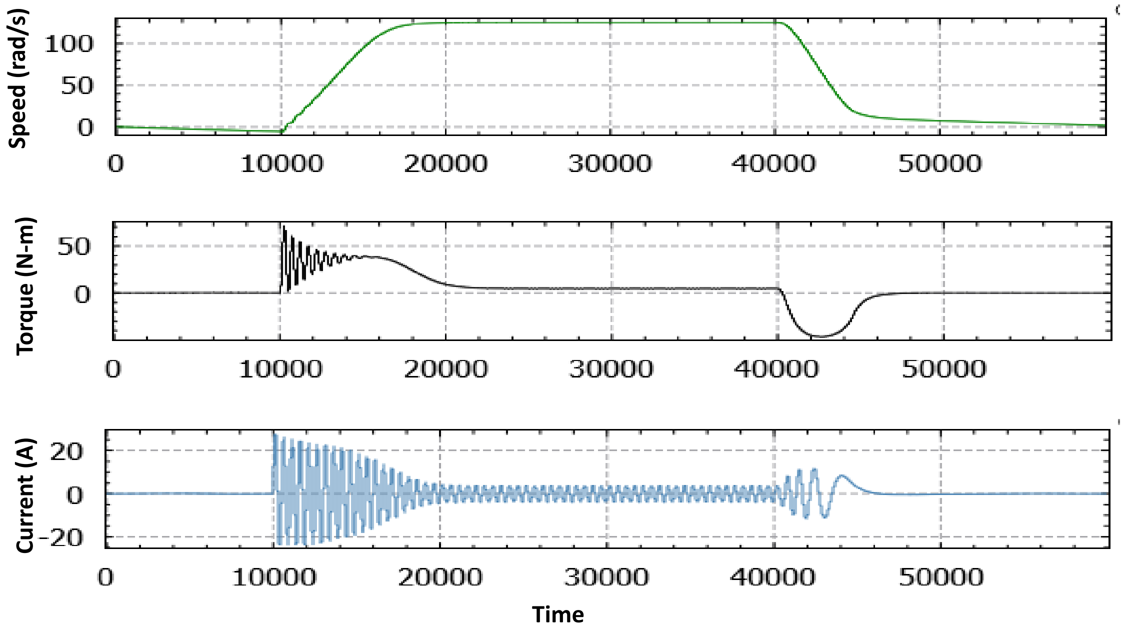

Fig. 3.8 FSS offline simulation for speed, torque and current

Similarly, the torque developed by the motor tracks the commanded value by keeping the proportionate value of the stator current. Small ripples in the developed torque and motor current are observed in simulation due to switching effect in the current controller. Fig. 3.9 (a)-(c) represents the real time simulation results of the IM operation with V/f control.

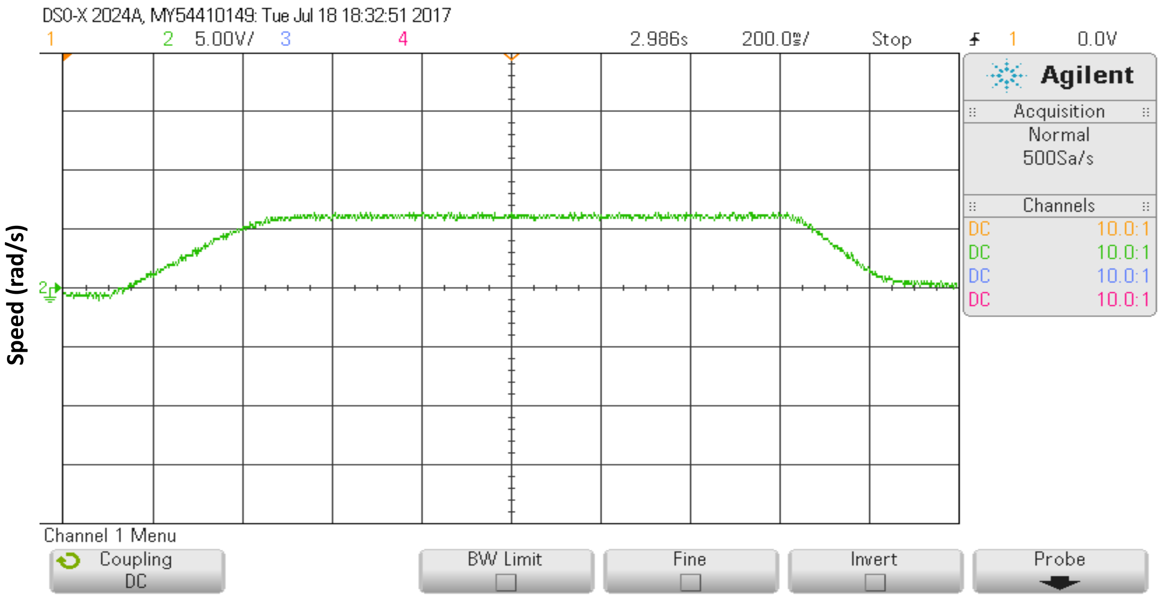

(a) Real time simulation of motor speed

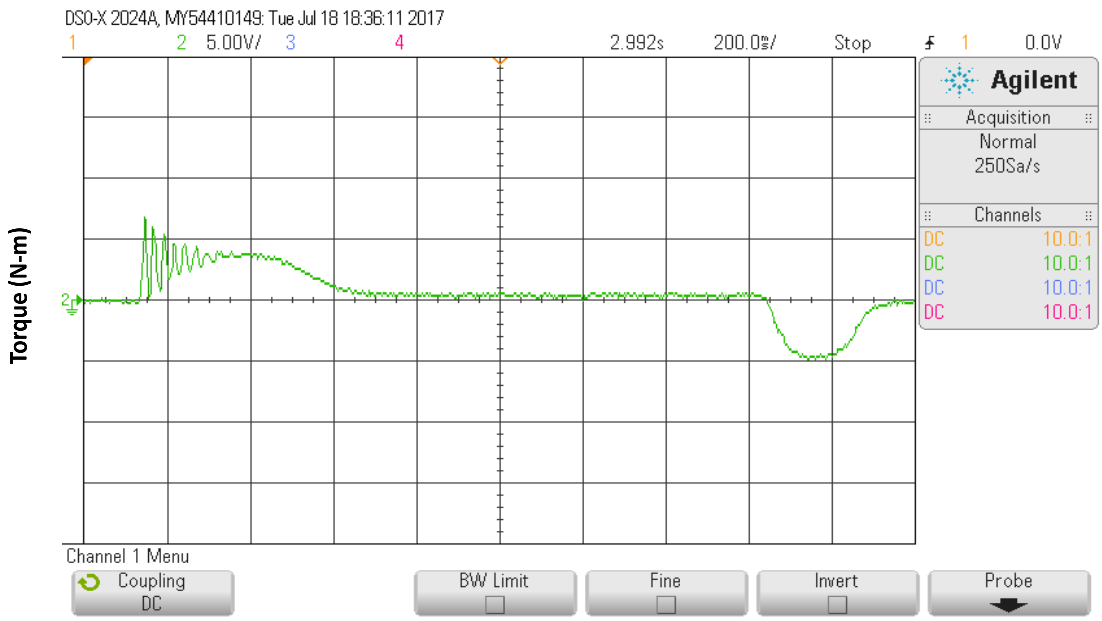

(b) Real time simulation of motor torque

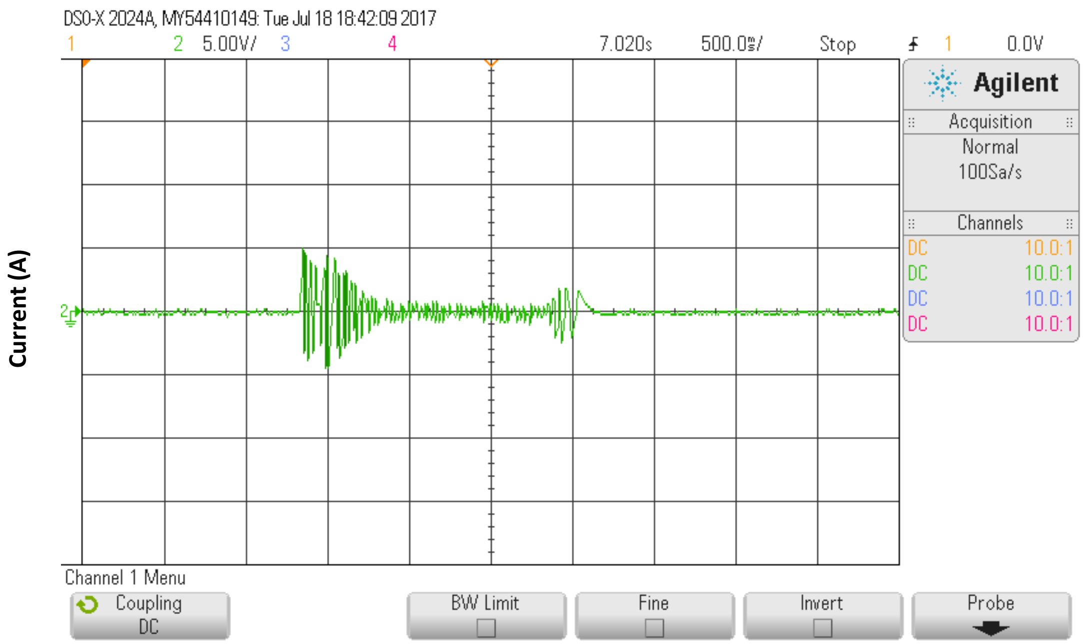

(c) Real time simulation of motor current

Fig. 3.9 FSS real time simulation for (a) speed, (b) torque, (c) current with V/f control

3.5.2 Simulation Results of Indirect Field Oriented Control (IFOC) Method

Simulation of the IFOC IM drive system is carried out in MATLAB/Simulink and FSS under sudden change in speed and torque. Fig. 3.10 represents dynamic performance of indirect FOC using MATLAB simulink. Fig. 3.11 and Fig. 3.12 show dynamic performance of IFOC drive using FSS offline and real time simulation respectively. Initially the motor is at rest and started with sudden speed command of 100 rad/sec at t = 0.5 sec and then again changed to zero rad/sec at t = 2 sec with a load torque of 5 Nm. Initially motor draws high starting current to develop the required starting torque which is shown in the Fig. 3.10. Small ripples in the developed torque and motor current are observed in simulation due to switching effect in the current controller. Fig. 3.12 (a)-(c) shows the real time simulation results of IFOC drive, which are in agreement with the simulated results.

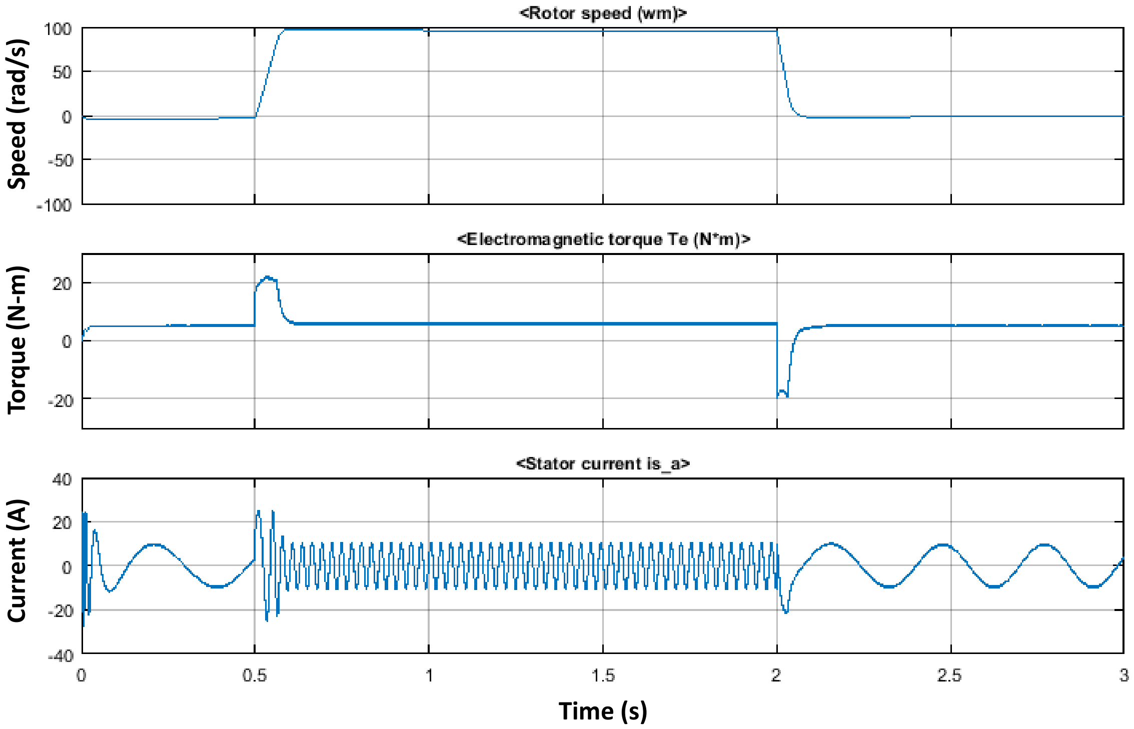

Fig. 3.10 Matlab Simulation for speed, torque and current with IFOC control

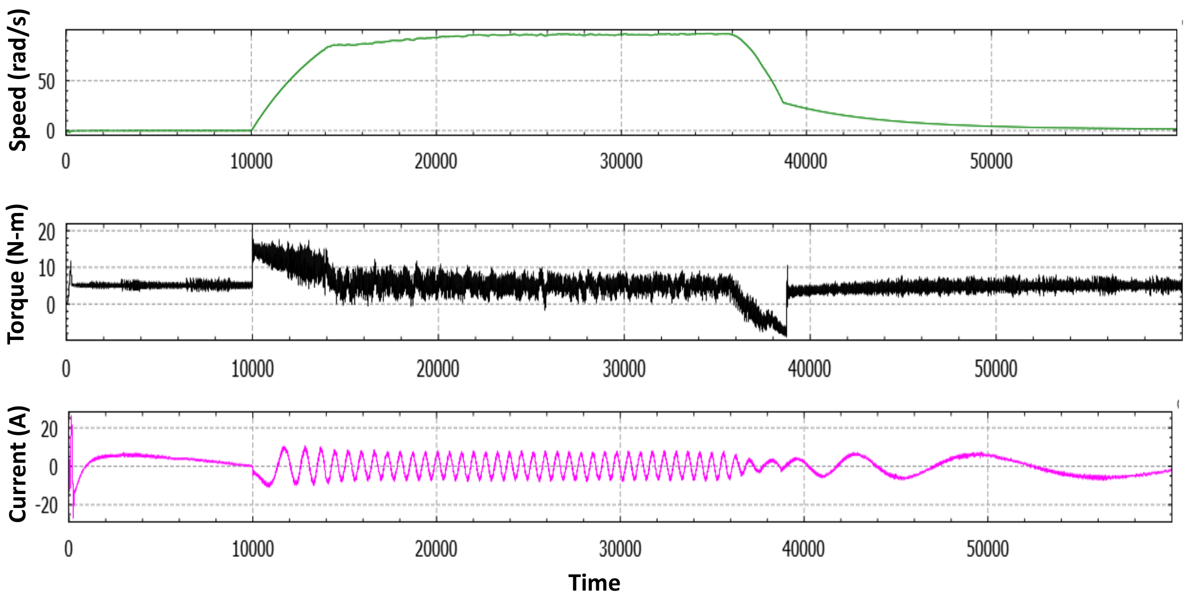

Fig. 3.11 FSS offline Simulation for speed, torque and current with IFOC control

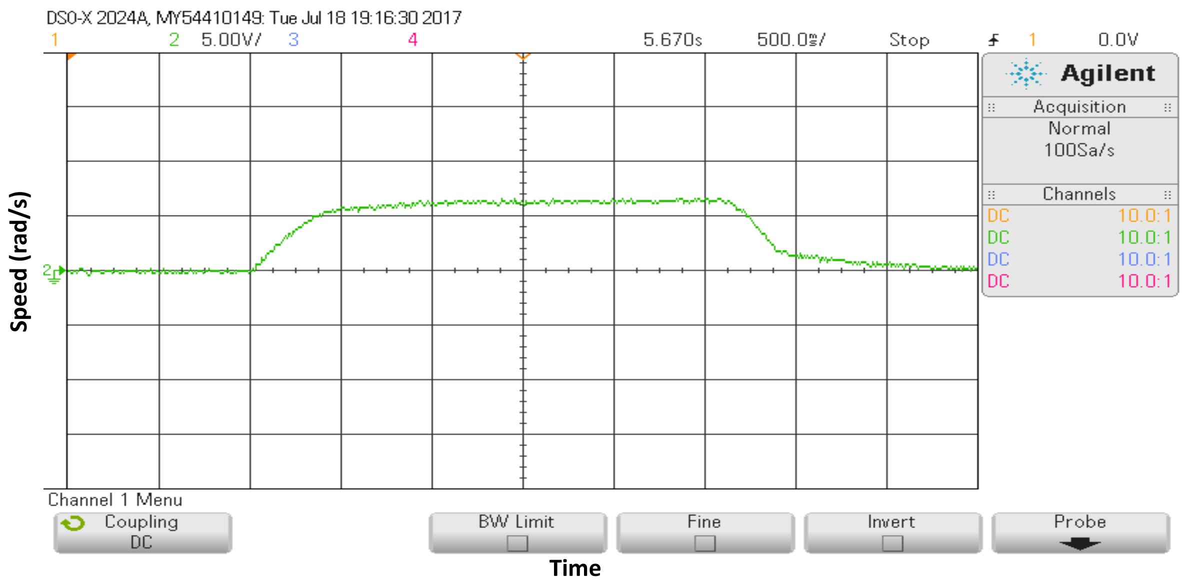

(a) Real time simulation of motor speed

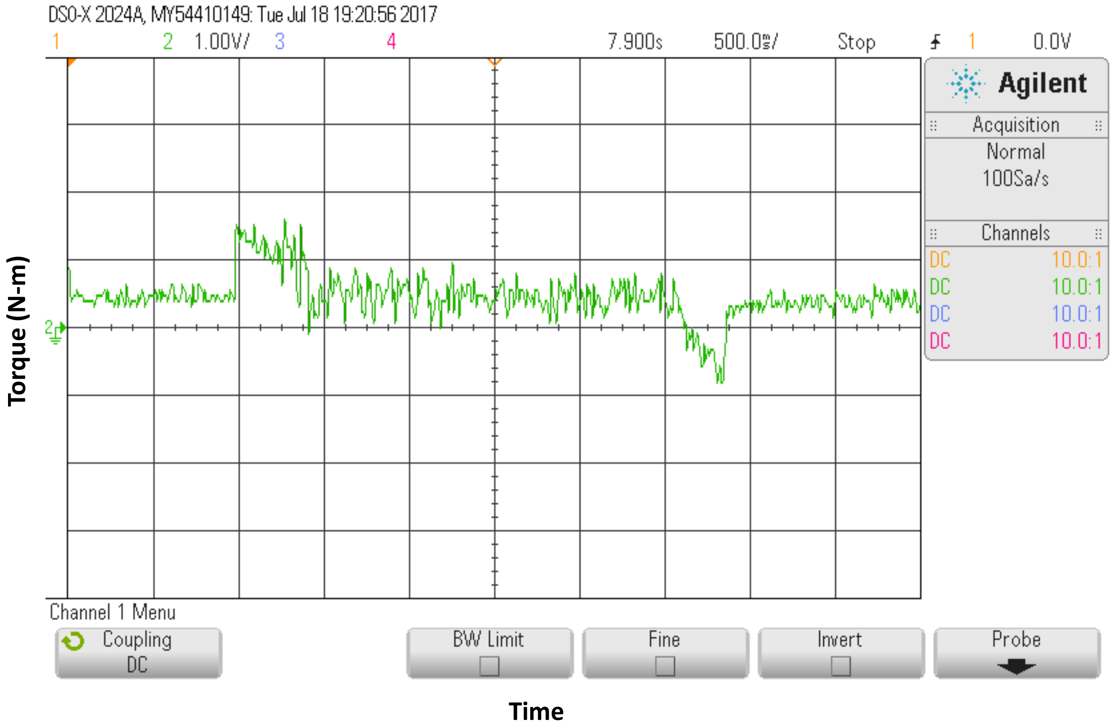

(b) Real time simulation of motor torque

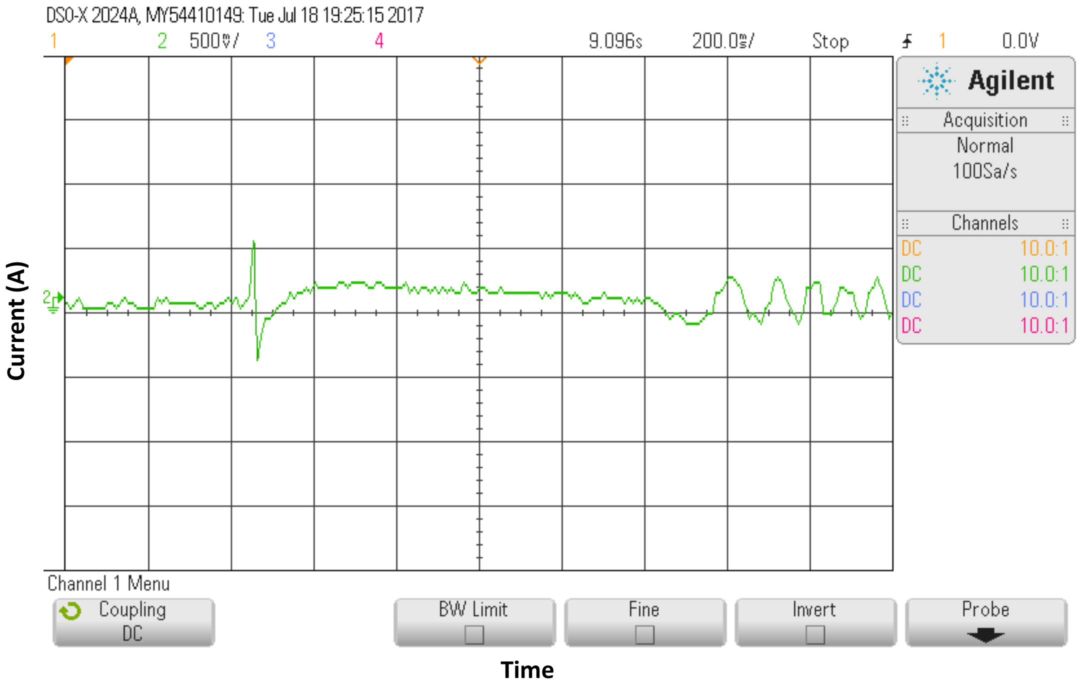

(c) Real time simulation of motor current

Fig. 3.12 FSS real time simulation for (a) speed, (b) torque, (c) current with IFOC control

3.6 CONCLUSION

Offline and online simulation of V/f and IFOC based IM drive is discussed in the MATLAB/ Simulink and FSS. The performance analysis under different speed and load conditions is discussed. Modeling and simulation for V/f and vector control (IFOC) of the IM have been developed by using MATLAB/ Simulink and full spectrum simulator (FSS) to understand the dynamics of induction motor for evaluation. It is observed that drive implementation in MATLAB is much easy as compared to developing system in FSS due to availability of necessary simulation blocks. However, in FSS user can develop system as per their requirements. It allows great flexibility in creating and modifying circuit element, which is very important in developing new system. Also, it is observed that the results obtained using FSS are superior then the result obtained using MATLAB and more close to real time operating conditions. However, the constant V/f method of speed control of the IM especially at low frequency is challenging, because of the stator resistance influence and the required rotor slip to generate torque. But, IFOC control method shows good dynamic response in the drive. Moreover, the apparent comparison of simulation results with MATLAB and FSS offline simulator are in full agreement with the FSS real time simulator.

CHAPTER IV

SENSITIVITY ANALYSIS OF INDUCTION MOTOR PERFORMANCE

4.1 GENERAL

The effect of parametric variations in three phase IM such as rotor resistance, stator resistance, leakage and mutual inductances on the induction motor performance variables such as output power, input power, stator current, magnetizing current, starting current, efficiency, power factor, developed torque and starting torque have been analyzed in this chapter. A nonlinear polynomial equation of the induction motor is derived and solved for finding the slip using computational methods to estimate the realistic value of slip of the induction motor under different load conditions. In operation of the drive system the motor parameters must be matched with actual parameter, otherwise motor performance deteriorates. Sensitivity analysis through computational and mathematical methods is carried out to predict the effect of parametric variations on the motor performance characteristics. The parametric analysis is carried out using the equivalent circuit of the induction motor, with and without core loss resistance. Induction motors are the most generally used and commonly encountered machines in industries due to their simple construction, simple design, low cost and less maintenance. Despite of these advantages, the induction motor also has some inherent drawbacks due to their nonlinear relationship among torque and supply voltage, small air gap, lower power factor and lower efficiency than those of synchronous motors. Control schemes used in AC machines and its variants, combined with the advances in both digital signal processing and power electronic devices has led to the increased use of AC machines in higher performance motor control applications. The control of the asynchronous motor, however, is complex because the dynamic performances of the machine are multivariable, non-linear and highly coupled. Despite of these limitations induction motors are popular in industries [109].

Induction motor parameters fluctuate considerably with operating conditions. The effects of model uncertainties and parameter variation become even more significant with speed sensor less control, calling for sophisticated techniques for the estimation of flux and torque. Therefore the performance of the drive differs from the desired result. Sensitivity analysis for a particular induction motor is carried out to identify the parameters which have the more effect on motor performance characteristic [90]. The induction motor parameters specified by manufacturer possess vagueness because it is based on the parameters for a similar size frame motor. Furthermore, the motor parameters may vary under changing operating conditions like temperature change and magnetic saturation in motor. Hence sensitivity analysis provides important information about variation in motor parameters and their effects on motor performance [85].

In this chapter a sensitivity analysis on a 2.2 kW induction machine is carried out as per the specifications of the motor given in Table 4.1 without considering the core loss equivalent resistance and to identify the parameters which have maximum effect on the performance of the machine. The core losses for the machine are constant when it is fed from a constant frequency, constant voltage source. The performances of motor have been expressed in terms of motor parameters. A similar analysis is carried out for an equivalent circuit by considering core loss equivalent resistance at different load conditions.

4.2 PARAMETERS CALCULATION OF INDUCTION MOTOR

The parameters of the IM as per the specifications of motor given in Table 4.1 are determined. The per phase steady state equivalent circuit of the induction motor when core loss resistance is taken in parallel with the mutual inductance is shown in Fig. 4.1. The equivalent circuit parameters of the motor are defined, where $R1$ is the per phase stator resistance, R_2 is the per phase rotor resistance referred to the stator, X_1 is the leakage reactance of stator, Rc is the core loss equivalent resistance, Xm is the mutual reactance, X_2 is the leakage reactance of rotor referred to the stator, and s is the slip. The blocked rotor test on IM provides the information about leakage impedances and rotor resistance. The no-load test on IM gives information about exciting current and rotational losses. The equivalent circuit parameters were obtained by performing the blocked rotor and no load tests for a 2.2 kW three-phase IM and are given in Table 4.2.

Table 4.1: Ratings of three phase IM

Rated power	Input voltage	Input current	Input frequency	Rated speed	Number of poles
2.2kW	430 V ±10%	4.8A	50 Hz	1430 rpm	4

Table 4.2: IM parameters

Equivalent circuit parameters					
R_1	R_2	Rc	X_1	X_2	Xm
1.33Ω	5.5 Ω	285.5 Ω	5.81 Ω	5.81 Ω	102.4 Ω

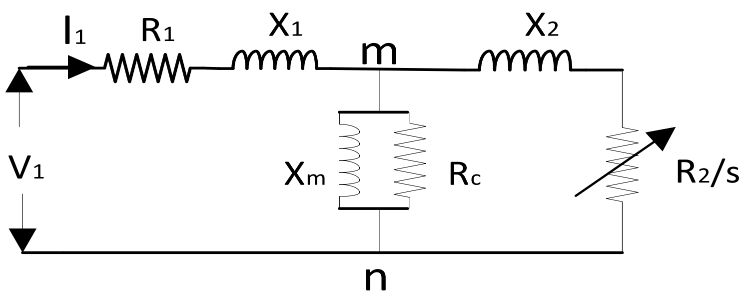

Fig. 4.1 Equivalent circuit of IM with Rc

4.3 PERFORMANCE CHARACTERISTICS OF INDUCTION MOTOR

The performances of three phase induction motor were evaluated by utiltzing the equivalent circuit as shown in Fig. 4.2, where core loss resistance is omitted, initially.

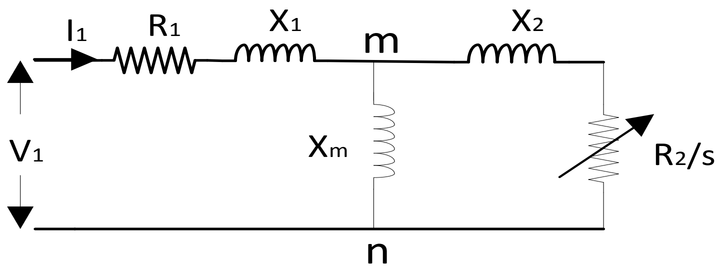

Fig. 4.2 Equivalent circuit of IM

The various performance variables have been represented in terms of the motor equivalent circuit parameters to recognize and analyze the effect of equivalent circuit parameters on these motor performance variables.

Power factor (cos θ) = $\cos\left(\tan^{-1}\frac{X_{mn}+X_1}{R_{mn}+R_1}\right)$ (4.1)

Where R_{mn} and X_{mn} are the resistive and reactive components of the equivalent impedance $Z_{mn} = (R_{mn} + jX_{mn})$ of parallel combination of jX_m and $(R_2/s + j\,X_2)$ across the point m and n in the equivalent circuit

Per phase input power (P_{in}) = $V_1 I_1 \cos\theta$ (4.2)

Where V_1 is the per phase stator voltage and I_1 is the stator current.

The air gap power and constant losses can be used to express the output power as:

Output power (P_{out}) = $P_g - sP_g -$ CL (4.3)

Where CL is the constant losses of the motor and can be obtained from the no-load test.

Stator current (I_1) = $\frac{V_1}{(Z_{mn} + R_1 + \mathrm{j}\,X_1)}$ (4.4)

Magnetizing current, (I_m) = $\frac{I_1\left(\frac{R_2}{s}+jX_2\right)}{R_2/s+j\,(X_2+X_m)}$ (4.5)

Per phase air gap power is given by the relation:

$P_g = I_1^2 R_{mn}$ (4.6)

The torque is given by the expression:

$T = (I_1^2 R_{mn})/\omega$ (4.7)

Where ω is the synchronous speed in radians per second

The starting current and starting torque is obtained from equation (4.4) and equation (4.7) by substituting slip, s = 1.

From equations (4.1) to (4.7), it shows that all the performance variables are induction motor parameters and slip (s) dependent.

4.4 SLIP CALCULATION

The slip of three phase IM depends on load and varies from zero to one. The slip can be expressed from equation (4.3) in term of the applied voltage, output power and motor parameters as below:

$s = 1 - \{(P_{out} + CL)/P_g\}$ (4.8)

Fig. 4.2 of the equivalent circuit of the IM is further simplified and redrawn as shown in Fig. 4.3.

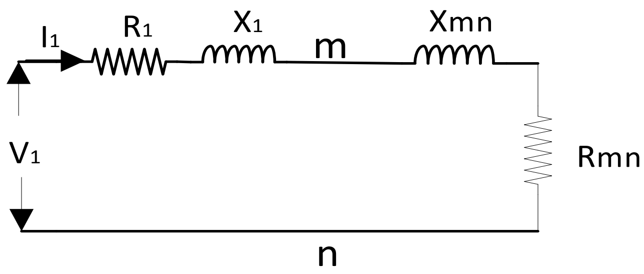

Fig. 4.3 Simplified equivalent circuit of IM

From Fig. 4.2, Z_{mn} is expressed as:

$$Z_{mn} = \frac{j X_m [R_2/s + j X_2]}{(R_2/s + j[X_2 + X_m])} \quad (4.9)$$

OR $$Z_{mn} = \frac{\mathrm{j}\,X_m\ [R_2/\mathrm{s}+\mathrm{j}\,X_2]}{(R_2/\mathrm{s}+\mathrm{j}[X_2+X_m])} * \frac{\left\{\frac{R_2}{\mathrm{s}} - \mathrm{j}[X_2+X_m]\right\}}{\left\{\frac{R_2}{\mathrm{s}} - \mathrm{j}[X_2+X_m]\right\}} \tag{4.10}$$

$$\Rightarrow\ Z_{mn} = \frac{X_m}{\left(\frac{R_2}{s}\right)^2+(X_2+X_m)^2} * \left[X_m\left(\frac{R_2}{s}\right) + j\left\{\left(\frac{R_2}{s}\right)^2 + X_2(X_2+X_m)\right\}\right] \tag{4.11}$$

By segregating the Z_{mn} into its resistive and reactive components, from (4.11)

$$R_{mn} = \frac{X_m^2\left(\frac{R_2}{s}\right)}{\left(\frac{R_2}{s}\right)^2+(X_2+X_m)^2} \tag{4.12}$$

$$X_{mn} = \frac{X_m}{\left(\frac{R_2}{s}\right)^2+(X_2+X_m)^2} * \left\{\left(\frac{R_2}{s}\right)^2 + X_2(X_2+X_m)\right\} \tag{4.13}$$

By substituting (4.3) and (4.6) in (4.8) we get:

$$s = 1 - \left(\frac{P_{out}+\mathrm{CL}}{V_1^2}\right) * \left(\frac{X_m^2\left(\frac{R_2}{s}\right)}{\left(\frac{R_2}{s}\right)^2+(X_2+X_m)^2}\right) + \left(\frac{P_{out}+\mathrm{CL}}{V_1^2}\right) *$$

$$\left\{\left(\frac{X_m}{\left(\frac{R_2}{s}\right)^2+(X_2+X_m)^2} * \left\{\left(\frac{R_2}{s}\right)^2 + X_2(X_2+X_m)\right\}\right)^2 * \left(\frac{\left(\frac{R_2}{s}\right)^2+(X_2+X_m)^2}{X_m^2\left(\frac{R_2}{s}\right)}\right)\right\} \tag{4.14}$$

Rearranging (4.14) in order to get the polynomial equation in terms of the slip we get:

$$(\mathrm{X}_2+\mathrm{X}_\mathrm{m})^2\left\{{V_1}^2R_2+(P_{out}+CL)X_2^2\right\}s^4 - {V_1}^2R_2(\mathrm{X}_2+\mathrm{X}_\mathrm{m})^2s^3 +$$

$$R_2^2\left\{{V_1}^2R_2+(P_{out}+CL)[X_m^2+X_2(X_2+X_m)]\right\}s^2 - V_1^2R_2^3s + (P_{out}+CL)R_2^4 = 0 \tag{4.15}$$

Equation (4.15) can further be represented as:

$$K_1\mathrm{s}^4 - K_2\mathrm{s}^3 + K_3\mathrm{s}^2 - K_4\mathrm{s} + K_5 = 0 \tag{4.16}$$

Where:

$$K_1 = (\mathrm{X}_2+\mathrm{X}_\mathrm{m})^2\left\{{V_1}^2R_2 + (P_{out}+CL)X_2^2\right\} \tag{4.17}$$

$$K_2 = {V_1}^2R_2(\mathrm{X}_2+\mathrm{X}_\mathrm{m})^2 \tag{4.18}$$

$$K_3 = R_2^2\left\{{V_1}^2R_2+(P_{out}+CL)[X_m^2+X_2(X_2+X_m)]\right\} \tag{4.19}$$

$$K_4 = V_1^2R_2^3 \tag{4.20}$$

$$K_5 = (P_{out}+CL)R_2^4 \tag{4.21}$$

The equation (4.16) is solved to determine different roots. During sensitivity analysis the unrealistic values of slip calculated from equation (4.16) are discarded. The value of slip for various loads has been determined and is shown in Table 4.3.

Table 4.3: Slip for various load

Load %age	Slip for various loads		
	s1	s2	s3 & s4
100	0.0780	0.8483	$-0.0000 \pm 0.0508i$
90	0.0701	0.8624	$-0.0000 \pm 0.0508i$
80	0.0625	0.8765	$-0.0000 \pm 0.0508i$
70	0.0550	0.8904	$-0.0000 \pm 0.0508i$
60	0.0476	0.9044	$-0.0000 \pm 0.0508i$
50	0.0404	0.9183	$-0.0000 \pm 0.0508i$
40	0.0333	0.9321	$-0.0000 \pm 0.0508i$
30	0.0263	0.9460	$-0.0000 \pm 0.0508i$
20	0.0194	0.9598	$-0.0000 \pm 0.0508i$
10	0.0127	0.9736	$0.0000 \pm 0.0508i$

4.5 PARAMETER SENSITIVITY ANALYSIS

The parameter sensitivity analysis is given by the expression shown in equation (4.22).

$$S_{\alpha}^{N} = \frac{\text{parameter of analysis } (\alpha)}{\text{performance variable } (N)} * \frac{\partial N}{\partial \alpha} \tag{4.22}$$

In industrial IM drives, requirements related to control, quality and price of drives are important. Hence in order to predict the impact of motor parameters on the performance variables, the sensitivity analysis is utilized by designers of machines. The sensitivity analysis of the performance variables of three phase IM like input power, output power, efficiency, power factor, magnetizing current, starting current, stator current, starting torque and developed torque, with respect to the different parameters of interest are computed and is expressed by the relation as shown in equation (4.23).

$$S_{\alpha}^{N} = \frac{(N_i - N_o)}{N_o} * 100 \tag{4.23}$$

Where N_o is the value of the performance variable with nominal value of the parameter and N_i is the value of the performance variable when the value of the nominal parameter of analysis α is raised by 1% . Similarly the values of slip with variation in rotor resistance (R_2) at different load have been obtained and are shown in Table 4.4.

Table 4.4: Slip at different rotor resistance

Rotor resistance (R2)	Slip Estimation at 100% Load (2200W)		
	s1	s2	s3 & s4
5.5 (100%)	0.0780	0.8483	-0.0000 ± 0.0508i
6.05 (110%)	0.0866	0.8459	0.0000 ± 0.0559i
6.6 (120%)	0.0954	0.8424	-0.0000 ± 0.0610i
7.15 (130%)	0.1044	0.8379	-0.0000 ± 0.0661i
7.7 (140%)	0.1136	0.8326	0.0000 ± 0.0712i
	Slip Estimation at 60% Load (1320W)		
5.5 (100%)	0.0476	0.9044	-0.0000 ± 0.0508i
6.05 (110%)	0.0526	0.9035	0.0000 ± 0.0559i
6.6 (120%)	0.0577	0.9019	0.0000 ± 0.0610i
7.15 (130%)	0.0629	0.8998	0.0000 ± 0.0661i
7.7 (140%)	0.0681	0.8971	0.0000 ± 0.0712i

An increase of rotor resistance causes a rise in slip as shown in table 4.4. Furthermore, the slip increases with increase of load. As a consequence of increase in the slip efficiency decreases and the maximum torque occur at low speed and at high value of slip (s = R_2/X_2 for maximum torque). Therefore by varying the rotor resistance maximum torque can be made at any desired motor speed.

In order to validate the sensitivity analysis carried out using computation (4.23), the mathematical approach using (4.22) was also carried out for stator current (I_1) with respect to stator resistance (R_1) and starting current (I_{st}) with respect to stator resistance (R_1) and with respect to rotor resistance (R_2). The results obtained of both the methods found comparable as shown below:

The sensitivity analysis by using (4.22) for stator current (I_1) with respect to the R_1 is given by the relation:

$$S_{R1}^{I_1} = \frac{R_1}{I_1} * \frac{\partial I_1}{\partial R_1} \tag{4.24}$$

Where stator current (I_1) = $\frac{V_1}{(Z_{mn} + R_1 + \mathrm{j}\, X_1)}$ (4.25)

By putting motor parameter values and stator current (I_1) in (4.24), we get:

$$S_{R_1}^{I_1} = -\frac{R_1(R_{mn} + R_1)}{(R_{mn} + R_1)^2 + (X_1 + X_{mn})^2} = -0.0169 \tag{4.26}$$

The sensitivity analysis by using (4.22) for starting current (I_{st}) with respect to the R_1 is given by the relation:

$$S_{R_1}^{I_{st}} = \frac{R_1}{I_{st}} * \frac{\partial I_{st}}{\partial R_1} \tag{4.27}$$

Where starting current (I_{st}) = $\frac{V_1}{\sqrt{(R_{mn} + R_1)^2 + (X_1 + X_{mn})^2}}$ (4.28)

By putting motor parameter values and starting current (I_{st}) in (4.27), we get:

$$S_{R_1}^{I_{st}} = -\left(R_1 + \frac{R_2 X_m}{X_2 + X_m}\right)\left\{\frac{R_1}{\left(R_1 + \frac{R_2 X_m}{X_2 + X_m}\right)^2 + \left(X_1 + \frac{X_2 X_m}{X_2 + X_m}\right)^2}\right\} = -0.040 \tag{4.29}$$

Sensitivity analysis for the starting current (I_{st}) with respect to R_2 using (4.22) is given by the relation:

$$S_{R_2}^{I_{st}} = \frac{R_2}{I_{st}} * \frac{\partial I_{st}}{\partial R_2} \quad (4.30)$$

By using values of the starting current (I_{st}) and motor parameters in (4.30), we get:

$$S_{R_2}^{I_{st}} = -\frac{R_2 X_m \{R_1(X_2+X_m)+R_2 X_m\}}{\{R_1(X_2+X_m)+R_2 X_m\}^2+\{X_1(X_2+X_m)+X_2 X_m\}^2} = -0.1994134 \quad (4.31)$$

4.6 OBSERVATIONS AND DISCUSSION

The normalized sensitivity of performance variables such as input power, output power, starting current, stator current, magnetizing current, efficiency, power factor, developed torque and starting torque with respect to each equivalent circuit parameters of motor are obtained for full load and at a slip of 0.078 for a 2.2 kW, 430 V, 4-pole, 50 Hz three-phase induction motor. This is achieved by utilizing the equivalent circuit of IM, where core loss resistance is neglected i.e. Ze and also using the equivalent circuit of the induction motor, where the core loss resistance R_c is considered i.e. Zm and is shown in Table 4.5 and is also shown as bar graph in Fig. 4.4.

Table 4.5: Sensitivity index of performance variables

(full load = 2200W, s = 0.0780)

Performance variables/Parameters	Ze/ Zm	R_1	R_2	X_1	X_2	X_m	**V**
Input power (P_{in})	Ze	-0.0066	-0.8477	-0.0620	-0.0145	0.0427	2.0111
	Zm	0.0228	-0.8186	-0.0509	0.0118	0.0753	1.8966
Output power (P_{out})	Ze	-0.0274	-0.9196	-0.0088	-0.0043	0.0339	2.2150
	Zm	0.0022	-0.8890	0.0205	0.0289	0.0798	2.0965
Stator current (I_1)	Ze	-0.0174	-0.6051	-0.0089	0.0256	-0.3133	0.9998
	Zm	-0.0191	-0.5002	-0.0108	0.0280	-0.4121	0.9302
Starting current (I_{st})	Ze	-0.0361	-0.1912	-0.3339	-0.2804	-0.0249	1.0000
	Zm	-0.0359	-0.1915	-0.3387	-0.2695	-0.0320	0.9301
Magnetizing current(I_m)	Ze	-0.0156	0.0223	-0.0071	0.00078	-0.9549	1.0017
	Zm	-0.0180	0.0208	-0.0097	0.00000	-0.9243	0.9313
Power factor (pf)	Ze	0.0079	-0.2469	-0.0560	-0.0430	0.3543	-0.0017
	Zm	0.0078	-0.3541	-0.0743	-0.0503	0.4552	-0.0072
Efficiency (eff)	Ze	-0.0261	-0.0779	0.0479	0.0049	-0.0142	0.1945
	Zm	-0.0339	-0.0842	0.0581	0.0038	-0.0088	0.1829
Torque (T)	Ze	-0.0345	-0.8479	-0.0175	-0.0134	0.0214	2.0100
	Zm	-0.0390	-0.8506	-0.0223	-0.0146	0.0317	1.8683
Starting torque (T_{st})	Ze	-0.0328	-0.3112	-0.0159	-0.0391	-0.5157	2.0117
	Zm	-0.0361	-0.1036	-0.0195	-0.0608	-0.6832	1.8713

.

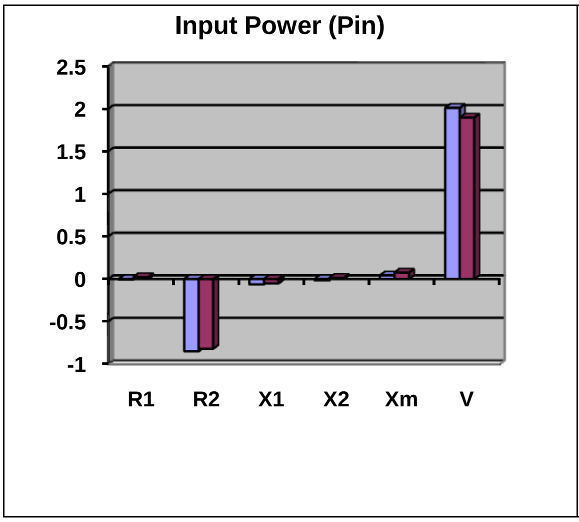
Input Power (Pin)
2.5
2
1.5
1
0.5
0
-0.5
-1
R1
R2
X1
X2
Xm
V

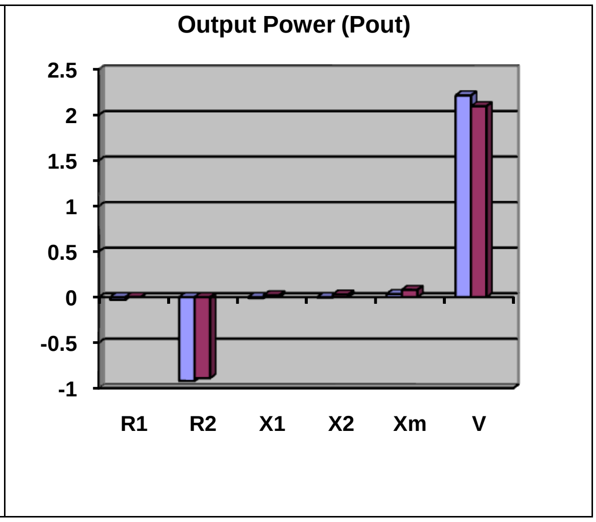
Output Power (Pout)
2.5
2
1.5
1
0.5
0
-0.5
-1
R1
R2
X1
X2
Xm
V

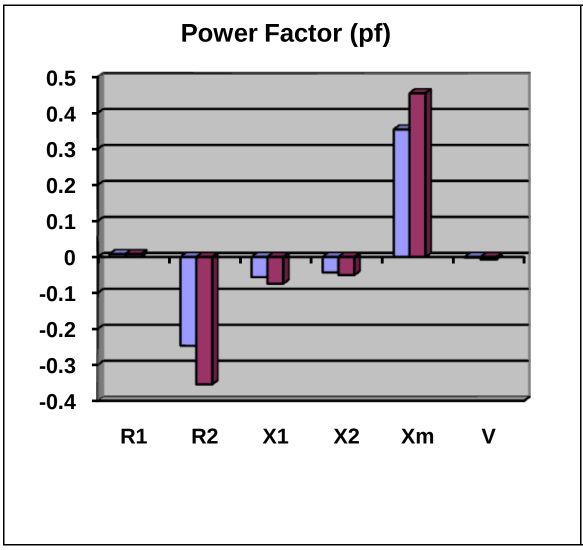
Power Factor (pf)
0.5
0.4
0.3
0.2
0.1
0
-0.1
-0.2
-0.3
-0.4
R1
R2
X1
X2
Xm
V

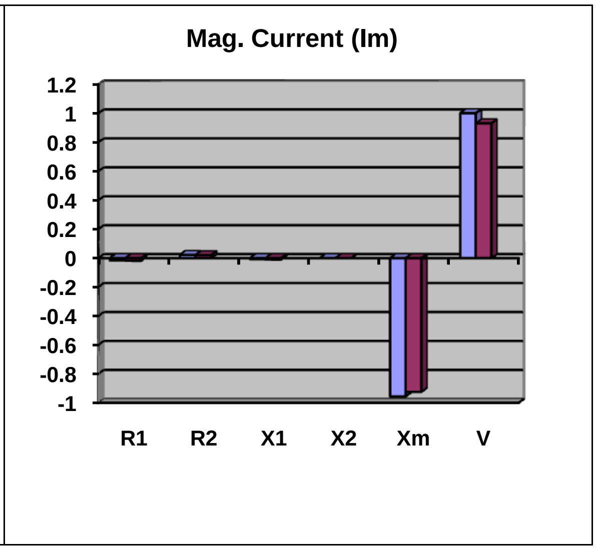
Mag. Current (Im)
1.2
1
0.8
0.6
0.4
0.2
0
-0.2
-0.4
-0.6
-0.8
-1
R1
R2
X1
X2
Xm
V

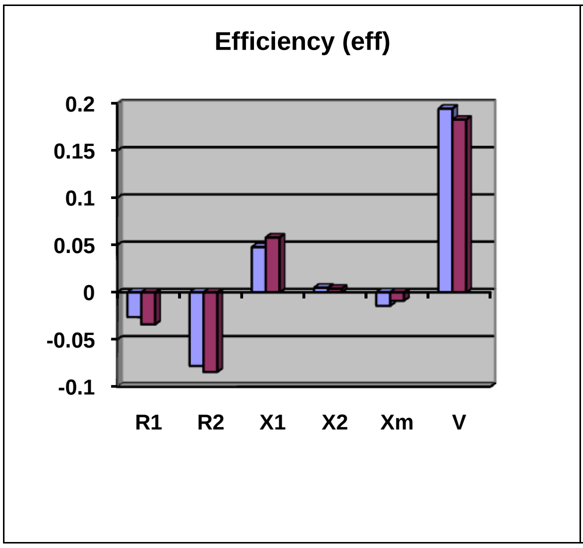
Efficiency (eff)
0.2
0.15
0.1
0.05
0
-0.05
-0.1
R1
R2
X1
X2
Xm
V

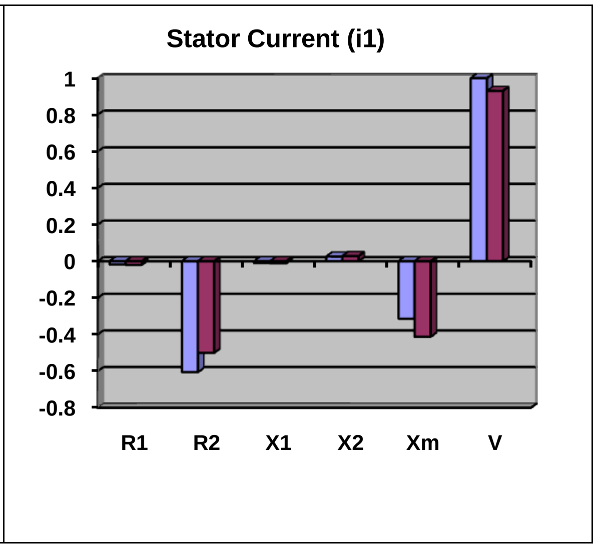
Stator Current (i1)
1
0.8
0.6
0.4
0.2
0
-0.2
-0.4
-0.6
-0.8
R1
R2
X1
X2
Xm
V

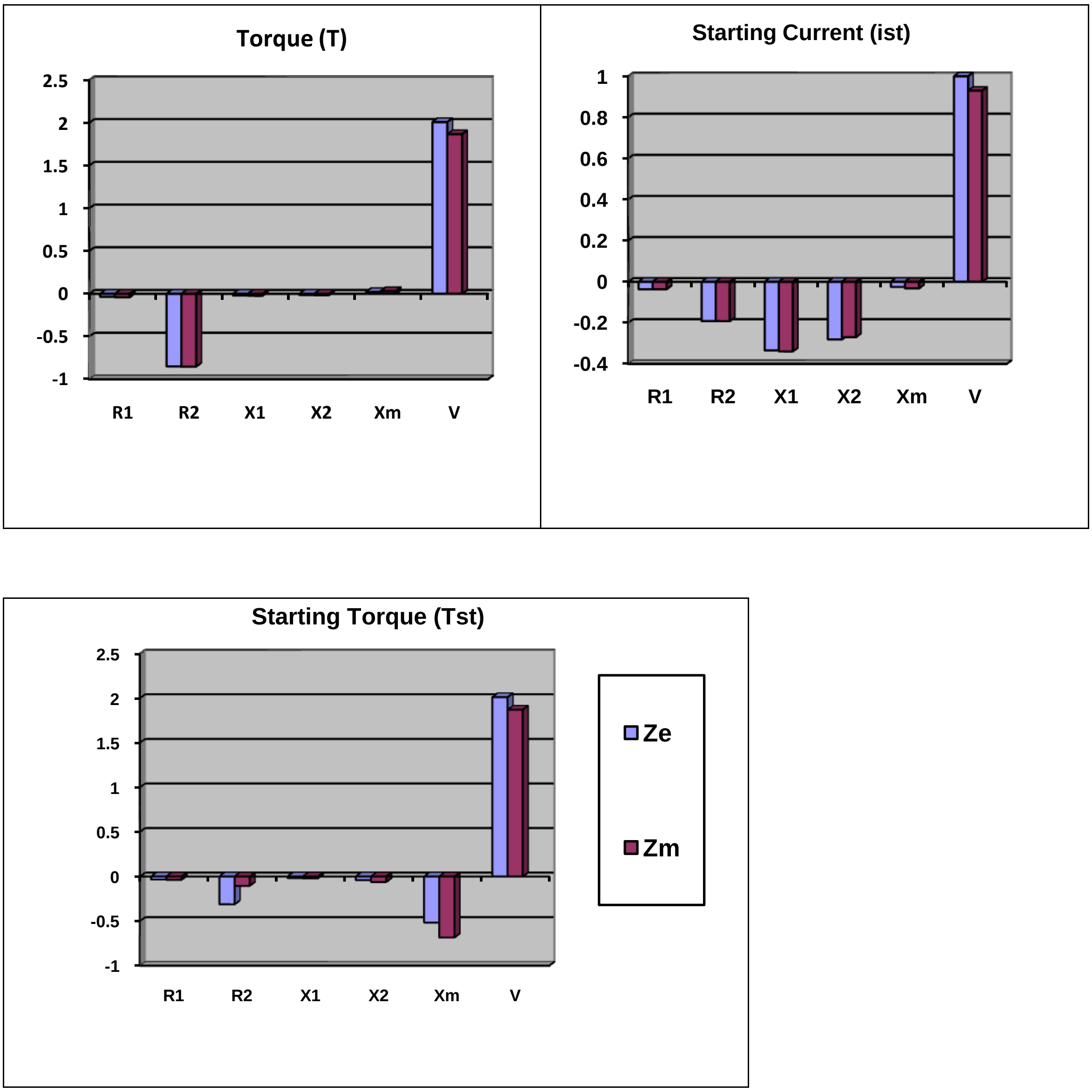

Fig.4.4 Bar graph of performance with full load: P_{in} , P_{out} , pf , I_m , eff, I_1 , T , I_{st} and T_{st}.

Furthermore, the normalized sensitivity are also obtained for 60% (1320W) of load and at a slip of 0.0476 by using the equivalent circuit of induction motor (IM), where core loss resistance is neglected i.e. Ze and also using the equivalent circuit of the induction motor, where the core loss resistance R_c is considered i.e. Zm and is shown in Table 4.6 and is also shown as bar graph in Fig. 4.5.

Table 4.6 Sensitivity index of performance variables

(60% load = 1320W, s = 0.0476)

Performance variables/Parameters	Ze/ Zm	R_1	R_2	X_1	X_2	X_m	**V**
Input power (P_{in})	Ze	-0.0033	-0.8727	-0.0566	-0.0083	0.0318	2.0073
	Zm	-0.0080	-0.8754	-0.0820	-0.0183	0.0218	1.8559
Output power (P_{out})	Ze	-0.0229	-1.0093	-0.0042	0.0013	0.0363	2.3368
	Zm	-0.0043	-0.9891	0.0152	0.0251	0.0737	2.2011
Stator current (I_1)	Ze	-0.0123	-0.4073	-0.0042	0.0197	-0.5253	1.0008
	Zm	-0.0147	-0.2974	-0.0063	0.0185	-0.6205	0.9309
Starting current (I_{st})	Ze	-0.0361	-0.1912	-0.3339	-0.2804	-0.0249	1.0000
	Zm	-0.0311	-0.1866	-0.3338	-0.2647	-0.0704	0.8914
Magnetizing current(I_m)	Ze	-0.0137	0.0090	-0.0056	-0.0011	-0.9554	0.9994
	Zm	-0.0164	0.0077	-0.0079	-0.0014	-0.9243	0.9293
Power factor (pf)	Ze	0.0111	-0.4652	-0.0502	-0.0258	0.5622	-0.0013
	Zm	0.0262	-0.5605	-0.0563	-0.0173	0.6659	0.0058
Efficiency (eff)	Ze	-0.0296	-0.1478	0.0423	−0.0052	-0.0057	0.3130
	Zm	-0.0408	-0.1590	0.0529	-0.0010	0.0074	0.2944
Torque (T)	Ze	-0.0248	-0.8760	-0.0087	-0.0040	0.0262	2.0113
	Zm	-0.0296	-0.8779	-0.0127	-0.0042	0.0377	1.8704
Starting torque (T_{st})	Ze	-0.0140	0.0946	0.0021	-0.0422	-0.9299	2.0223
	Zm	-0.0226	0.3089	-0.0057	-0.0750	-1.0936	1.8775

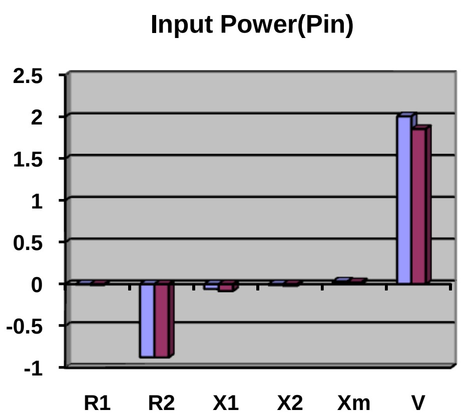
Input Power(Pin)
2.5
2
1.5
1
0.5
0
-0.5
-1
R1
R2
X1
X2
Xm
V

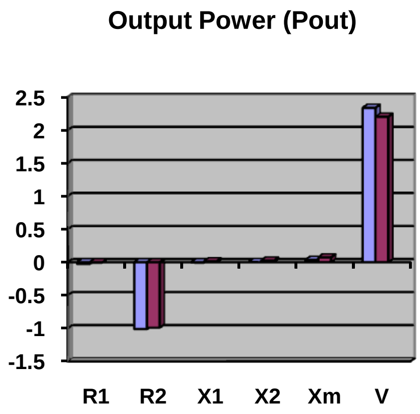
Output Power (Pout)
2.5
2
1.5
1
0.5
0
-0.5
-1
-1.5
R1
R2
X1
X2
Xm
V

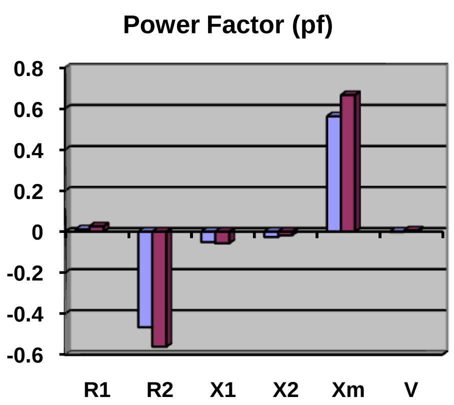
Power Factor (pf)
0.8
0.6
0.4
0.2
0
-0.2
-0.4
-0.6
R1
R2
X1
X2
Xm
V

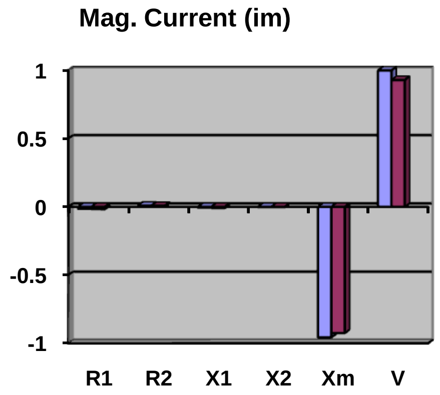
Mag. Current (im)
1
0.5
0
-0.5
-1
R1
R2
X1
X2
Xm
V

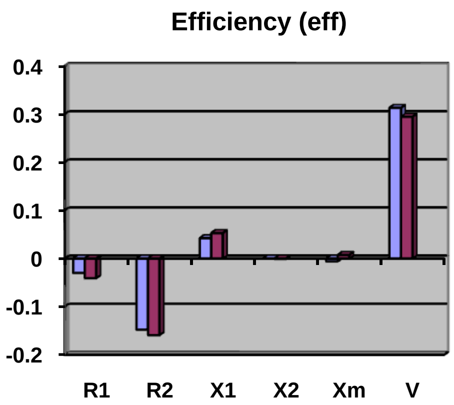
Efficiency (eff)
0.4
0.3
0.2
0.1
0
-0.1
-0.2
R1
R2
X1
X2
Xm
V

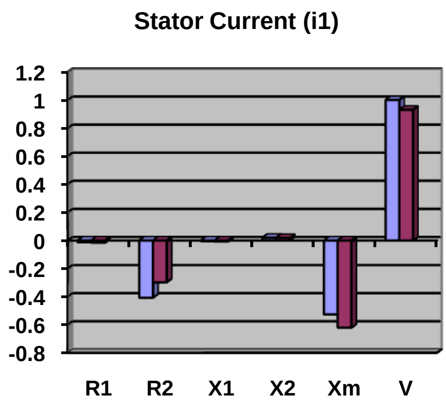
Stator Current (i1)
1.2
1
0.8
0.6
0.4
0.2
0
-0.2
-0.4
-0.6
-0.8
R1
R2
X1
X2
Xm
V

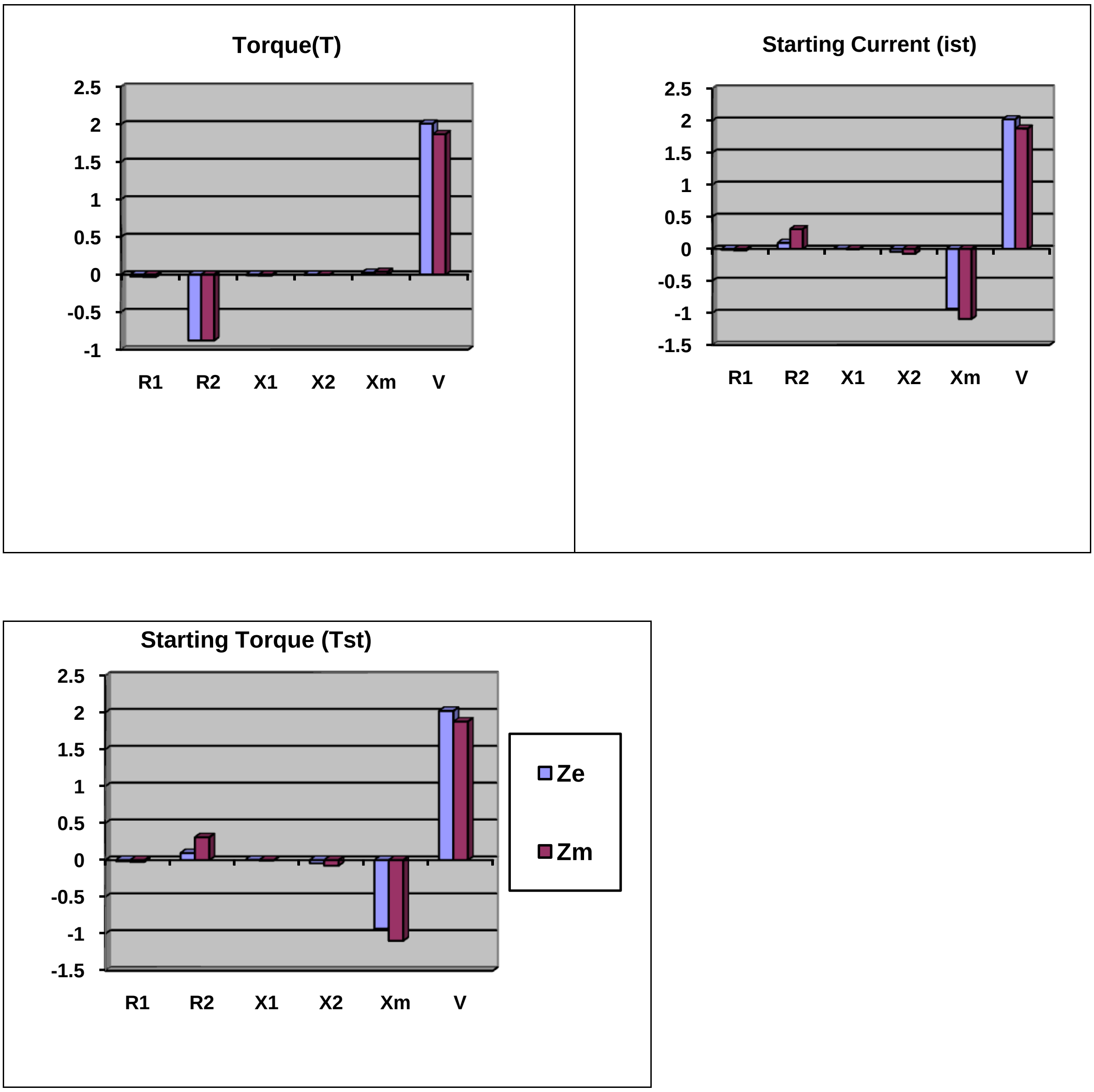

Fig. 4.5 Bar graph of performance with 60% load: P_{in} , P_{out} , pf , I_m , eff, I_1 , T , I_{st} and T_{st}.

In addition, a comparative study is carried out on variation in equivalent circuit parameters and their effect on motor performance variables using an equivalent circuit with and without core loss resistance.

4.7 SENSITIVITY ANALYSIS OF MOTOR PERFORMANCES

By considering table 4.5 and table 4.6 it is seen that the supply voltage variation has considerable effect on almost all performance variables except on power factor where it has least effect. The effect of supply voltage on efficiency of motor is more at lower load (60% of load) in comparison to the full load. The effect of supply voltage variation is more on the efficiency if the core loss resistance (Rc) is not considered. However the power factor of motor is not much affected by voltage variation. The motor performances like input power, output power, starting torque and developed torque are highly sensitive to supply voltage variation at all load conditions and the effect on these performance variables is more if the core loss resistance (Rc) is not considered. The performance variables like stator current, magnetizing current and starting current are moderately sensitive with respect to voltage at all load conditions and the effect on these variables are more if the core loss resistance (Rc) is not considered i.e. Ze.

Furthermore, apart from the variation of supply voltage the effect of other parameters on performance are also considered. The sensitivity of the input power and output power with respect to rotor resistance R_2 is highest while it is lowest with respect to rotor reactance X_2 and R_1. The motor efficiency and power factor are less sensitive to the motor equivalent circuit parameters however the rotor resistance R_2 and mutual reactance X_m variations have maximum affect on the power factor and R_2 and X_1 variations have maximum affect on the efficiency compared to the other motor parameters. The stator current sensitivity with respect to rotor resistance R_2 is maximum and it further increases with increase of load. Similarly the stator current sensitivity with respect to mutual reactance X_m is high and it further increases with decrease of load and slightly affected by other parameters. The starting current sensitivity with respect to X_2 and X_1 is maximum and with respect to X_m is minimum. The magnetizing current sensitivity with respect to X_m is maximum and slightly affected by other parameters. The developed torque is affected maximum by R_2 and slightly affected by other parameters. The starting torque is affected maximum by X_m, moderately by R_2 and slightly affected by other parameters.

From the above observation it is clear that R_2 and X_m are the two parameters of motor, which have maximum impact on the performances of motor. It is further observed that R_2 as compared to any other motor parameters affects performance variables P_{in}, P_{out}, T and T_{st} the most for every load conditions and stator current I_1 at full load condition only. Similarly X_m in comparison to any other motor parameters affects power factor the most for every load conditions. It is also observed that the effects of parameters on motor performances are different while using the equivalent circuit with and without core loss resistance as shown in bar graph of Fig. 4.4 and Fig. 4.5.

4.8 STABILITY ANALYSIS

The state space model of the induction motor gives us the possibility to develop and analyse different control strategies for the induction motor for control purposes. Hence the mathematical description of the induction motor is developed through the state space approach.

By considering the d-axis and the q-axis equivalent circuit of the induction motor, as shown in Fig. 3.4, the following voltage equations can be written:

$$v_{qs} = R_1 i_{qs} + \frac{\partial \varphi_{qs}}{\partial t} + \omega \varphi_{ds} \tag{4.32}$$

$$v_{ds} = R_1 i_{ds} + \frac{\partial \varphi_{ds}}{\partial t} - \omega \varphi_{qs} \tag{4.33}$$

$$v_{qr} = R_2 i_{qr} + \frac{\partial \varphi_{qr}}{\partial t} + (\omega - \omega_r) \varphi_{dr} \tag{4.34}$$

$$v_{dr} = R_2 i_{dr} + \frac{\partial \varphi_{dr}}{\partial t} - (\omega - \omega_r) \varphi_{qr} \tag{4.35}$$

The time derivative of the fluxes from the above voltage equations can be evaluated and written in state space form as:

$$\begin{bmatrix} \frac{\partial}{\partial t}\varphi_{qs} \\ \frac{\partial}{\partial t}\varphi_{ds} \\ \frac{\partial}{\partial t}\varphi_{qr} \\ \frac{\partial}{\partial t}\varphi_{dr} \end{bmatrix} = \begin{bmatrix} \frac{-R_1}{L_s - \frac{L_m{}^2}{L_r}} & -\omega & \frac{R_1 * L_m}{L_r\left(L_s - \frac{L_m{}^2}{L_r}\right)} & 0 \\ \omega & \frac{-R_1}{L_s - \frac{L_m{}^2}{L_r}} & 0 & \frac{R_1 * L_m}{L_r\left(L_s - \frac{L_m{}^2}{L_r}\right)} \\ \frac{-R_2}{L_m - \frac{L_r * L_s}{L_m}} & 0 & \frac{R_2 * L_s}{L_m\left(L_m - \frac{L_r * L_s}{L_m}\right)} & -\omega + \omega_r \\ 0 & \frac{-R_2}{L_m - \frac{L_r * L_s}{L_m}} & \omega - \omega_r & \frac{R_2 * L_s}{L_m\left(L_m - \frac{L_r * L_s}{L_m}\right)} \end{bmatrix} \begin{bmatrix} \varphi_{qs} \\ \varphi_{ds} \\ \varphi_{qr} \\ \varphi_{dr} \end{bmatrix} + \begin{bmatrix} v_{qs} \\ v_{ds} \\ v_{qr} \\ v_{dr} \end{bmatrix} \quad (4.36)$$

This is equivalent to the general form of state equation: $\frac{d(x)}{dt} = Ax + Bu$

The local stability can be analysed by calculating the eigen values of the system. The state equations can be used to find the eigen values directly without converting the state equation into transfer function.

By using the parameters of IM shown in table 4.1 and 4.2, the numerical values of the matrix A represented by nonlinear state equation (4.36) is as follows:

$$A = \begin{bmatrix} -36.7400 & -50.0000 & 34.7680 & 0 \\ 50.0000 & -36.7400 & 0 & 34.7680 \\ 144.7360 & 0 & -152.9470 & -2.0000 \\ 0 & 144.7360 & 2.0000 & -152.9470 \end{bmatrix} \quad (4.37)$$

The eigen values of matrix A ($\det|\lambda I - A| = 0$) obtained are as follows:

$$\lambda_{1,2} = -4.99 \pm 41.52i$$

$$\lambda_{3,4} = -184.69 \pm 10.48i$$

It is clear that the real parts of the eigen values obtained are negative which shows that the roots of the system are located in the left hand side of the s-plane. Therefore the system is stable about the given operating point.

Furthermore, the rotor resistance of the motor if increased by 50 percent, the numerical values of the matrix A is as follows:

$$A=\begin{bmatrix}-36.7400 & -50.0000 & 34.7680 & 0\\ 50.0000 & -36.7400 & 0 & 34.7680\\ 217.1040 & 0 & -229.4205 & -2.0000\\ 0 & 217.1040 & 2.0000 & -229.4205\end{bmatrix} \quad (4.38)$$

The eigen values of matrix A ($\det|\lambda I - A| = 0$) obtained are:

$$\lambda_{1,2} = -4.33 \pm 43.96i$$

$$\lambda_{3,4} = -261.83 \pm 8.04i$$

This shows that the roots of closed loop poles lie in the left side of the s-plane and the system is stable. Similarly, the stability can be checked with variation in other parameters of the matrix A.

4.9 CONCLUSION

Sensitivity computational function and analytical methods were used to find out the sensitivity analysis of the performance variables like efficiency, input power, output power, power factor, stator current, starting current, magnetizing current, starting torque and developed torque of induction motor with respect to parameters of the induction motor. This is achieved by using the equivalent circuit of induction motor (IM), where core loss resistance is neglected and also using the equivalent circuit of the induction motor, where the core loss resistance is taken. From the sensitivity analysis it is observed that how the different parameters of the induction motor affects the performance of the IM and a good general picture of the induction motor behaviour was achieved. With the help of this sensitivity analysis, the engineers can choose and change the physical parameters of the motor to obtain a better efficiency, robustness and reliability. Hence the design engineer can optimize the design of the IM. The simple nonlinear state equation of an induction motor has been used to find out the stability of the system and it has been found that the model is locally asymptotically stable with regards to an operating state.

CHAPTER V

SPEED AND STATOR RESISTANCE ESTIMATION OF SPEED SENSORLESS IM DRIVE

5.1 GENERAL

This chapter presents speed and stator resistance estimation for speed sensorless vector controlled IM drive. The effectiveness of sensorless vector controlled drives depends on the correct information of the motor parameters such as stator and rotor resistances, which usually vary with working conditions of the motor. An accurate estimation of stator resistance is important for the proper estimation of the flux, speed and torque in the sensorless IM drive. Therefore, the flux estimation in IM drive is prone to incorrect due to variation in stator resistance especially at low frequency region. Stator resistance and motor speed estimation methods based on model reference adaptive control (MRAS) system in a sensorless IM drive is discussed in details. The proposed algorithm utilizes the measured stator currents and voltages for the estimation of speed and stator resistance so as to reduce the computational complexities. Adaptive mechanism for stator resistance estimation utilizes adaptive neuro-fuzzy inference system and the estimated stator resistance is used for building the motor speed estimation system independent of stator resistance. Moreover, the stability analysis of the drive using frequency domain method is carried out over a broad range of stator resistance variation. The proposed algorithm is simulated for IFOC IM drive in MATLAB environment and the results obtained are analyzed for different operating conditions.

The induction motor (IM) parameters are used for high precision motor control drive system. The parameters vary considerably with operating conditions. Therefore the result of the drive deteriorates during working conditions. It becomes necessary for the controller to adopt stator resistance value of the motor for accurate estimation and control of the motor speed [67]. Currently sensorless vector controlled drive is popular and commercially accessible, but the parameter variation creates difficulty for speed estimation accuracy [99].

In the literature numerous speed estimation methods have been proposed. Some of these like machine model-based methods, voltage/current model, speed estimation using model reference adaptive system and adaptive observer are very popular [100]. These methods are not very sensitive to motor parameters and perform well even at low and zero speed operation. There are other types of speed estimation methods available in literature such as slip control, state equations, flux observer, artificial intelligence, EKF, slot harmonics, reactive power and neural adaptive system etc.

The methods based on artificial intelligence such as adaptive neuro-fuzzy inference system (ANFIS) and artificial neural networks (ANN) are commonly used for estimation of speed. Model reference adaptive system has drawn a lot of attention for parameter estimation because MRAS is easy to implement, it needs less computation and shows good stability. Different MRASs based on flux, torque, reactive power and back electromotive force are projected in literatures [106] for speed estimation and have shown acceptable performance. Flux and Back-emf based MRAS estimate motor speed efficiently but the flux based method suffers from integrator problem and back emf based method suffers from low back-emf related problems at very low rotor speed operation. These problems of low speed operation can be conquered by using reactive power based model reference adaptive system but it suffers from stability related problems when operating in the regenerative mode. Hence, X-MRAS can be used to overcome this stability linked problem by using the steady state and instantaneous values of the stator voltage and current vectors [111],[112].

In the present chapter, X-MRAS is used for speed estimation. However, this depends on stator resistance which is compensated by another MRAS used for stator resistance estimation. On-line stator resistance estimation by utilizing ANFIS controller is used, where stator resistance is updated through an adaptive mechanism each time for estimation of the speed. The small signal stability analysis with large deviation of stator resistance is done by linearizing the motor equations around the stable operating point.

5.2 IMPLEMENTATION OF ANFIS CONTROLLER

Artificial intelligence based controllers like genetic algorithm, neural network, fuzzy logic, etc. are being used to control the high precision drive systems. ANFIS is a hybrid neuro fuzzy system which contains the advantages of fuzzy logic controller along with the artificial neural network. It is a more powerful intelligent system for getting the improved performance and design features, where a neural network designs the fuzzy system by determining the rules and membership functions of the fuzzy system. ANN is based on the biological nervous system of human brain whereas fuzzy logic is based on knowledge of the system and human intelligence.

ANFIS designs the fuzzy inference system (FIS) systematically with the help of neural network design method. This designs the rules and membership functions of the fuzzy model by training of neural network from the desired input and output data available for a fuzzy system. The ANFIS structure is shown in Fig. 5.1, where it generates output corresponding to the inputs. It is divided into five layer system where the first layer shows inputs to the system, second layer shows the input membership functions of the fuzzy system, next layer shows the rules of the fuzzy inference system, further next layer shows output membership function and the fifth layer shows the output.

The training error generated during ANFIS training to the workspace is shown in Fig. 5.2. The error signal generated is used to train the FIS and updates the weights by back propagation algorithm to minimize the error. Five membership functions were used for input and output data set in the fuzzy system. The trained FIS so obtained is used for the sensorless drive system.The estimated value of stator resistance by using the PI and ANFIS controller is shown in Fig. 5.3. It is observed that ANFIS controller gives a lower rise time (0.05 sec) and a smooth steady state value of stator resistance because it contains epoches and training. Training repeats until the minimum error is reached [11],[12].

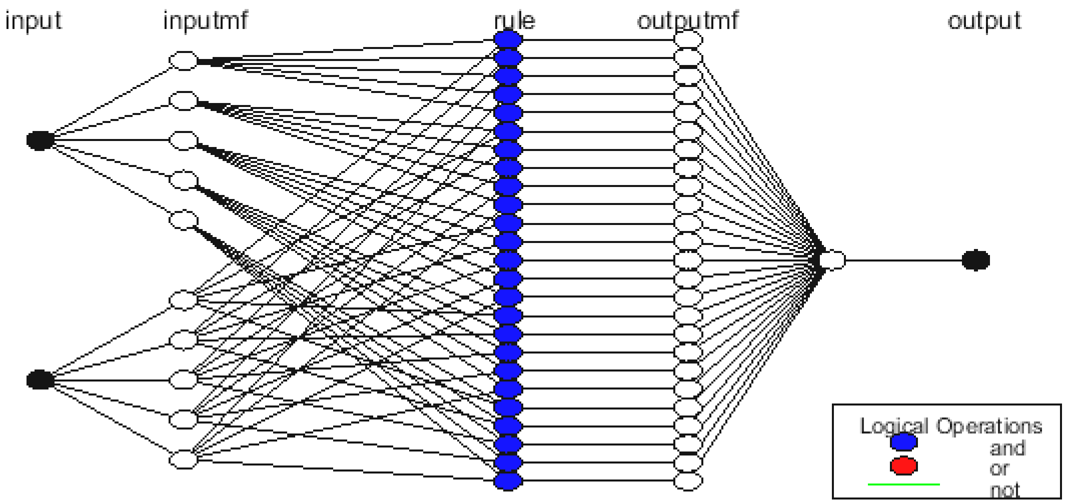

Fig. 5.1 ANFIS structure

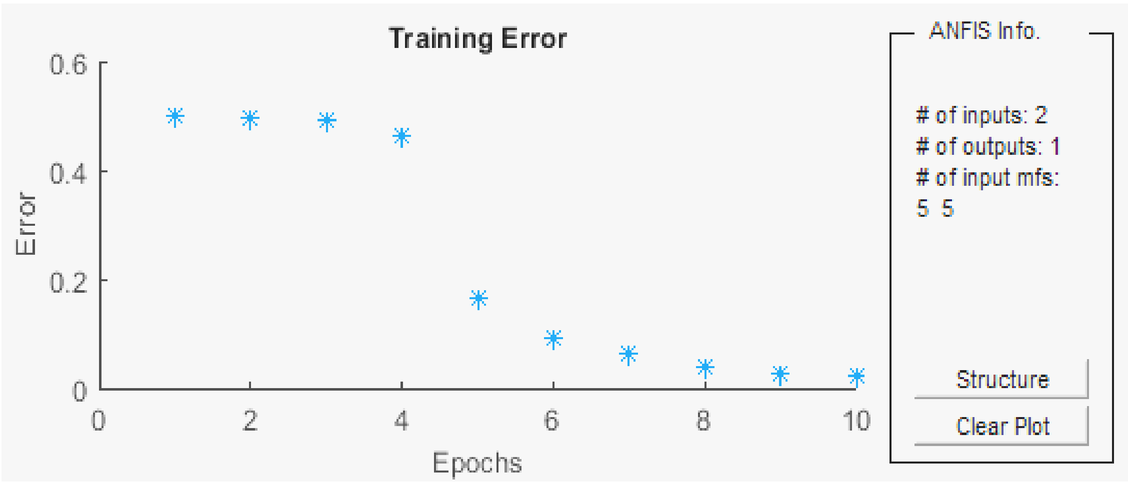

Fig. 5.2 Training error variations with epochs

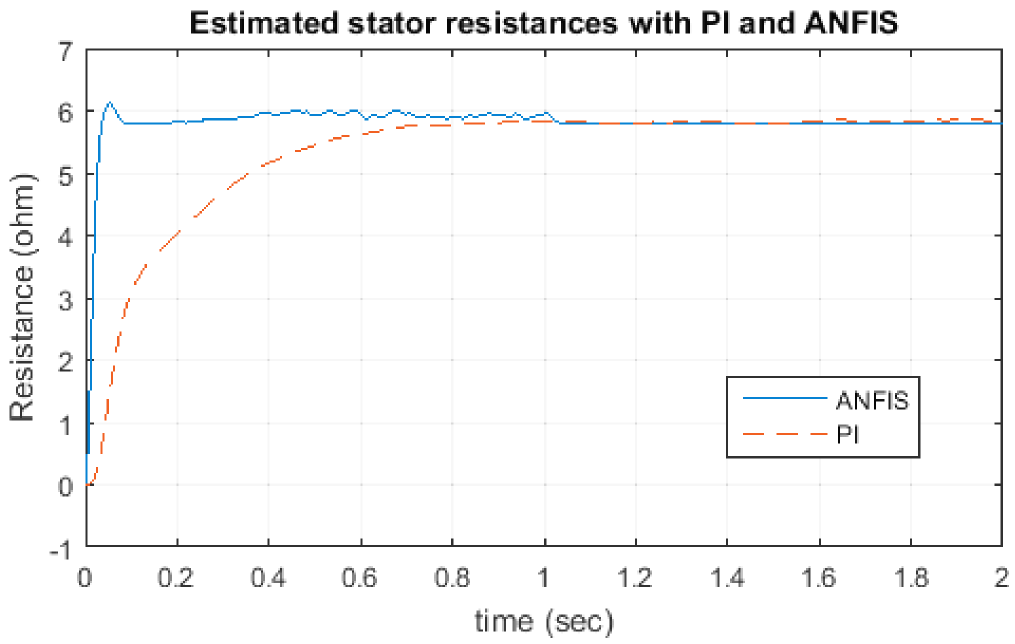

Fig. 5.3 Stator resistance estimation using PI and ANFIS controller

5.3 MODEL FORMULATION

The proposed structure of X-MRAS is presented in Fig. 5.4 for speed estimation, where the instant value of the fictitious quantity $X = \vec{v} \times \vec{i}$ is utilized for the reference model and the steady state value is used in the adaptive model [112]. Difference of these two models is used to estimate the speed which is further fed back to the adaptive model to reduce the difference to zero. In synchronously rotating reference, stator voltages of IM are given as:

$$v_{ds} = R_1 i_{ds} - \omega\sigma L_s i_{qs} + \frac{\partial}{\partial t}\sigma L_s i_{ds} - \frac{L_m}{L_r}(\omega\varphi_{qr} - \frac{\partial}{\partial t}\varphi_{dr}) \tag{5.1}$$

$$v_{qs} = R_1 i_{qs} + \omega\sigma L_s i_{ds} + \frac{\partial}{\partial t}\sigma L_s i_{qs} + \frac{L_m}{L_r}(\omega\varphi_{dr} + \frac{\partial}{\partial t}\varphi_{qr}) \tag{5.2}$$

The Instantaneous value of $X = \vec{v} \times \vec{i}$ can be written as:

$$X_1 = v_{ds} i_{qs} + v_{qs} i_{ds} \tag{5.3}$$

The term X_1 is independent of motor speed, consequently it is taken for the reference model

For steady state $(\frac{\partial}{\partial t} = 0)$ and in rotor flux oriented drive

$$\varphi_{dr} = \varphi_r = L_m i_{ds} \tag{5.4}$$

$$\varphi_{qr} = 0 \tag{5.5}$$

By substituting v_{ds} and v_{qs} from (5.1) and (5.2) into (5.3)

$$X_2 = \omega\left(L_s {i_{ds}}^2 - \sigma L_s {i_{qs}}^2\right) + 2R_1 i_{ds} i_{qs} \tag{5.6}$$

$$\text{Where } \sigma = 1 - \frac{{L_m}^2}{L_s L_r} \tag{5.7}$$

The term X_2 depends on motor speed and is chosen for the adaptive model. But it depends on stator resistance which has to be compensated by another MRAS used for stator resistance estimation.

From equation (5.1) and (5.2), the steady state stator voltages in rotor flux oriented drive can be written as:

$$v_{ds} = R_1 i_{ds} - \omega\sigma L_s i_{qs} \tag{5.8}$$

$$v_{qs} = R_1 i_{qs} + \omega\left(\frac{{L_m}^2}{L_r} + \sigma L_s\right) i_{ds} \tag{5.9}$$

R_1 can be derived by eliminating ω from (5.8) and (5.9)

$$\Rightarrow \quad R_1 = \frac{v_{ds} i_{ds} + \sigma v_{qs} i_{qs}}{L_s(\sigma {i_{qs}}^2 + {i_{ds}}^2)} \tag{5.10}$$

By using voltage and current vectors, the value of R_1 in (5.10) is estimated as shown in Fig. 5.5, where the adaptive model is dependent on R_1.

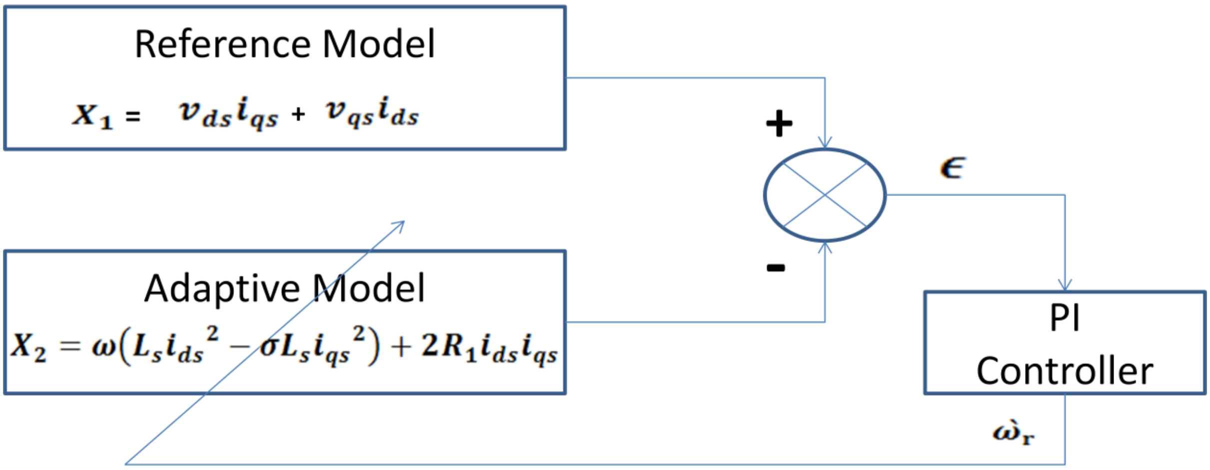

Fig. 5.4 X-MRAS based speed estimation

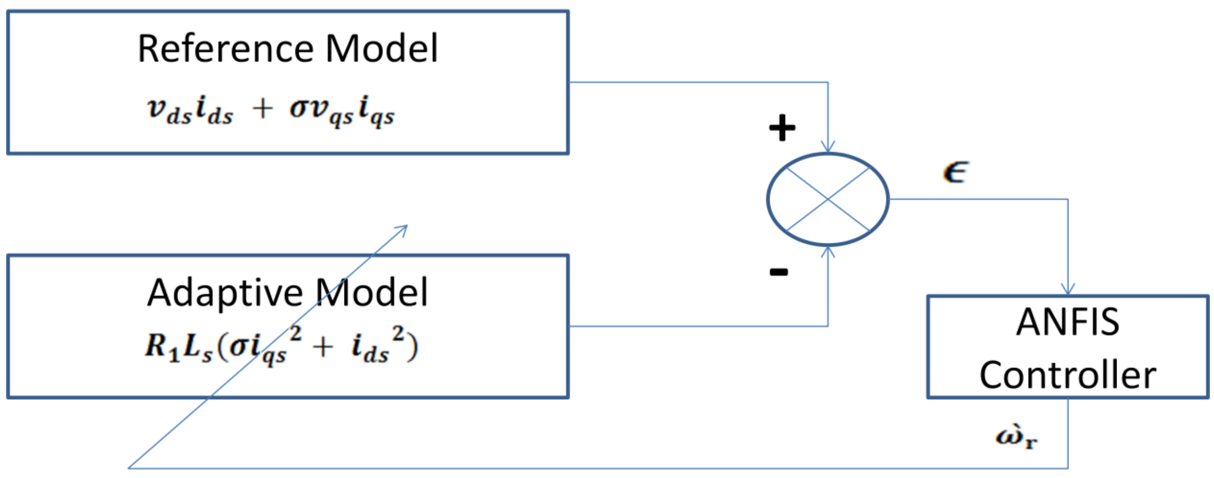

Fig. 5.5 Stator resistance estimation

5.4 DRIVE SYSTEM BLOCK DIAGRAM

A 1.5 HP, 415 V, 1430 rpm, 50 Hz, three phase IM with sensorless speed control is modeled in MATLAB/ Simulink for simulation study. A stator resistance estimation is developed using ANFIS controller which further decides the estimated speed. The current (i_{qs}^*) for torque is obtained from the motor speed loop controller, while the current (i_{ds}^*) for flux is kept constant at the rated value. For executing the vector control strategy, the motor line currents and stator voltages are sensed and transformed into d-q components (i_{ds} , i_{qs} , v_{ds} , v_{qs}) using Clark's/Park's transformation for estimating speed and stator resistance. Stator resistance modified each time for estimation of the speed. Fig. 5.6 shows the complete block diagram of drive system.

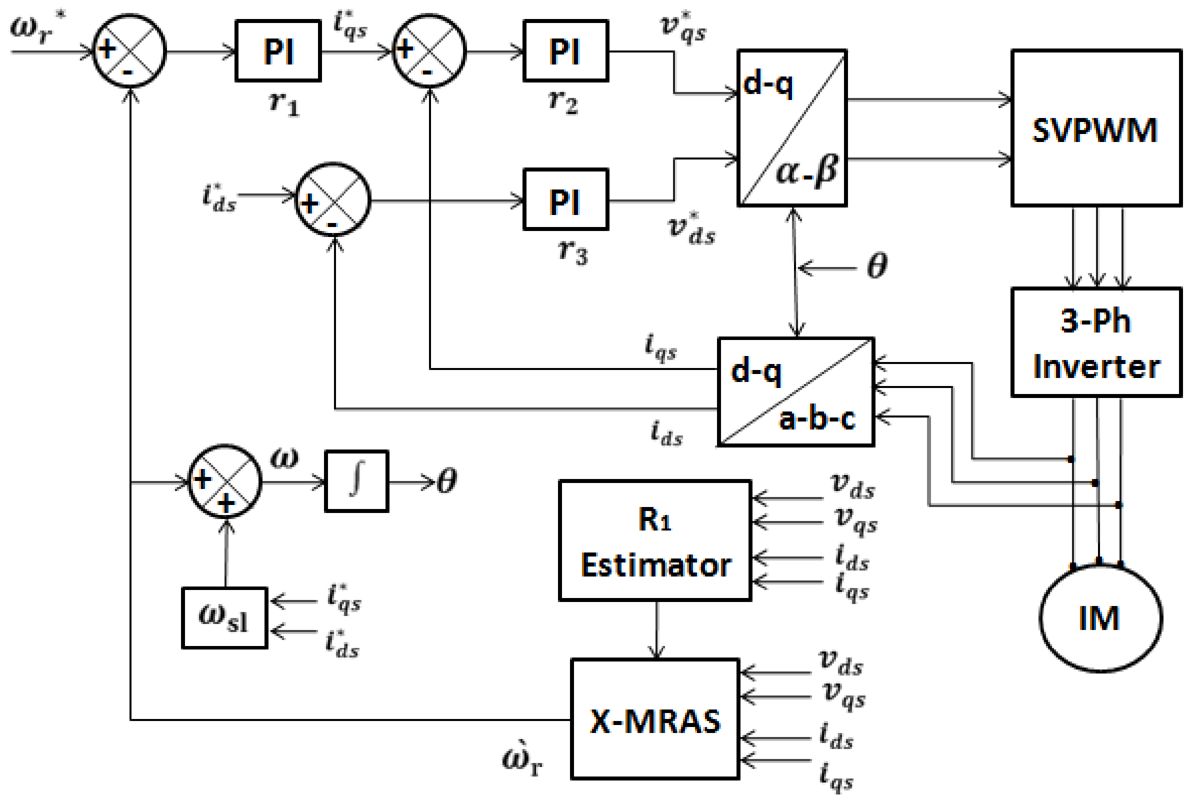

Fig. 5.6 Block diagram of sensorless drive system

5.5 SYSTEM STABILITY ANALYSIS

A stability analysis of drive system is carried out by linearizing the machine equations around stable operating point and by considering the values of PI controllers over a wide variation of stator resistance [111]. The state space equation using stator current and rotor flux in synchronous rotating reference frame as the state variable of the induction machine is represented by:

$$\frac{d}{dt}\begin{bmatrix} i_{ds} \\ i_{qs} \\ \varphi_{dr} \\ \varphi_{qr} \end{bmatrix} = \begin{bmatrix} -b_1 & \omega & b_2 & b_3\omega_r \\ -\omega & -b_1 & -b_3\omega_r & -b_2 \\ b_4 & 0 & -b_5 & \omega_{sl} \\ 0 & b_4 & -\omega_{sl} & -b_5 \end{bmatrix}\begin{bmatrix} i_{ds} \\ i_{qs} \\ \varphi_{dr} \\ \varphi_{qr} \end{bmatrix} + \frac{1}{\sigma L_s}\begin{bmatrix} 1 & 0 \\ 0 & 1 \\ 0 & 0 \\ 0 & 0 \end{bmatrix}\begin{bmatrix} v_{ds} \\ v_{qs} \end{bmatrix} \tag{5.11}$$

$$\begin{bmatrix} i_{ds} \\ i_{qs} \end{bmatrix} = \begin{bmatrix} 1 & 0 & 0 & 0 \\ 0 & 1 & 0 & 0 \end{bmatrix}\begin{bmatrix} i_{ds} \\ i_{qs} \\ \varphi_{dr} \\ \varphi_{qr} \end{bmatrix} \tag{5.12}$$

Where $b_1 = \frac{1}{\sigma L_s} R_1 + \frac{{L_m}^2 R_2}{\sigma L_s {L_r}^2}$ (5.13)

$b_2 = \frac{L_m R_2}{\sigma L_s {L_r}^2}$ (5.14)

$b_3 = \frac{L_m}{\sigma L_s L_r}$ (5.15)

$b_4 = \frac{L_m R_2}{L_r}$ (5.16)

$b_5 = \frac{R_2}{L_r}$ (5.17)

Equations (5.11) and (5.12) are equivalent to the general form of state equations:

$\dot{x} = Ax + Bu$ (5.18)

$y = Cx + Du$ (5.19)

Where $x = [i_{ds}\, i_{qs}\, \varphi_{dr}\, \varphi_{qr}]^T$ (5.20)

$u = [v_{ds}\, v_{qs}]^T$ (5.21)

$y = [i_{ds}\, i_{qs}]^T$ (5.22)

Linearising the above state equations about a stable point x_0, small signal representation will become:

$\Delta\dot{x} = A\Delta x + \Delta A x_0$ (5.23)

$\Delta y = C\Delta x$ or $\Delta y = C(sI - A)^{-1}\Delta A x_0$ (5.24)

Where $x_0 = [i_{dso}\ i_{qso}\ \varphi_{dro}\ \varphi_{qro}]^T$ represent the operating point.

ΔA can be represented in terms of $\Delta\omega_r$ for inspecting the practicability of the algorithm for speed estimation and is given by:

$$\Delta A = \begin{bmatrix} 0 & 0 & 0 & b_3 \\ 0 & 0 & -b_3 & 0 \\ 0 & 0 & 0 & -1 \\ 0 & 0 & 1 & 0 \end{bmatrix} \Delta\omega_r \quad (5.25)$$

Equation (5.24) for Δy can be represented as:

$$\Delta y = \begin{bmatrix} 1 & 0 & 0 & 0 \\ 0 & 1 & 0 & 0 \end{bmatrix} (sI - A)^{-1} \begin{bmatrix} 0 & 0 & 0 & b_3 \\ 0 & 0 & -b_3 & 0 \\ 0 & 0 & 0 & -1 \\ 0 & 0 & 1 & 0 \end{bmatrix} \begin{bmatrix} i_{dso} \\ i_{qso} \\ \varphi_{dro} \\ \varphi_{qro} \end{bmatrix} \Delta\omega_r \tag{5.26}$$

$$\Rightarrow \Delta y = \begin{bmatrix} (c_{14} - c_{12}b_3) * \varphi_{dro} + (c_{11}b_3 - c_{13}) * \varphi_{qro} \\ (c_{24} - c_{22}b_3) * \varphi_{dro} + (c_{21}b_3 - c_{23}) * \varphi_{qro} \end{bmatrix} \tag{5.27}$$

Where c_{ij} = adjoint $(sI - A)$

From (5.27) the transfer functions for $\frac{\Delta_{i_{ds}}}{\Delta\omega_r}$ and $\frac{\Delta_{i_{qs}}}{\Delta\omega_r}$, can be represented as:

$$\frac{\Delta_{i_{ds}}}{\Delta\omega_r} = \frac{(c_{14} - c_{12}b_3)\varphi_{dro} + (c_{11}b_3 - c_{13})\varphi_{qro}}{|sI - A|} \tag{5.28}$$

$$\frac{\Delta_{i_{qs}}}{\Delta\omega_r} = \frac{(c_{24} - c_{22}b_3)\varphi_{dro} + (c_{21}b_3 - c_{23})\varphi_{qro}}{|sI - A|} \tag{5.29}$$

At steady state, under rotor flux orientation

$$\varphi_{dro} = \varphi_r \tag{5.30}$$

$$\varphi_{qro} = 0 \tag{5.31}$$

From Fig. 5.6 the following equations can be depicted:

$$v_{ds}^* = \left(k_{p3} + \frac{k_{i3}}{s}\right)(i_{ds}^* - i_{ds}) = r_3(i_{ds}^* - i_{ds}) \tag{5.32}$$

$$\text{OR} \quad v_{ds}^* = r_3(i_{ds}^* - i_{ds}) \tag{5.33}$$

$$v_{qs}^* = \left(k_{p2} + \frac{k_{i2}}{s}\right)\left\{\left(k_{p1} + \frac{k_{i1}}{s}\right)(\omega_r{}^* - \omega_r) - i_{qs}\right\} \tag{5.34}$$

$$\text{OR} \quad v_{qs}^* = r_2\{r_1(\omega_r{}^* - \omega_r) - i_{qs}\} \tag{5.35}$$

$$\text{Where} \quad r_1 = \left(k_{p1} + \frac{k_{i1}}{s}\right) \tag{5.36}$$

$$r_2 = \left(k_{p2} + \frac{k_{i2}}{s}\right) \tag{5.37}$$

$$r_3 = \left(k_{p3} + \frac{k_{i3}}{s}\right) \tag{5.38}$$

r_1 , r_2 and r_3 are the transfer functions of PI controllers.

By linearising equations (5.33) and (5.35), we get

$$\Delta v_{ds} = r_3 \Delta i_{ds} \tag{5.39}$$

$$\Delta v_{qs} = -r_2(r_1\Delta\omega_r + \Delta i_{qs} \tag{5.40}$$

For X-MRAS, the small signal error can be given by:

$$\epsilon = X_1 - X_2 = v_{qs} i_{ds} + v_{ds} i_{qs} - \omega(L_s i_{ds}{}^2 - \sigma L_s i_{qs}{}^2) - R_1 i_{ds} i_{qs} \tag{5.41}$$

Where $\omega = \grave{\omega}_r + \grave{\omega}_{sl}$ (5.42)

The variables in (5.41) are perturbed as:

$$i_{ds} = i_{dso} + \Delta i_{ds}\ , \quad i_{qs} = i_{qso} + \Delta i_{qs}\ , \quad \grave{\omega}_{sl} = \grave{\omega}_{slo} + \Delta\grave{\omega}_{sl}\ , \quad \grave{\omega}_r = \grave{\omega}_{ro} + \Delta\grave{\omega}_r \tag{5.43}$$

Hence, $\Delta\epsilon$ for X-MRAS can be represented as:

$$\Delta\epsilon = k_1\Delta i_{ds} + k_2\Delta i_{qs} + k_3\Delta\grave{\omega}_{sl} + k_4\grave{\omega}_r \tag{5.44}$$

Where $k_1 = v_{qso} - 2R_1 i_{qso} - 2\omega_o L_s i_{dso} - r_3 i_{qso}$ (5.45)

$$k_2 = v_{dso} - 2R_1 i_{dso} + 2\sigma\omega_o L_s i_{qso} - r_2 i_{dso} \tag{5.46}$$

$$k_3 = \sigma L_s i_{qso}{}^2 - L_s i_{dso}{}^2 \tag{5.47}$$

$$k_4 = \sigma L_s i_{qso}{}^2 - L_s i_{dso}{}^2 - r_1 r_2 i_{dso} \tag{5.48}$$

Any increment (small) in the estimated speed causes the decrement of slip speed. If the speed (ω) of rotor flux remains same after the perturbation, then from (5.43):

$$\Delta\grave{\omega}_r = -\Delta\grave{\omega}_{sl} \tag{5.49}$$

Substituting (5.49) into (5.44) yields:

$$\Delta\epsilon = k_1\Delta i_{ds} + k_2\Delta i_{qs} + (k_4 - k_3)\Delta\grave{\omega}_r \tag{5.50}$$

Dividing both sides of (5.50) by $\Delta\grave{\omega}_r$

$$\frac{\Delta\epsilon}{\Delta\grave{\omega}_r} = \frac{k_1\Delta i_{ds}}{\Delta\grave{\omega}_r} + \frac{k_2\Delta i_{qs}}{\Delta\grave{\omega}_r} + (k_4 - k_3) = G_s \tag{5.51}$$

The closed loop transfer function for rotor speed estimator is represented as:

$$\frac{\grave{\omega}_r}{\omega_r} = \frac{G_s(k_p + \frac{k_i}{s})}{1 + G_s(k_p + \frac{k_i}{s})} \tag{5.52}$$

where $(k_p + \frac{k_i}{s})$ shows PI controller transfer function for adaptive mechanism. Fig. 5.7 shows the X-MRAS based closed loop rotor speed estimator.

Close loop transfer function as per the equation (5.52) for a three-phase induction motor with ratings as given in Table 5.1 and for an operating point at a rotor speed of 10 rad/sec and a load torque of 5 Nm has been derived. The bode plot for this transfer function with a stator resistance of 5.85 ohm (rated value) is shown in Fig. 5.8 and for a stator resistance of 11.7 ohm (double to rated value) is shown in Fig. 5.9. It is observed from Fig. 5.8 and Fig. 5.9 of bode plot, the gain margin as well as the phase margin is positive, therefore X-MRAS represents a stable system.

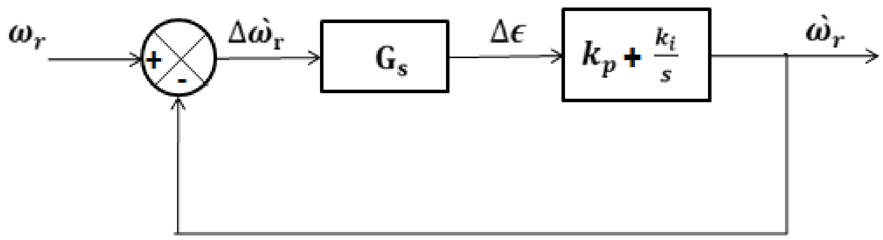

Fig. 5.7 Closed loop speed estimator

Table 5.1 Three phase induction motor parameters

Name of Parameter	**Value**
Rating	1.5 hp, , 415V, 1430 rpm
No. of pole	4
Stator /rotor resistance	5.85/ 6.08 ohm
Mutual inductance L_m	0.489H
Stator /rotor self-inductance L_s ,L_r	0.51H/ 0.52H
Moment of inertia J	0.0178Kg-m^2

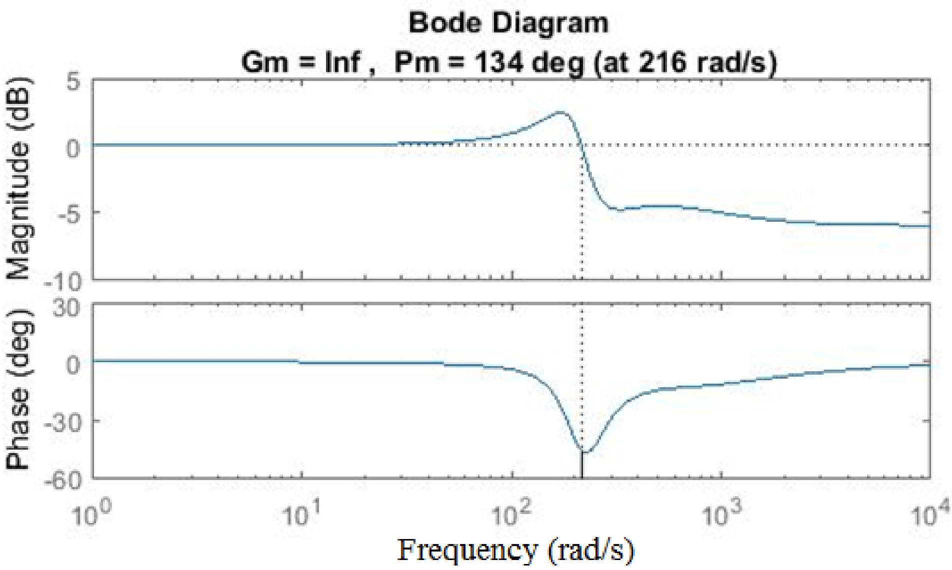

Fig. 5.8 Bode plot of IM drive system with R_1 = 5.85 ohm

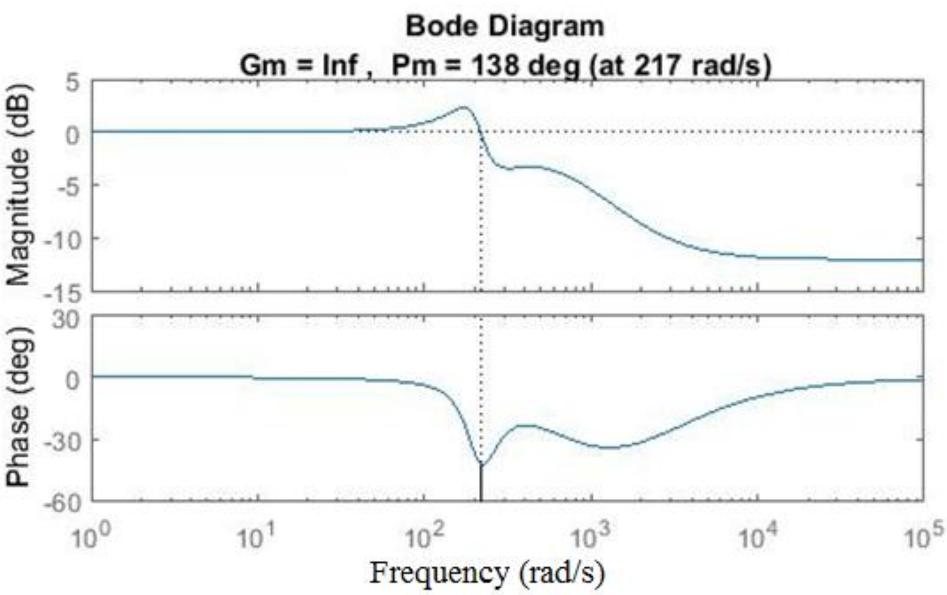

Fig. 5.9 Bode plot of IM drive system with R_1 = 11.7 ohm

5.6 SIMULATION RESULTS AND ANALYSIS

The X-MRAS based speed estimation method for induction motor is simulated in MATLAB/ Simulink for a 1.5 HP, 415 V, 1430 rpm 50 Hz. The performance of speed estimator is first checked at no load condition and then under loaded condition. For speed sensorless drive system, the performance at zero and low speed is not satisfactory. Therefore, low rotor speed performance for X-MRAS based drive is highlighted in this chapter.

5.6.1 Dynamic Response of IM Drive for Variation in Stator Resistance

Fig. 5.10 shows the performance of the drive system for stator resistance variation, where motor stator resistance is increased suddenly from 5.85 ohm to 10.6 ohm and again decreased suddenly to 5.85 ohm. The reference speed along with the actual speed and estimated rotor speed was observed as presented in Fig. 5.11 and Fig. 5.12. The d and q-axis rotor flux orientation is also maintained throughout, as shown in Fig. 5.13. In the simulation result it is observed that the rotor speed estimator as shown in Fig. 5.2 is independent of stator resistance variation.

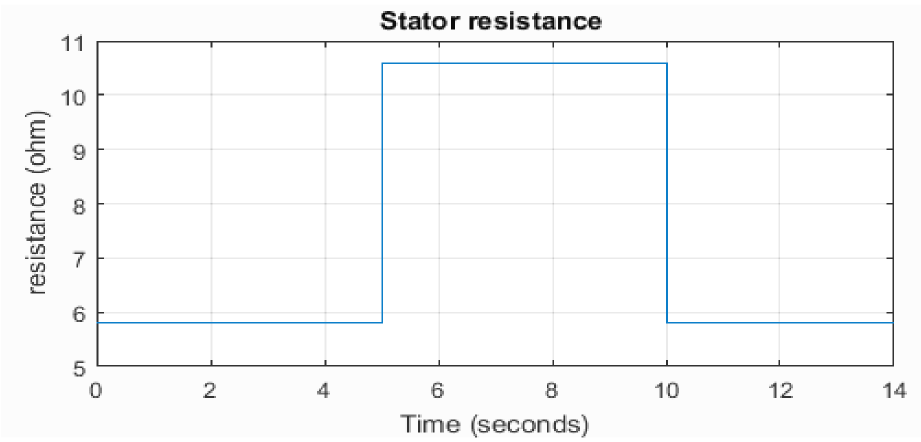

Fig. 5.10 Variation of stator resistance

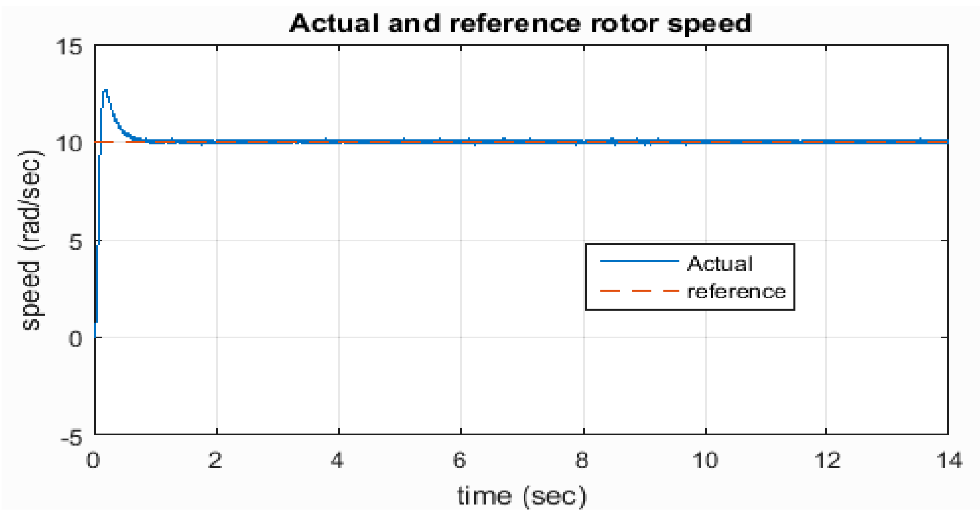

Fig. 5.11 Actual and reference speed

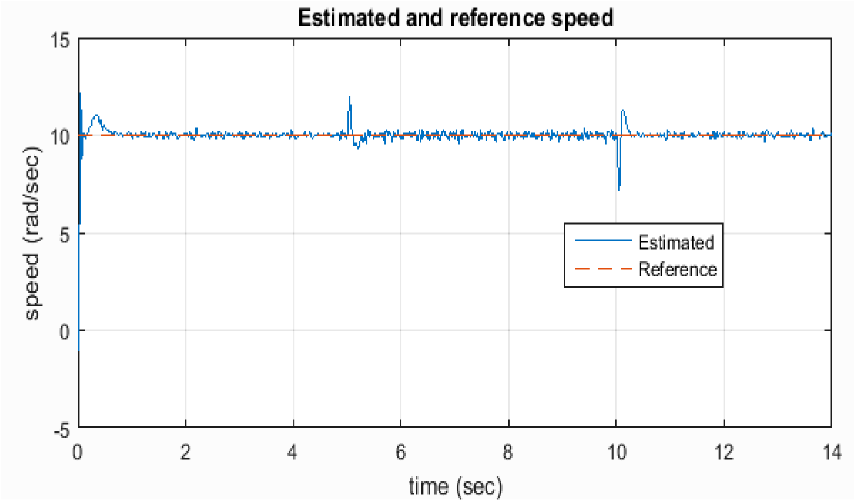

Fig. 5.12 Estimated and reference speed

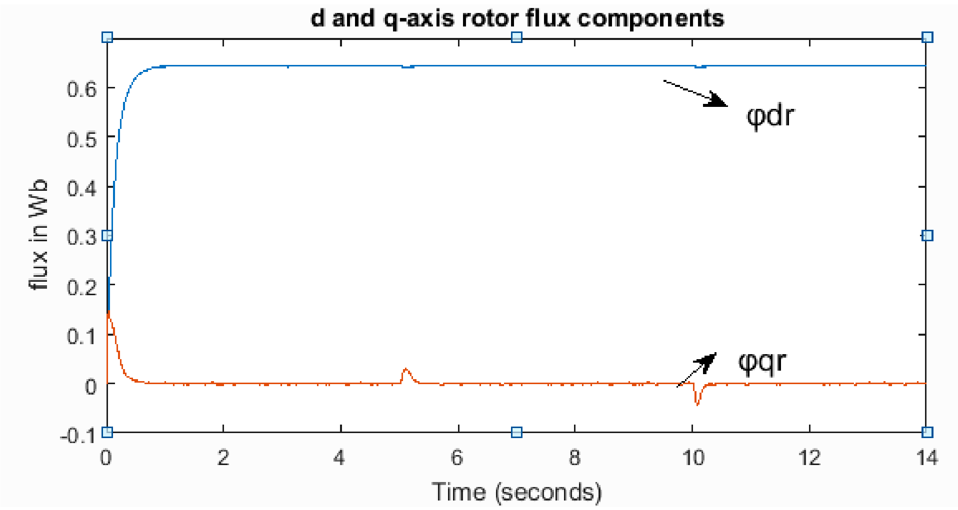

Fig. 5.13 d and q-axis rotor flux components

5.6.2 Dynamic Response of Drive for Sudden change in Speed

The characteristic of the drive system for a step speed command is analyzed, where the step speed command is set to 0 from t=0 to t=5 sec and changed suddenly from zero to 15 rad/sec at t=5 sec. The actual rotor speed along with the reference and the estimated rotor speed is observed in Fig. 5.14 and Fig. 5.15, which show that the speed follows suitably with the estimated speed. The estimated stator resistance is also observed, as shown in Fig. 5.16. The dq-axis rotor flux orientation is also maintained throughout, as shown in Fig. 5.17.

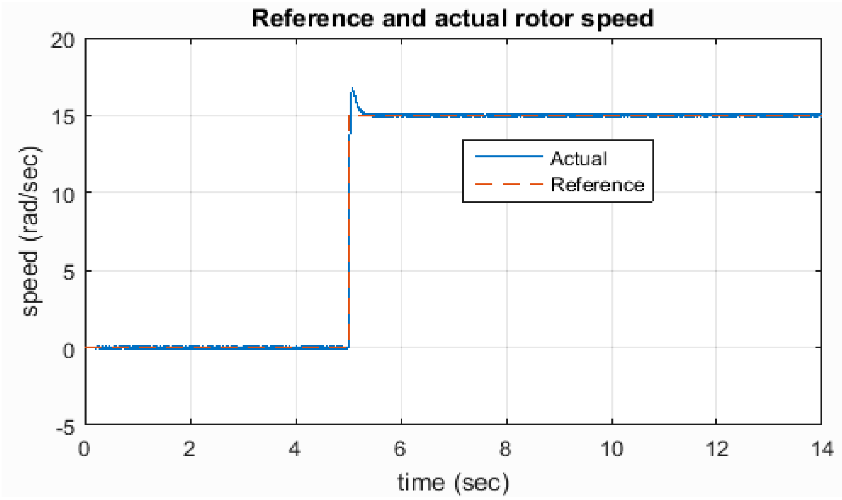

Fig. 5.14 Reference and actual rotor speed

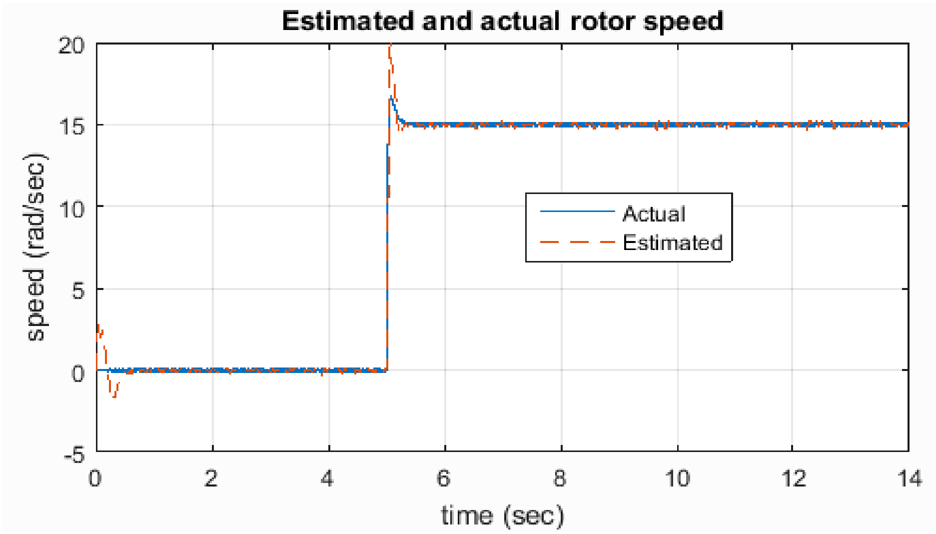

Fig. 5.15 Actual and estimated speed

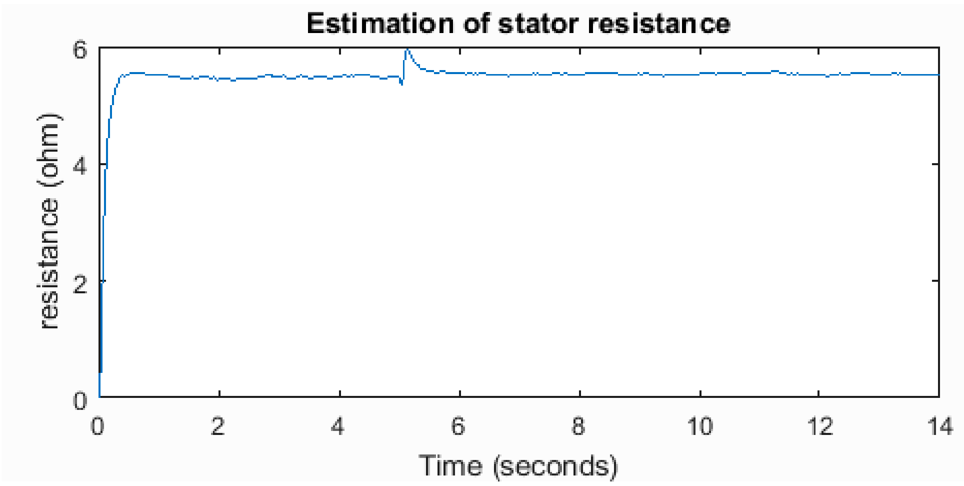

Fig. 5.16 Estimation of stator resistance

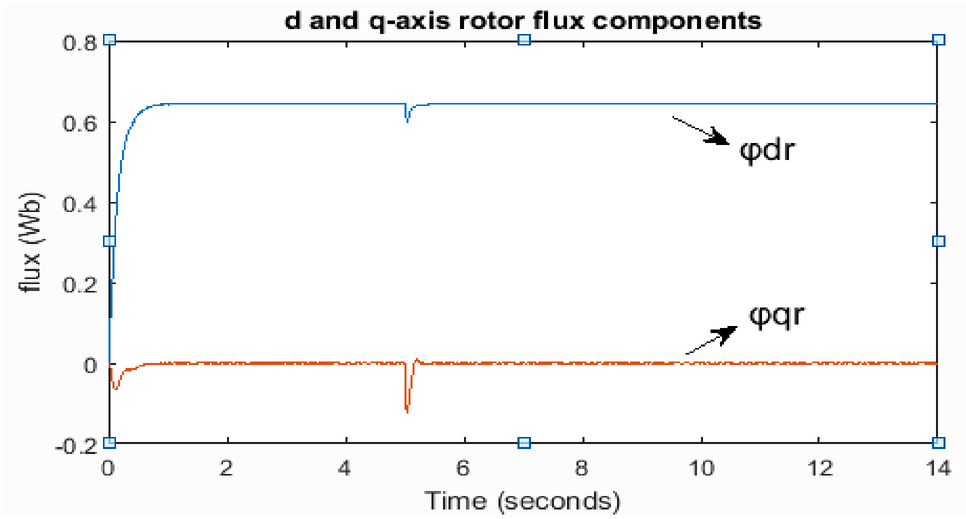

Fig. 5.17 d and q-axis rotor flux components

5.6.3 Dynamic Response of the Drive in Regenerative Mode

Rotor speed estimator performance in regenerative mode is analyzed, where the speed starts from initial value of zero, changed to +10 rad/s at 5 s and −10 rad/s at 10 s. The actual rotor speed along with the reference rotor speed is observed as shown in Fig. 5.18. The actual speed along with the estimated speed is observed and shown in Fig. 5.19, where the estimated and actual speed follows the speed command satisfactorily. The estimated stator resistance also maintained throughout, as shown in Fig. 5.20. The dq-axis rotor flux orientation is maintained throughout, as shown in Fig. 5.21. The response of torque is also presented in Fig. 5.22.

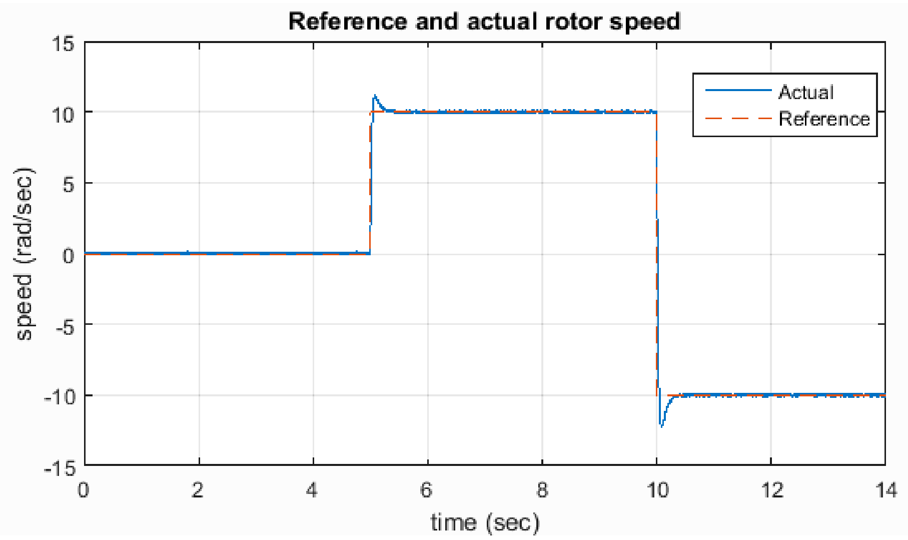

.

Fig. 5.18 Reference and actual rotor speed

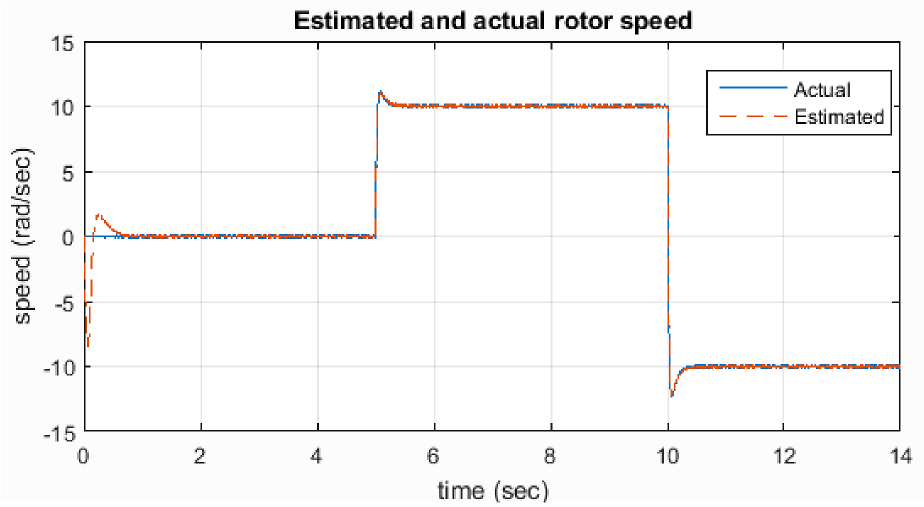

Fig. 5.19 Estimated and actual rotor speed

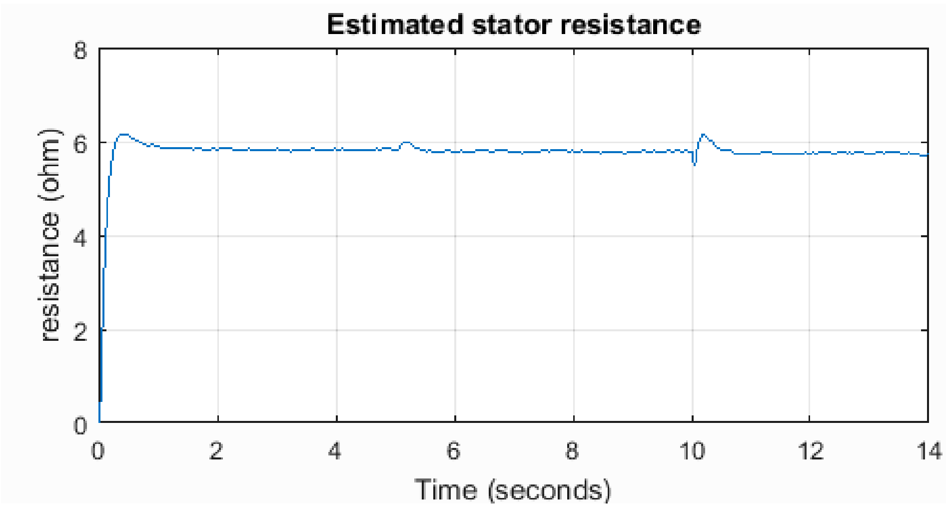

Fig. 5.20 Estimated stator resistance

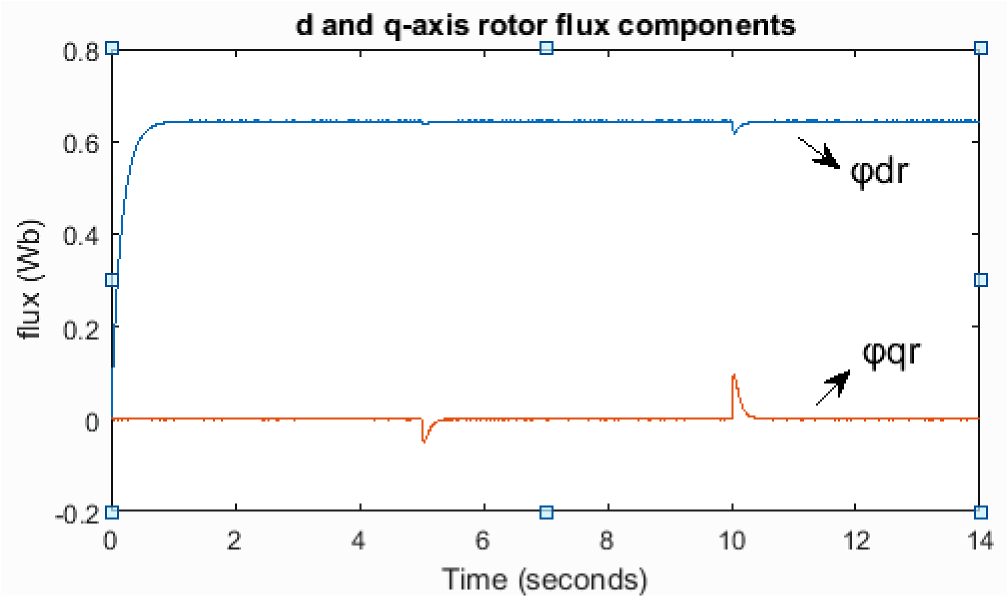

Fig. 5.21 d and q-axis rotor flux components

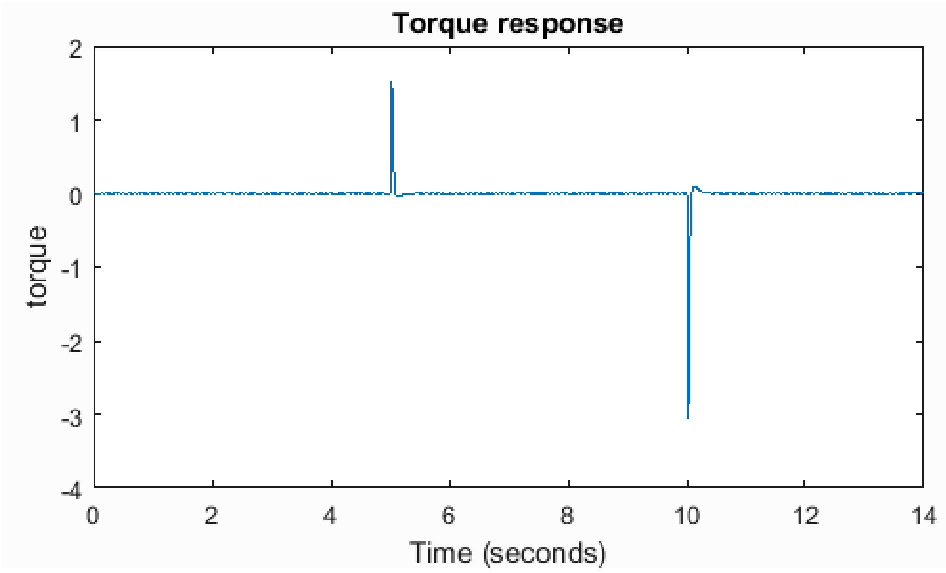

Fig. 5.22 Torque (N-m) response

5.6.4 Dynamic Response of the IM Drive with Sudden Change in Load

The dynamic performance of the X-MRAS based sensorless IM drive with a constant torque of 3 N-m and sudden change in speed from zero to 50 rad/s at 5 s and then reversed to −10 rad/s at 10 s. It is observed from Fig. 5.23 that motor tracks the reference speed with an initial small overshoot and settles at the reference speed. Fig. 5.24 shows estimated and actual rotor speed. The estimated stator resistance is maintained throughout, as shown in Fig. 5.25. The dq-axis rotor flux orientation is maintained and shown in Fig. 5.26. The response of the torque is shown in Fig. 5.27.

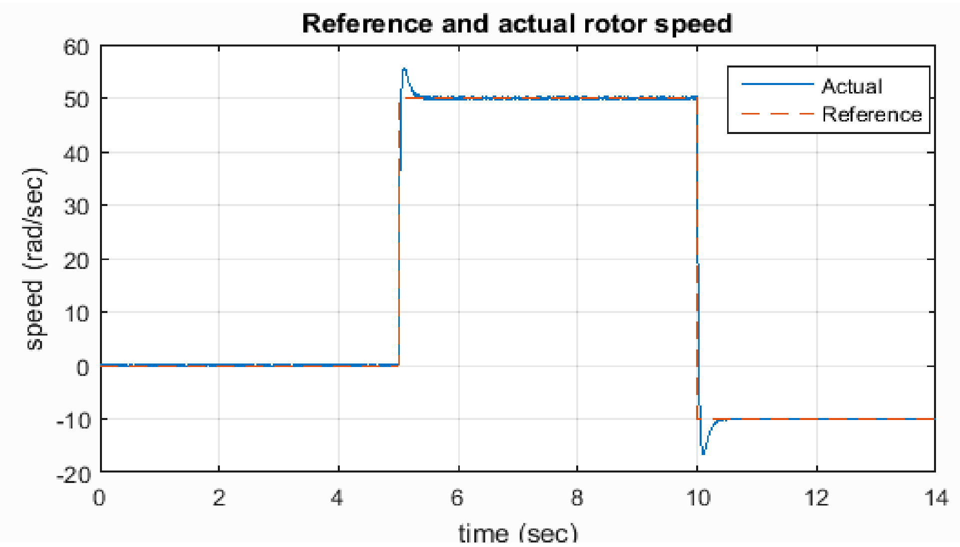

Fig. 5.23 Reference and actual rotor speed

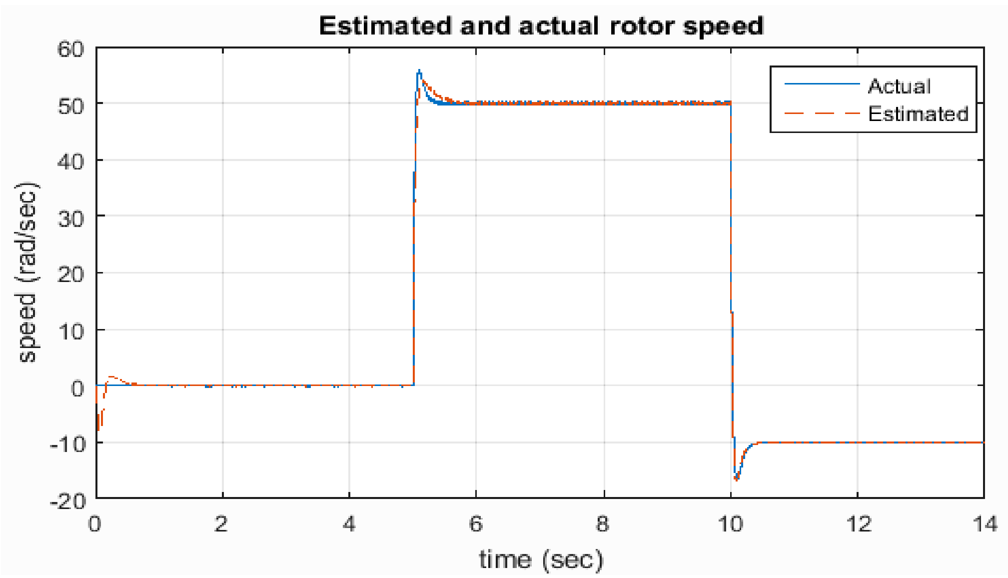

Fig. 5.24 Actual and estimated Speed

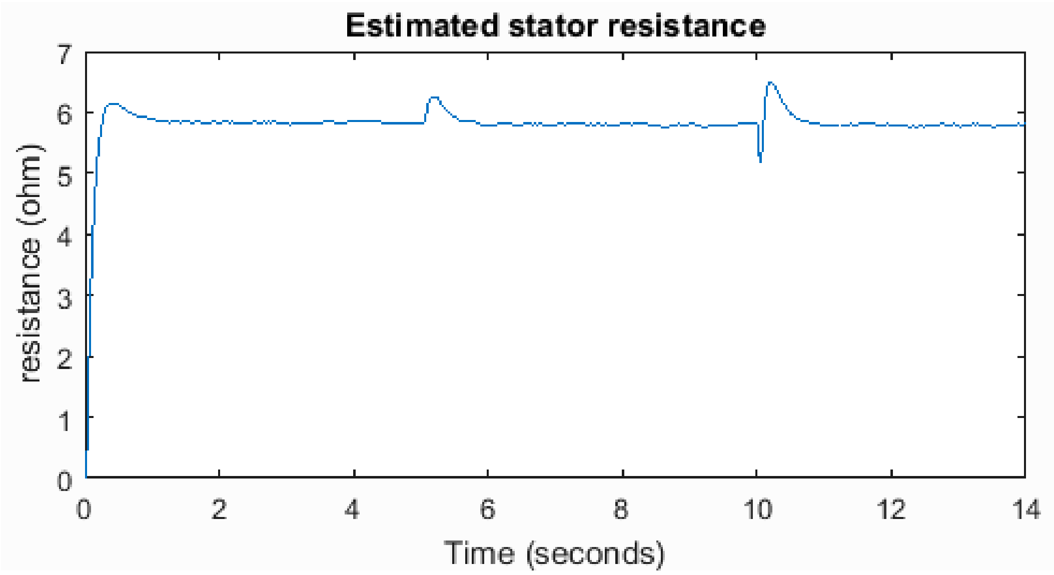

Fig. 5.25 Estimated stator resistance

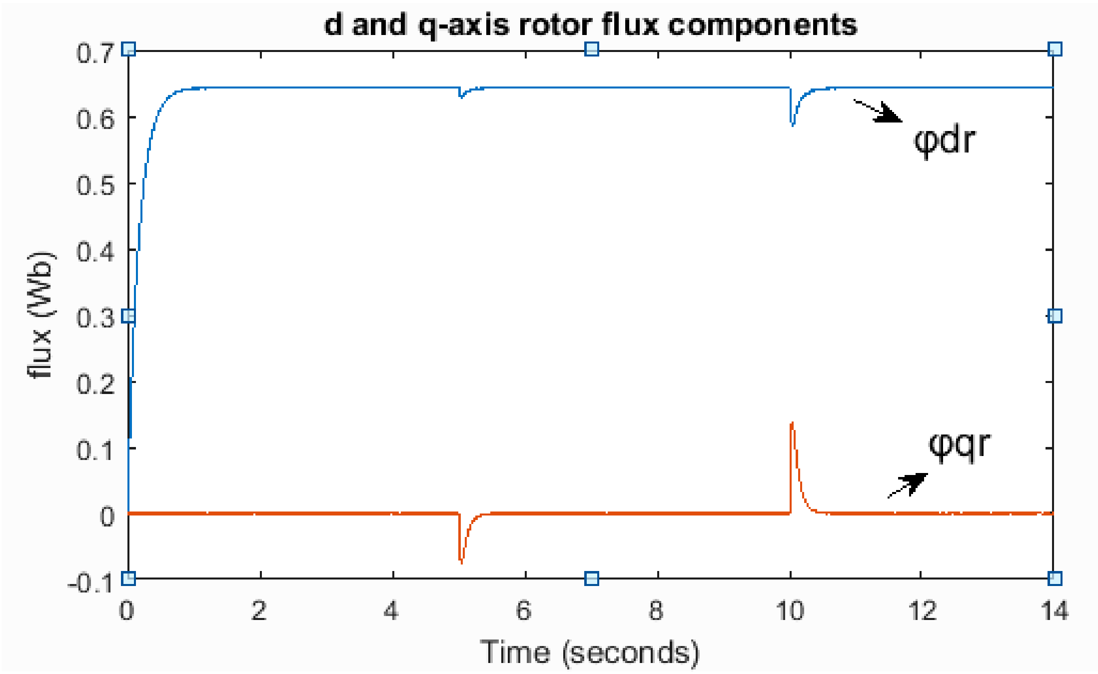

Fig. 5.26 d and q-axis rotor flux components

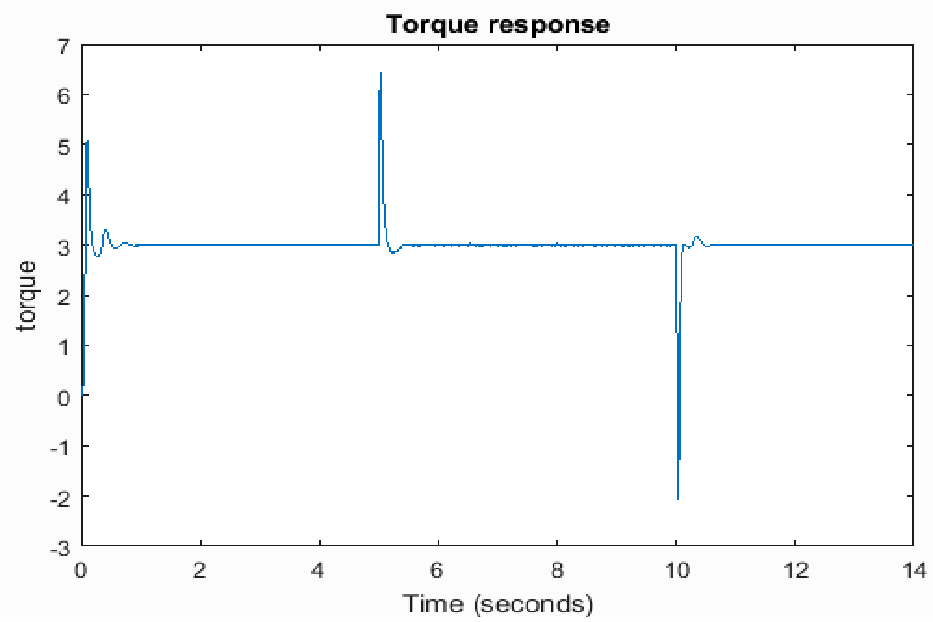

Fig. 5.27 Torque (N-m) response

5.7 CONCLUSION

The performance of sensorless IM drive with X-MRAS speed estimator is presented in this chapter. The proposed estimation algorithm for stator resistance is updated through an adaptive mechanism each time for estimation of the speed, hence making the motor speed estimation independent of stator resistance. Adaptive mechanism for stator resistance estimation utilized ANFIS controller. The small signal stability analysis with a large variation of stator resistance is also discussed after linearizing the motor equations around the operating point. The transfer function of the drive is developed from the linearized model and used to find out the stability of the IM drive system using Bode plots.

CHAPTER VI

EFFICIENCY OPTIMIZATION IN IFOC IM DRIVE BASED ON LOSS MODEL CONTROL

6.1 GENERAL

Technological advancements in digital signal processing and power electronics have resulted in induction motor drives finding widespread usage in high performance industrial control applications. For conservation of energy the operation of IM at optimal efficiency is paramount. Induction motors (IM) are designed and constructed with maximum efficiency of operation at rated speed and torque. However, for most of the period during routine operations, IMs are generally operated at loads less than the rated torque. It is therefore, essential to increase the efficiency of the IM drive for such operating conditions for optimizing the energy requirements, reducing the cost of operation and to minimize adverse effect on the environment. To increase the efficiency of motor at light loads, the flux current component must be decreased for obtaining a balance between iron and copper losses. This is achieved by optimal control of the flux producing current of the IM drive to decrease the core losses for light load conditions.

In recent years, there have been vast studies on new nature inspired algorithms, which are based on different sources of inspiration within the biological and natural world. Many of these algorithms are very efficient in solving real world optimization problems. Some of the nature inspired algorithms have been used to improve the motor efficiency at different load conditions. The approaches for efficiency improvement are mainly separated into two parts, namely search controller (SC) and loss-model controller (LMC). In LMC the machine model is used to compute the motor losses by choosing a flux value to minimize the core losses [57].

This method is machine parameter dependent, but the response is fast [121]. In SC the power input of the machine is measured frequently at fixed intervals and the value of flux is reduced continuously till the measured power input settles down to the minimum level for the commanded speed and torque. The SC is machine parameter independent optimization and torque ripples are always present in this method because of the oscillations in the air gap flux. The search control is relatively sluggish due to the search process [171].

In this chapter, efficiency optimization in an indirect vector controlled (IFOC) IM drive through optimal control of direct axis stator current is developed. An attempt is made to optimize the motor efficiency by minimizing the iron losses only and total losses independently by selecting an optimal flux value which minimizes these losses. The complete drive system and control schemes are implemented in MATLAB/Simulink environment by using PI controller and FLC.

6.2 MATHEMATICAL MODEL OF IM

The dynamic control of an induction motor is complex as the coupling coefficient between rotor and stator windings changes continuously with respect to the rotor position. In addition, torque and voltage equations that explain the dynamic behaviour of an IM is time varying. The time varying variables can be removed by shifting the rotor and stator variables to a common reference frame that can rotate at any motor speed. Synchronously rotating reference frame is taken in this paper, where each sinusoidal variables (voltage, current or flux linkage) appear as DC quantities. The dq equivalent circuit of the IM in synchronously rotating frame is as shown in Fig. 6.1.

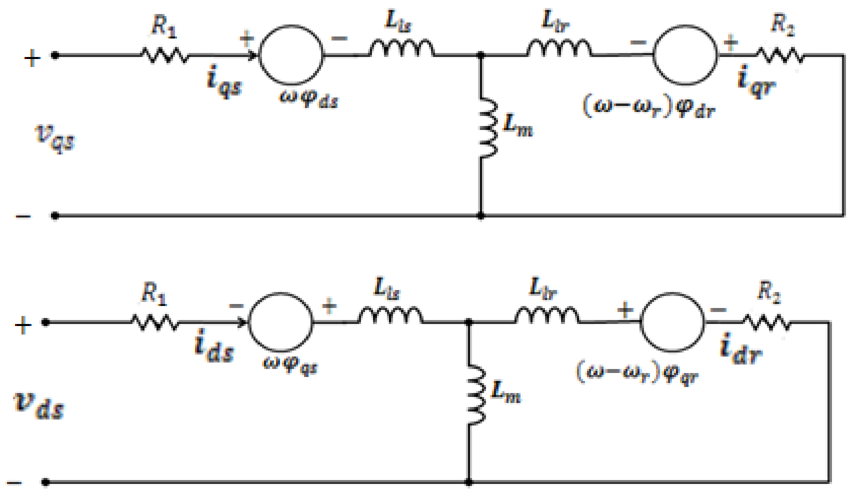

Fig. 6.1 d-q equivalent circuit of IM

Considering the *d-q* axes equivalent circuit of a three phase IM in the synchronously rotating reference frame, the voltage equations can be written as:

$$v_{qs} = R_1 i_{qs} + \frac{\partial \varphi_{qs}}{\partial t} + \omega\varphi_{ds} \tag{6.1}$$

$$v_{ds} = R_1 i_{ds} + \frac{\partial \varphi_{ds}}{\partial t} - \omega\varphi_{qs} \tag{6.2}$$

$$v_{qr} = 0 = R_2 i_{qr} + \frac{\partial \varphi_{qr}}{\partial t} + (\omega - \omega_r)\varphi_{dr} \tag{6.3}$$

$$v_{dr} = 0 = R_2 i_{dr} + \frac{\partial \varphi_{dr}}{\partial t} - (\omega - \omega_r)\varphi_{qr} \tag{6.4}$$

The motor torque (T_e) equation is given by:

$$T_e = \frac{3P}{4}\frac{L_m}{L_r}(\varphi_{dr} i_{qs} - \varphi_{qr} i_{ds}) \tag{6.5}$$

6.3 VECTOR CONTROL

The stator current is controlled in the vector control IM drive with its flux current locked on the rotor flux vector in a synchronously rotating reference frame. The orientation of d-axis component of the current i_{ds} is possible with rotor flux, stator flux and air gap flux in vector control. The orientation of rotor flux has been used in the developed algorithm, as it provides natural decoupling control between torque and flux. The unit vector assures accurate alignment of i_{ds} with rotor flux vector and keeps i_{qs} perpendicular to it. In rotor flux oriented drive the rotor flux equations are represented as:

$$\varphi_{qr} = 0 \quad (6.6)$$

$$\varphi_{dr} = \varphi_r \quad (6.7)$$

Relation between i_{qs} and i_{qr} is given by the expression:

$$i_{qr} = -\frac{L_m}{L_r} i_{qs} \quad (6.8)$$

Putting these values in (6.3) and (6.5), yields slip frequency (ω_{sl}) and torque (T_e) as:

$$0 = R_2 i_{qr} + (\omega - \omega_r)\varphi_{dr} \quad (6.9)$$

$$\Rightarrow (\omega - \omega_r) = \omega_{sl} = \frac{L_m}{L_r}\frac{R_2}{\varphi_{dr}} i_{qs} \quad (6.10)$$

$$T_e = \frac{3P}{4}\frac{L_m}{L_r}\varphi_{dr} i_{qs} \quad (6.11)$$

For the steady state condition

$$\varphi_{dr} = L_m i_{ds} \quad (6.12)$$

The expression of slip frequency and torque will become as:

$$\omega_{sl} = \frac{R_2}{L_r}\frac{i_{qs}}{i_{ds}} \quad (6.13)$$

$$T_e = \frac{3P}{4}\frac{{L_m}^2}{L_r} i_{ds} i_{qs} \quad (6.14)$$

6.4 EFFICIENCY OPTIMIZATION

The losses in an IM consist of iron losses, rotor copper losses, stator copper losses, and mechanical losses. Among these iron and copper losses constitutes the major portion of the total motor losses. The iron losses include eddy current and hysteresis losses. The hysteresis and eddy currents losses are proportional to ω and ω^2 respectively. The iron losses are given by the relation [121]:

$$P_{Fe} = \frac{3}{2}(k_h \omega {\varphi_m}^2 + k_e \omega^2 {\varphi_m}^2) \quad (6.15)$$

Where

$$\varphi_m{}^2 = \varphi_{dm}{}^2 + \varphi_{qm}{}^2 \tag{6.16}$$

$$\varphi_{qm} = L_m\left(i_{qs} + i_{qr}\right) \tag{6.17}$$

$$\varphi_{dm} = L_m(i_{ds} + i_{dr}) \tag{6.18}$$

The mechanical losses are given by:

$$P_{mec\,h} = k_m \omega_r{}^2 \tag{6.19}$$

The total copper losses are given by:

$$P_{cu} = \frac{3}{2}\{R_1\left(i_{qs}{}^2 + i_{ds}{}^2\right) + R_2\left(i_{qr}{}^2 + i_{dr}{}^2\right)\} \tag{6.20}$$

By using (6.15), (6.19) and (6.20), the total motor losses are represented as:

$$P_{Total} = \frac{3}{2}(k_h \omega \varphi_m{}^2 + k_e \omega^2 \varphi_m{}^2) + \frac{3}{2}\left\{R_1\left(i_{qs}{}^2 + i_{ds}{}^2\right) + R_2\left(i_{qr}{}^2 + i_{dr}{}^2\right)\right\}$$

$$+ k_m \omega_r{}^2 \tag{6.21}$$

Substituting (6.6) and (6.7) in (6.16) for the steady state condition ($\varphi_{dr} = L_m i_{ds}$) yields:

$$\varphi_m{}^2 = \frac{L_m{}^2}{L_r{}^2}\{L_r{}^2 i_{ds}{}^2 + (L_r - L_m)^2 i_{qs}{}^2\} \tag{6.22}$$

Where

$$i_{qr} = -\frac{L_m}{L_r} i_{qs} \tag{6.23}$$

$$i_{dr} = \frac{\varphi_r}{L_r} - \frac{L_m}{L_r} i_{ds}) \tag{6.24}$$

Substituting (6.22) in (6.15) yields:

$$P_{Fe} = A\{i_{ds}{}^2 + \frac{(L_r - L_m)^2}{L_r{}^2} i_{qs}{}^2\} \tag{6.25}$$

Where

$$A = \frac{3}{2} L_m{}^2 (k_h \omega + k_e \omega^2) \tag{6.26}$$

From (6.14) i_{qs} can be written as:

$$i_{qs} = \frac{4 T_e L_r}{3 P L_m{}^2 i_{ds}} \tag{6.27}$$

Substituting (6.27) in (6.25) yields:

$$P_{Fe} = A\{{i_{ds}}^2 + \frac{B}{{i_{ds}}^2}\} \tag{6.28}$$

Where

$$B = \frac{16(L_r - L_m)^2 {T_e}^2}{9P^2 {L_m}^4} \tag{6.29}$$

For getting the optimal value of magnetic flux producing current component that minimizes the iron losses, differentiate iron losses (6.28) with respect to i_{ds} and equate it to zero ($\frac{\partial P_{Fe}}{\partial i_{ds}} = 0$).

$$\Rightarrow \quad i_{ds\,opt\ (iron)} = \frac{2}{L_m} \sqrt[4]{\frac{(L_r - L_m)^2 {T_e}^2}{9P^2}} \tag{6.30}$$

Substituting (6.22) and (6.27) in (6.21) yields:

$$P_{Total} = \frac{3}{2}\left\{\mathrm{m}{i_{ds}}^2 + n\left(\frac{4T_e L_r}{3P{L_m}^2 i_{ds}}\right)^2\right\} + k_m {\omega_r}^2 \tag{6.31}$$

Where

$$\mathrm{m} = R_1 + {L_m}^2(k_h\omega + k_e\omega^2) \tag{6.32}$$

$$\mathrm{n} = R_1 + \frac{{L_m}^2}{{L_r}^2}\{R_2 + (k_h\omega + k_e\omega^2)(L_r - L_m)^2\} \tag{6.33}$$

For getting the optimal value of magnetic flux producing current component that minimizes the total losses, differentiate total losses (6.31) with respect to i_{ds} and equate it to zero ($\frac{\partial P_{Total}}{\partial i_{ds}} = 0$).

$$\Rightarrow \quad i_{ds\,opt\ (total)} = \frac{2}{L_m} \sqrt[4]{\frac{n}{m}\left(\frac{4T_e L_r}{3P{L_m}^2}\right)^2} \tag{6.34}$$

Optimal value of i_{ds} in equation (6.34) depends on k_e , k_h and ω, while in (6.30) it is independent of these parameters.

6.5 INDIRECT VECTOR CONTROL IM DRIVE

The indirect vector controlled (IVC) IM drive consists of IGBT based VSI, three-phase squirrel cage induction motor, PI and fuzzy controllers. In order to analyze the drive performance, the three phase IM drive with ratings as given in Table 6.1 is simulated using the Matlab/Simulink. The torque command current (i_{qs}^*) is created from the speed loop controller, while the flux command current (i_{ds}^*) is generated according to the implemented efficiency optimization algorithm. Hysteresis current controller is used for generating the gate drive pulses for the inverter. For execution of the vector control method, motor line currents are controlled using a hysteresis band current controller to track the reference current commands. Unit vector is achieved by integrating the sum of the rotor speed and slip frequency. The slip frequency is generated by using i_{qs}^* in feed forward manner and the motor speed is obtained from the speed encoder. The schematic representation of the IVC IM drive with the developed optimization algorithm is shown in Fig. 6.2.

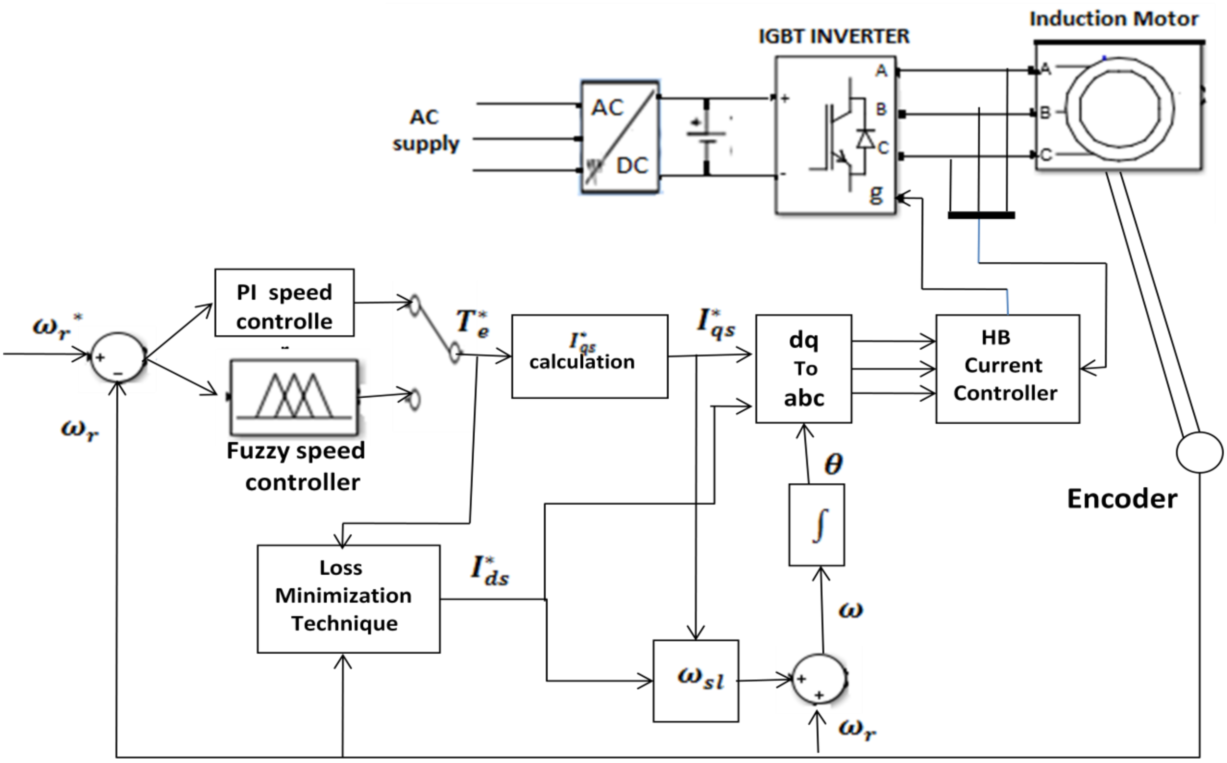

Fig. 6.2 A block diagram of indirect vector controlled IM drive with optimization

Table 6.1: Ratings of IM

Rated power	Input voltage	Input current	Input frequency	Rated speed	No. of Pole
2.2kW	430 V ±10%	4.8A	50 Hz	1430rpm	4

6.6 FUZZY LOGIC CONTROLLER

The FLC controls the process by incorporating the human knowledge into a pattern containing the relationship between output and input. The membership functions and rule table are generated with the experience of system operation. The rules are framed as per the requirement of the speed. FLC performance will be better when more number of rules is framed. The major processes of the FLC include fuzzification, rule base, inference and defuzzification. Defuzzification provides output in terms of crisp value on the basis of defined set of membership function and rules. The block diagram of the FLC is given in Fig. 6.3.

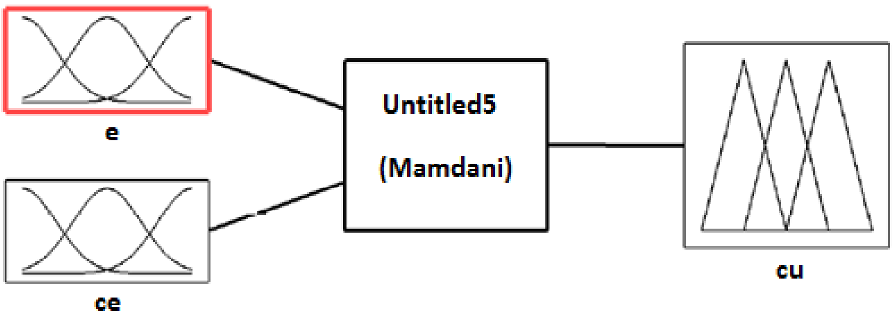

Fig. 6.3 Block diagram of FLC.

In the developed algorithm, FLC is used to find the torque command current (i_{qs}^{*}) from the actual and reference speed under the variation of load torque and parameters. The normalized values of two input linguistic variables in terms of speed error (*e*), change in speed error (*ce*) and defuzzified value of torque command (*cu*) as an output are reflected. Centroid and Mamdani methods are used for defuzzification and fuzzification respectively. The normalized membership functions (MF) of error (e), change in error and output are revealed in Fig. 6.4, Fig. 6.5 and Fig. 6.6. A 3-D surface view of all the three variables is shown in Fig. 6.7. It is observed from Fig. 6.7 that the output cu is positive big when both error and change of error are positive big. The FLC is implemented with 25 linguistic rules as shown in Table 6.2 and gives the change of the output in terms of two inputs. The fuzzy sets used are: NS (negative small), NB (negative big), Z (zero), PS (positive small) and PB (positive big). The linguistic rules are in the form of IF-THEN rules. For example if *e* is PS and *ce* is Z then *cu* is PS as highlighted in Table 6.2.

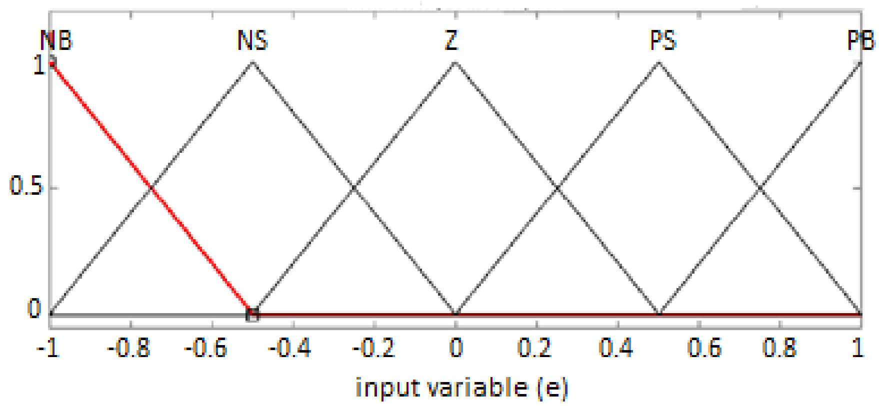

Fig. 6.4 MF for speed error (e)

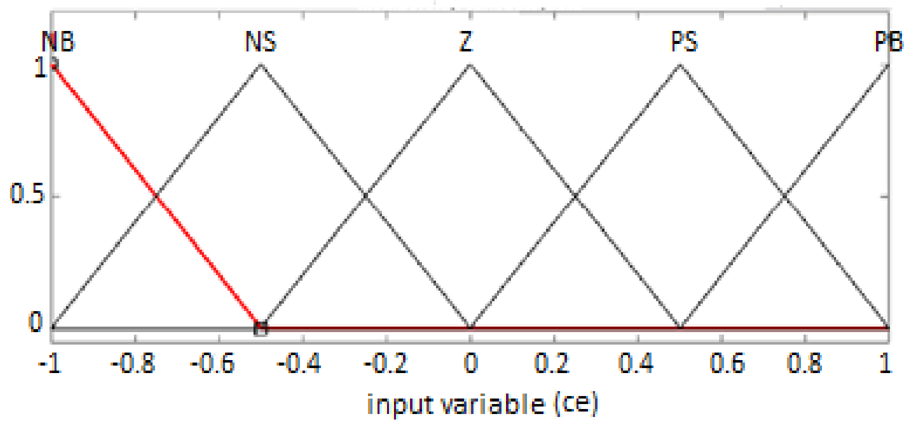

Fig. 6.5 MF for change in speed error (ce)

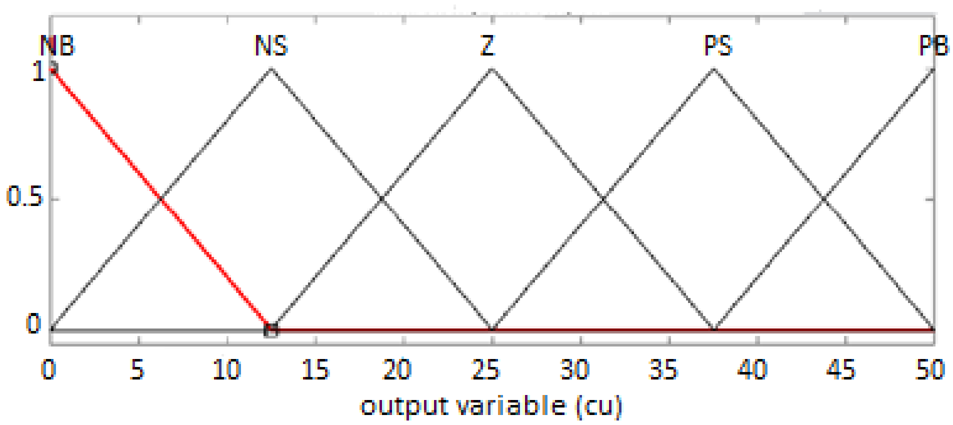

Fig. 6.6 MF for output (cu)

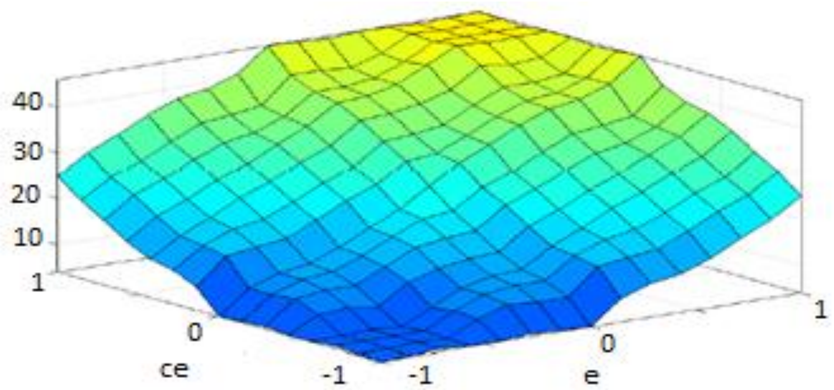

Fig. 6.7 3-D surface view

Table 6.2: Fuzzy logic controller rule table

e \ ce	NB	NS	Z	PS	PB
NB	NB	NB	NB	NS	Z
NS	NB	NB	NS	Z	PS
Z	NB	NS	Z	PS	PB
PS	NS	Z	**PS**	PB	PB
PB	Z	PS	PB	PB	PB

6.7 RESULTS AND DISCUSSIONS

The dynamic behavior of the IM drive is discussed for different operating conditions like sudden variation in speed and sudden change in load torque. The operation of the drive at rated speed with varying load torque and operation at rated torque with varying speed is demonstrated with PI controller and FLC.

6.7.1 Performance of IM Drive during Sudden Change in Speed and Load Torque

The dynamic behavior of the IM drive using PI controller for a sudden variation in speed and load torque is analyzed. The simulation results for total loss optimization algorithm are shown in the Fig. 6.8 and without optimization are shown in Fig. 6.9. A step change in speed is applied at t = 0.4 sec from a speed of 49.9 rad/sec (33% of rated value) to 149.7 rad/sec (rated value) and a step change in torque from 5 Nm (33% of rated torque) to 15Nm (rated torque) is applied at t = 0.7 sec. Initially to develop the required starting torque motor takes high current with low frequency. But when motor picks up the speed, then frequency starts increasing with the decreasing of stator current and the motor speed starts tracking the commanded speed. Similarly, the electromagnetic torque developed in the machine follows the commanded torque by maintaining a proportionate value for the stator current. Some ripples in the the developed torque and in current are observed due to switching effect of the current controller. It is also observed that in Fig. 6.8, torque ripples during transient period are less as compared to that in Fig. 6.9, where optimization is not used.

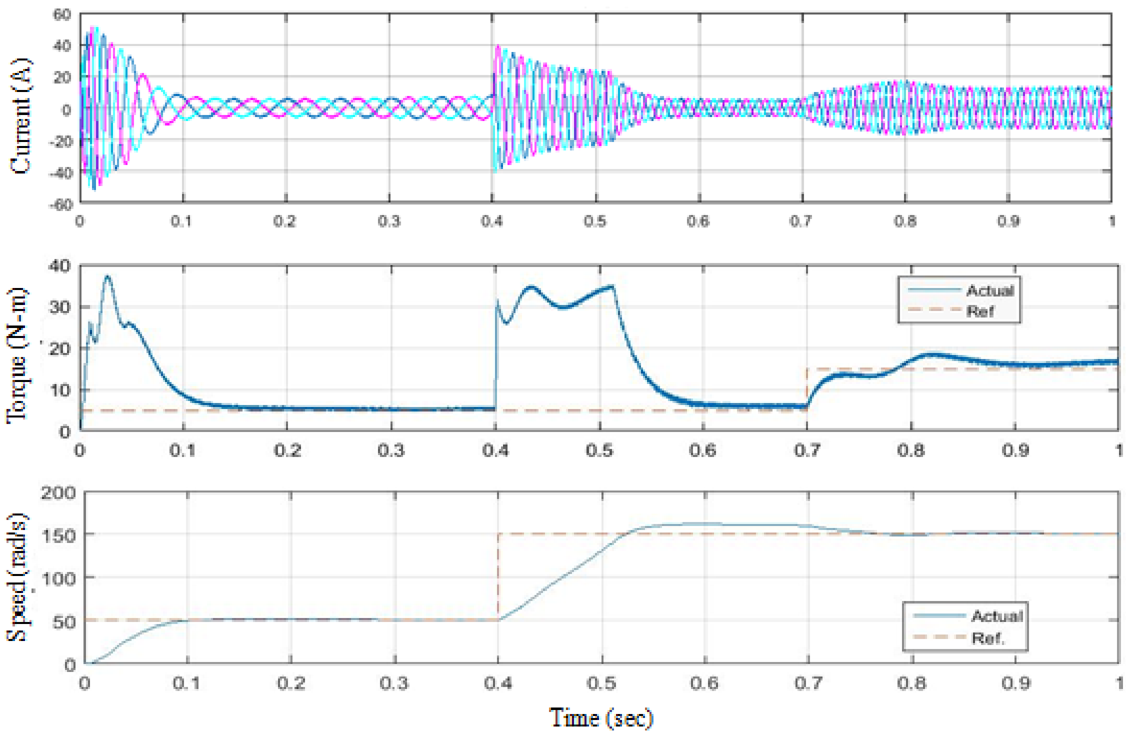

Fig. 6.8 Dynamic response of IM for current, torque and speed
with total loss optimization

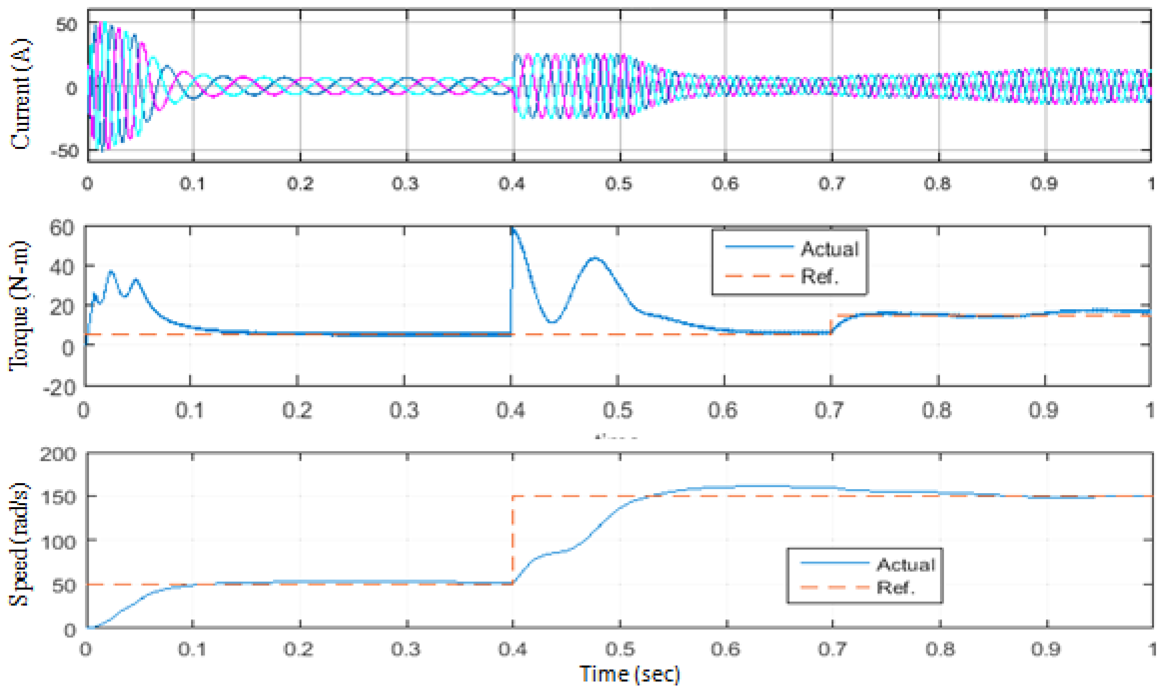

Fig. 6.9 Dynamic response of IM for current, torque and speed
without optimization

6.7.1.1 Effect of change in speed and torque on efficiency

Fig. 6.10, Fig. 6.11 and Fig. 6.12 show the efficiency of the IM drive system using PI controller and FLC for without optimization, with iron loss optimization and with total losses optimization respectively. Very small improvement in efficiency of the IM drive is obtained with the use of FLC as compared to the PI controller.

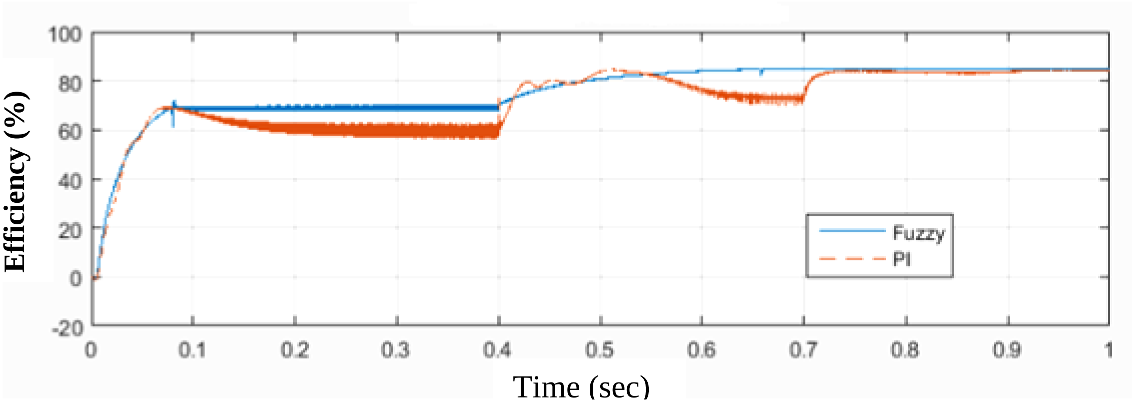

Fig. 6.10 Efficiency of IM drive without optimization

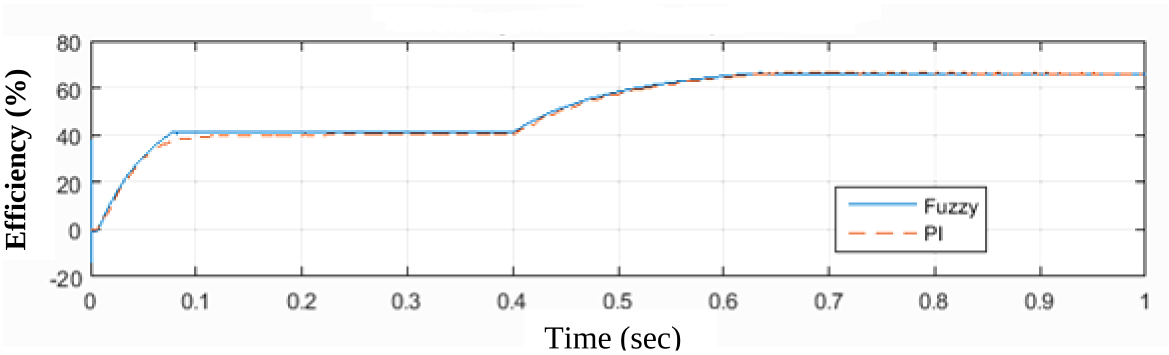

Fig. 6.11 Efficiency of IM drive with iron loss optimization

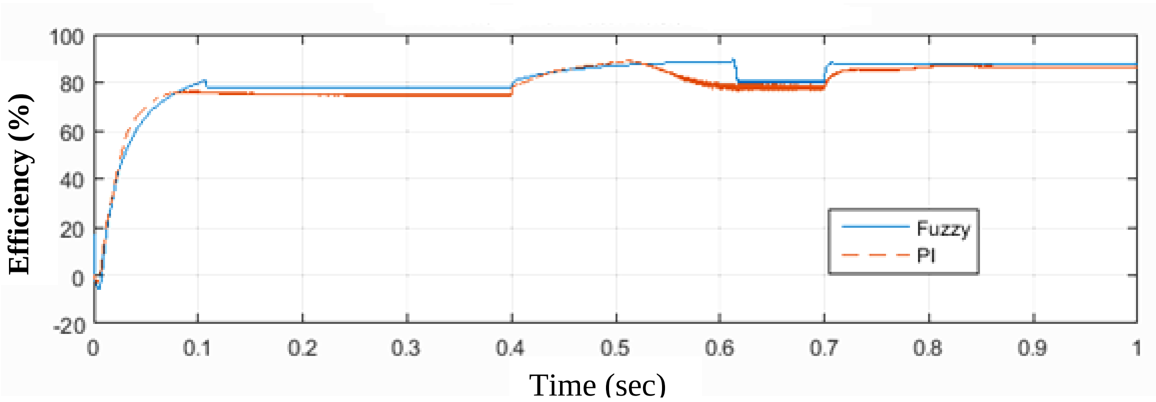

Fig. 6.12 Efficiency of IM drive with total losses optimization

Fig. 6.13 and Fig. 6.14 show the dynamic variation of efficiency of the IM drive system based on total losses optimization, iron loss optimization and without optimization using the PI controller and FLC respectively. The simulation results showed an improvement in efficiency of the IM drive with total losses optimization as compared to the iron loss optimization and without optimization. Fig. 6.14 with the use of FLC shows better response as compared to the Fig. 6.13 with the use of PI controller during transient period.

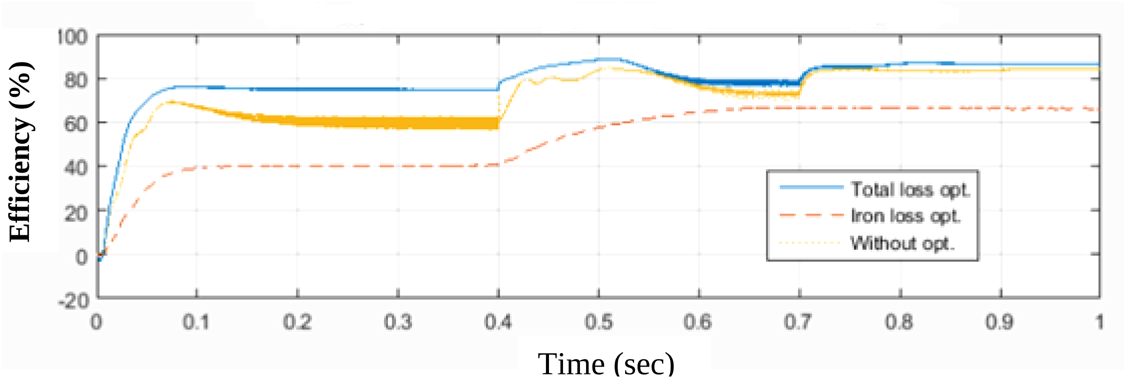

Fig. 6.13 Efficiency with PI controller

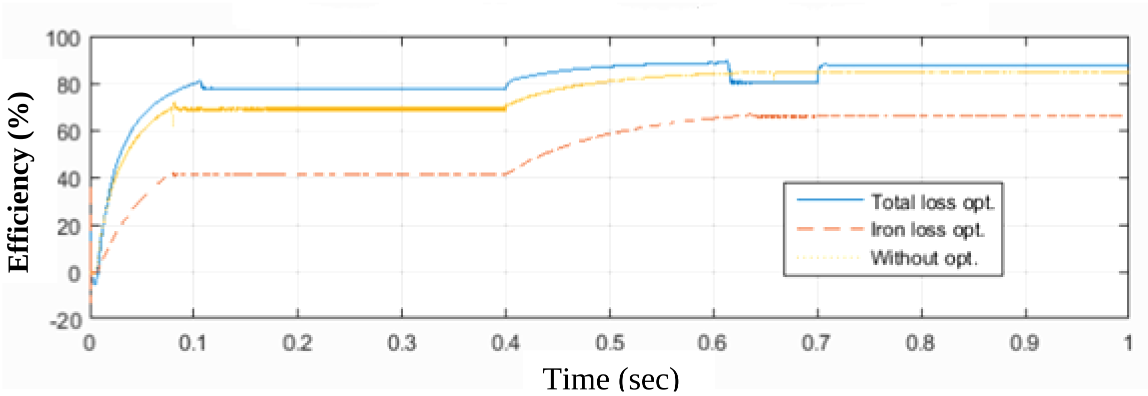

Fig. 6.14 Efficiency with fuzzy controller

6.7.1.2 Effect of optimization algorithm on speed

Fig. 6.15, Fig. 6.16 and Fig. 6.17 show the dynamic speed response of the IM drive using PI controller and FLC for without optimization, with iron loss optimization and with total losses optimization respectively. Better and smooth speed response is observed for the IM drive with the use of FLC as compared to the PI controller.

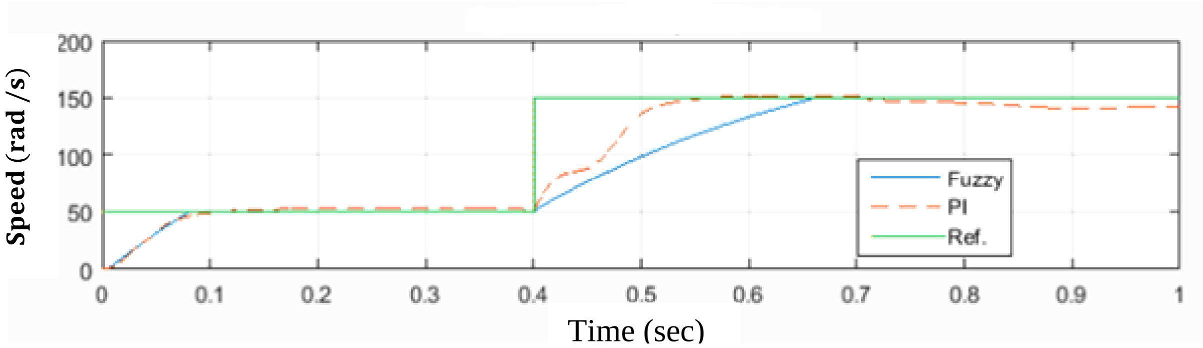

Fig. 6.15 Speed response of IM drive without optimization

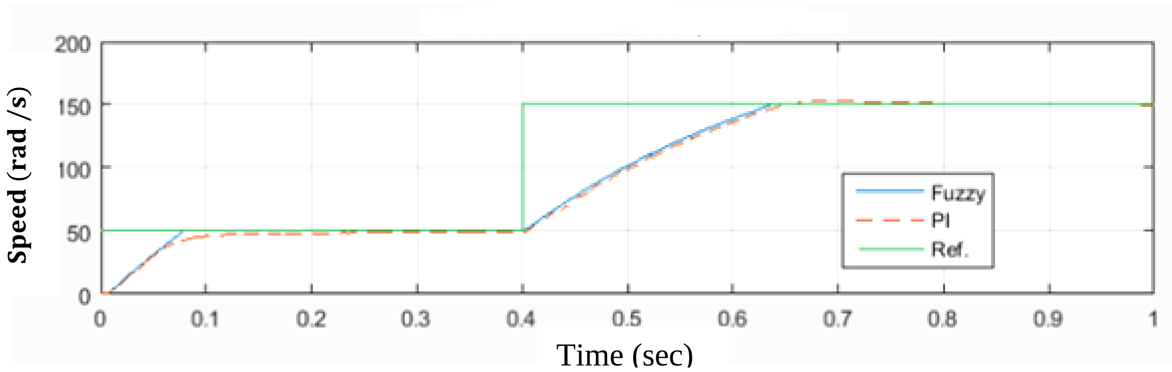

Fig. 6.16 Speed response of IM drive with iron loss minimization

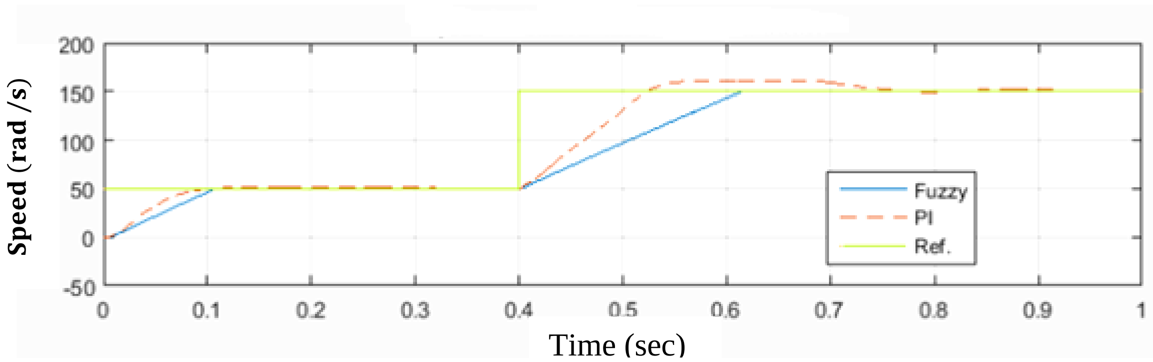

Fig. 6.17 Speed response of IM drive with total losses minimization

Fig. 6.18 and Fig. 6.19 show the speed performance based on total losses optimization, iron loss optimization and without optimization of the IM drive system for the PI and fuzzy controller respectively. The simulation result shows that the motor speed tracks the commanded speed more smoothly with the use of fuzzy controller as compared to the PI controller for all the cases of optimization.

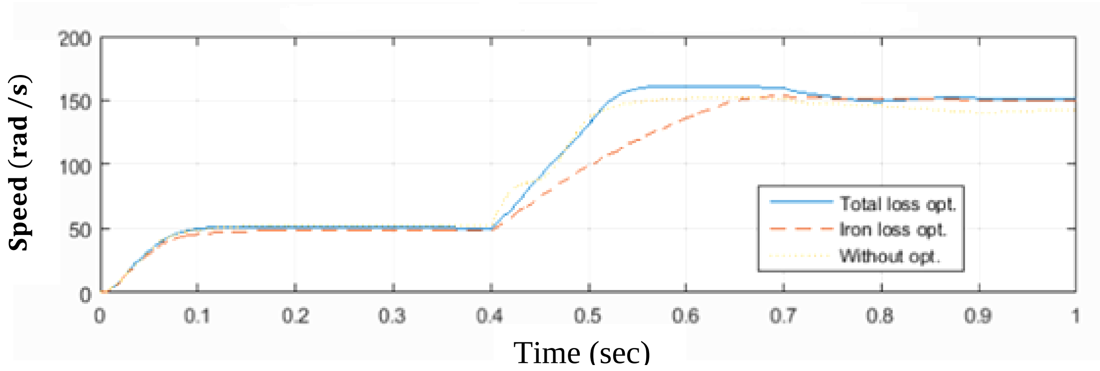

Fig. 6.18 Speed response of IM drive with PI controller

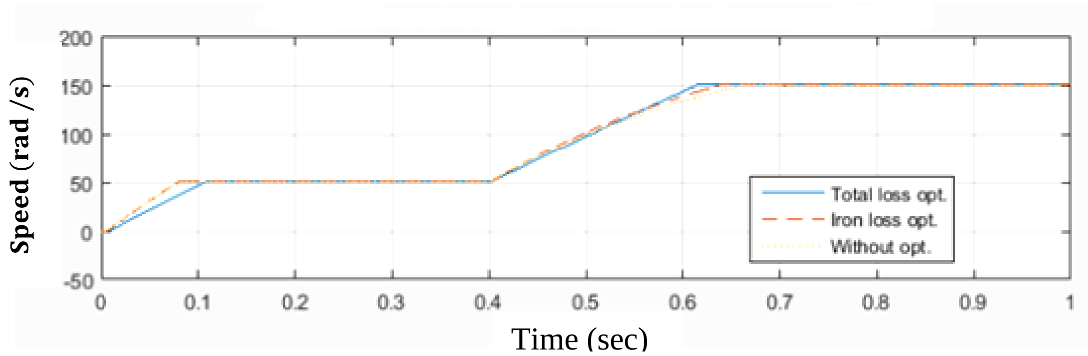

Fig. 6.19 Speed response of IM drive with FLC

6.7.1.3 Effect of optimization algorithm on torque

Fig. 6.20, Fig. 6.21 and Fig. 6.22 show the dynamic torque response of the IM drive using PI controller and FLC for without optimization, with iron loss optimization and with total losses optimization respectively. Reduction in the pulsation of the torque of the IM drive is observed with the use of FLC as compared to the PI controller. Moreover, the reduction in the torque pulsation is more pronounced for the iron loss minimization scheme with the use of FLC.

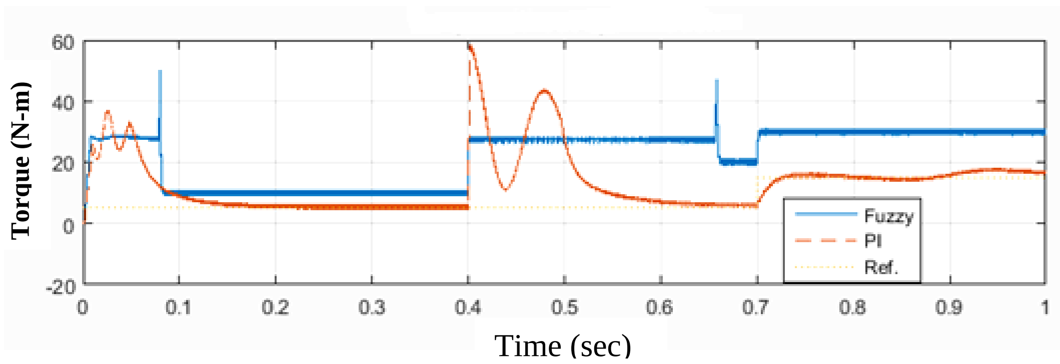

Fig. 6.20 Torque response of IM drive without optimization

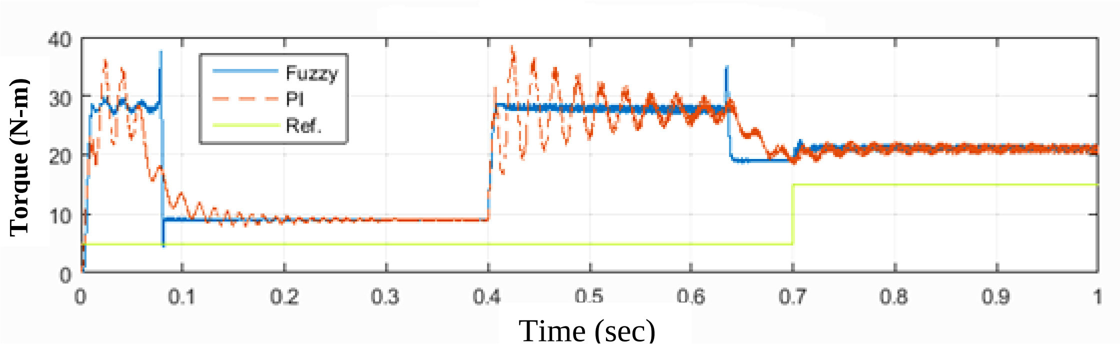

Fig. 6.21 Torque response of IM drive with iron loss optimization

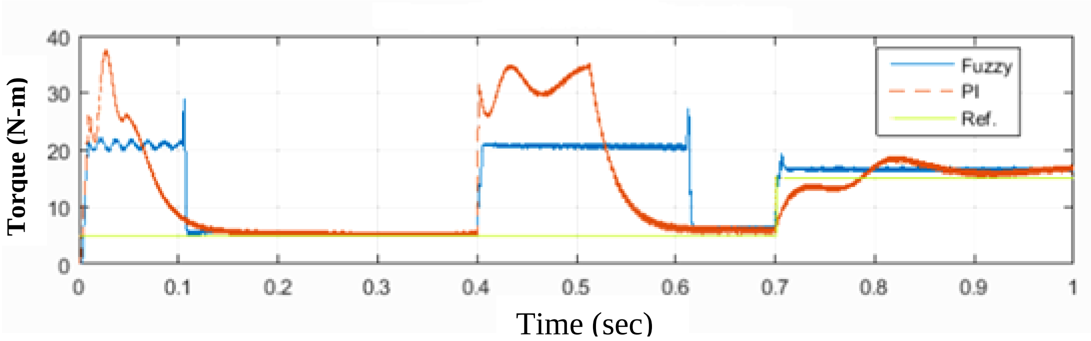

Fig. 6.22 Torque response of IM drive with total losses optimization

Fig. 6.23 and Fig. 6.24 show the dynamic torque response of the IM drive with total losses optimization, iron loss optimization and without optimization using the PI controller and FLC respectively. Higher reduction in the torque pulsation is observed for total losses optimization with the use of PI controller.

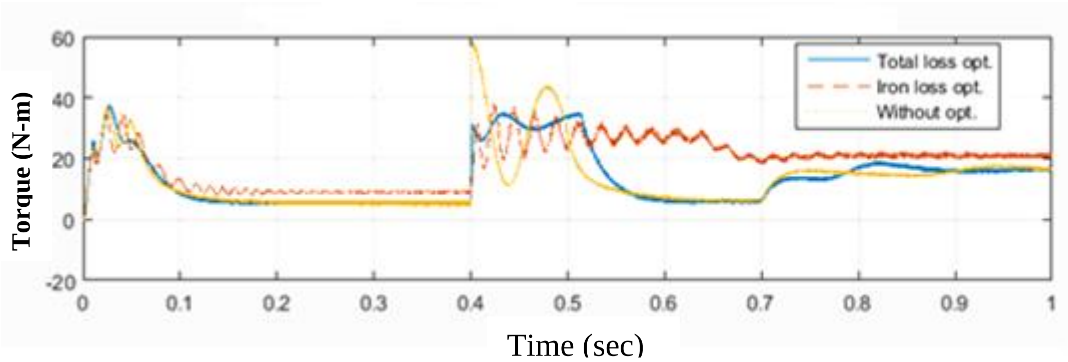

Fig. 6.23 Torque response of IM drive with PI controller

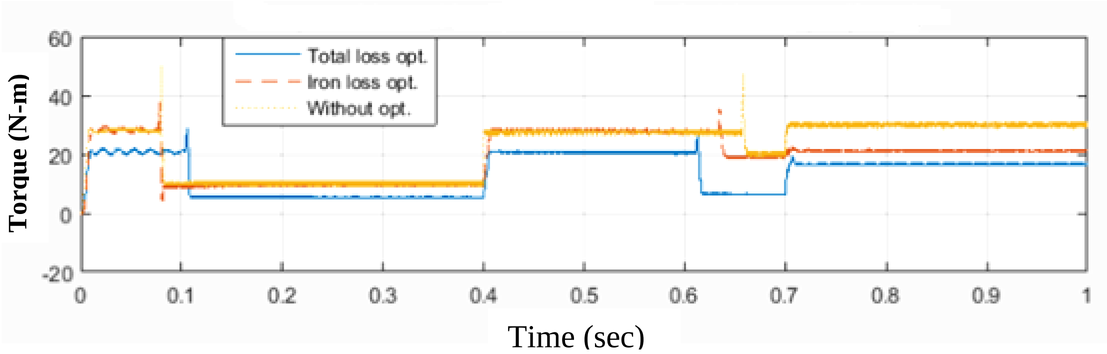

Fig. 6.24 Torque response of IM drive with fuzzy controller

6.7.2 Performance of IM Drive under Different Speed and Torque

The performance of the IM drive for different speed and different torque conditions for without optimization, with iron loss optimization and with total losses optimization using PI controller and FLC is tabulated in Table 6.3. It is observed that the efficiency is greatly improved at all operating conditions with total losses optimization. At rated speed and light load condition, efficiency increases about 9% by using PI controller and about 2% by using FLC for total losses optimization as compared to without optimization. Similarly at 25% rated speed and light load condition, efficiency increases about 13% by using PI controller and about 5% by using FLC.

6.7.2.1 Performance analysis at rated speed condition

Fig. 6.25 and Fig. 6.26 show the efficiency of the IM drive based on total losses optimization, iron loss optimization and without optimization using the PI controller and FLC respectively at the rated speed operation under different load conditions. Improvement in efficiency of the IM drive is observed at rated speed with increase in the torque for both PI controller and FLC. It is seen that the percentage improvement in efficiency achieved with total losses optimization and without optimization control is more as compared to the iron loss optimization. Slight improvement in efficiency is observed with iron loss optimization for both PI controller and FLC at rated speed.

Table 6.3: Performance under different speed and load torque

Eff. Load	Without optimization		Iron loss optimization		Total loss optimization	
	PI	Fuzzy	PI	Fuzzy	PI	Fuzzy
100% of rated speed in rad/sec = 149.7						
0.2	62.56	72.83	65.99	65.60	71.12	74.32
0.4	75.45	76.57	66.32	66.94	74.61	80.34
0.6	75.12	80.54	65.14	65.73	78.12	83.69
0.8	82.68	83.03	64.42	64.91	82.69	84.88
1.0	83.23	84.28	62.93	64.54	84.71	85.78
75% of rated speed in rad/sec = 112.27						
0.2	64.18	73.34	59.42	59.01	73.46	75.67
0.4	68.43	78.47	60.52	60.62	75.13	81.69
0.6	75.71	80.55	60.86	60.91	79.35	82.01
0.8	81.37	81.47	60.91	60.85	81.67	82.21
1.0	81.21	81.39	60.51	60.64	81.91	82.43
50% of rated speed in rad/sec = 74.85						
0.2	56.64	71.58	50.52	50.62	72.03	75.08
0.4	72.05	74.13	50.39	50.43	74.92	76.75
0.6	75.31	76.87	50.65	50.52	76.78	78.19
0.8	77.81	77.63	50.89	51.47	77.75	77.83
1.0	78.15	79.13	51.32	52.82	78.35	79.71
25% of rated speed in rad/sec = 37.42						
0.2	51.12	58.67	33.04	33.53	63.69	63.93
0.4	54.61	63.23	32.17	34.34	63.71	64.51
0.6	58.79	64.77	31.47	34.74	63.98	66.72
0.8	63.93	65.32	30.81	34.69	64.43	65.98
1.0	65.43	65.42	30.49	34.75	65.61	66.32

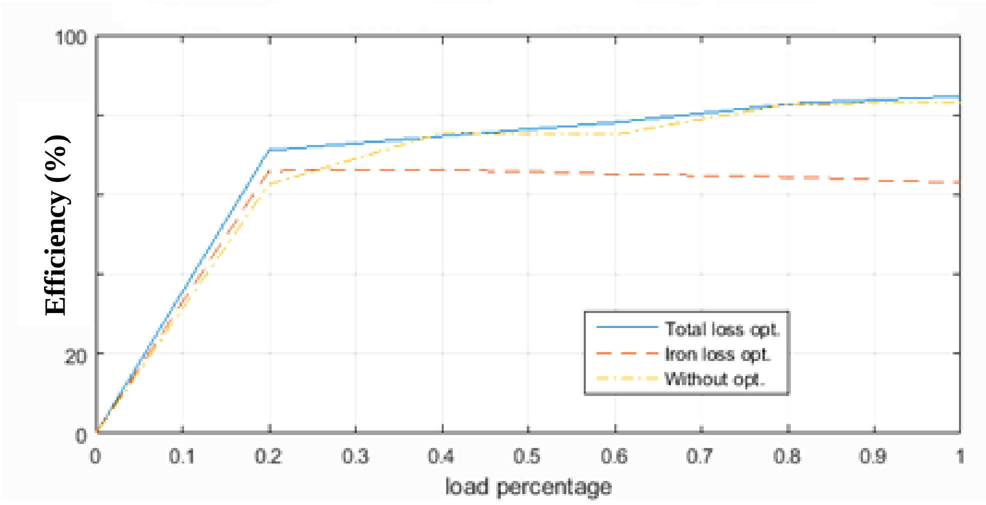

Fig. 6.25 Efficiency using PI controller

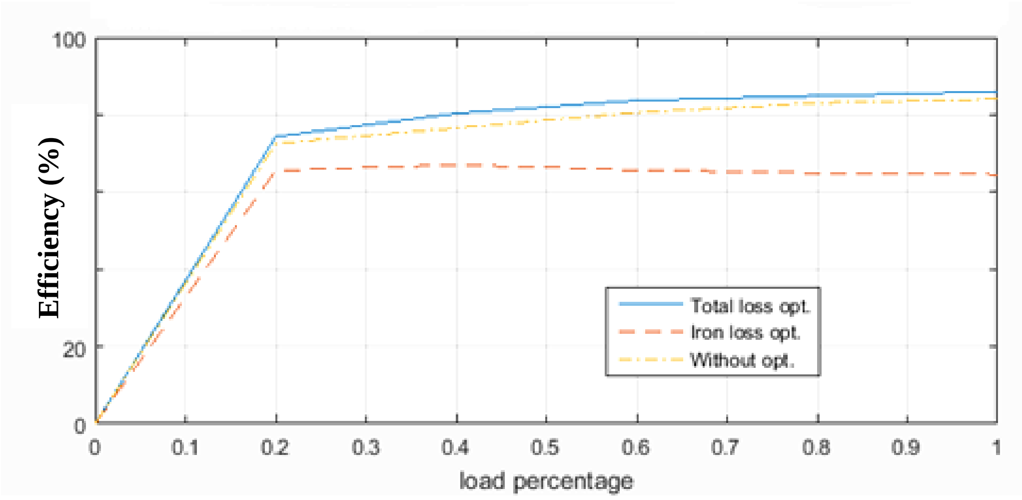

Fig. 6.26 Efficiency using FLC

6.7.2.2 Performance analysis at rated torque condition

Fig. 6.27 and Fig. 6.28 show the efficiency of the IM drive based on total losses optimization, iron loss optimization and without optimization using PI controller and FLC respectively at the rated torque with different operating speeds. With the increase in motor speed from 25% to rated value, 19.1 and 19.46 percent improvement in efficiency of the IM drive is observed with the use of PI controller and FLC respectively for total losses optimization. Similarly, 17.8 and 18.86 percent improvement in efficiency of the IM drive is observed with the use of PI controller and FLC respectively for without optimization. Efficiency of the IM drive for total losses optimization and without optimization is comparable but higher than the iron loss optimization.

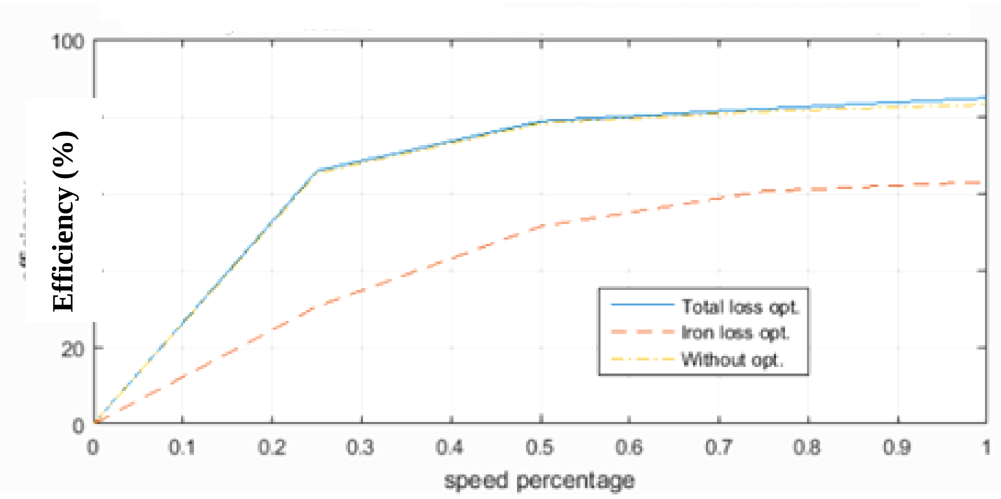

Fig. 6.27 Efficiency during variable speed operation for PI

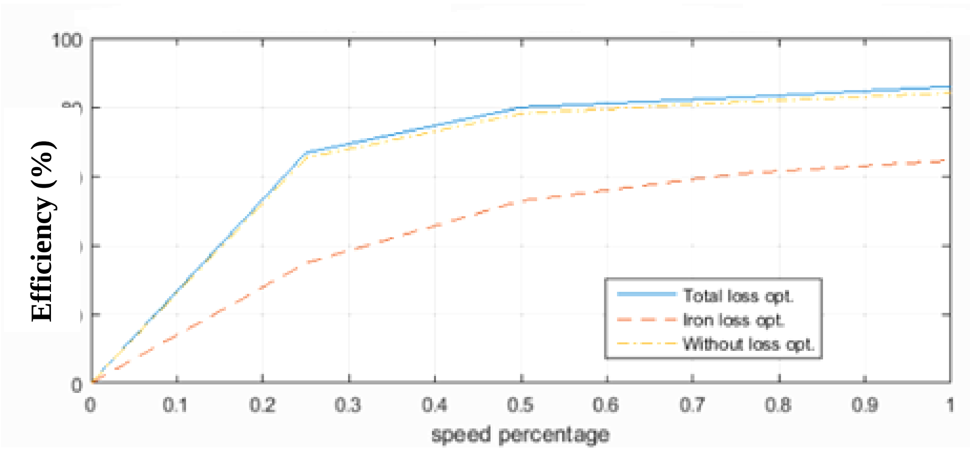

Fig. 6.28 Efficiency during variable speed operation for FLC

6.8 CONCLUSION

Efficiency optimization in IFOC controlled IM drive is implemented by using the optimal control of d-axis current component using a loss model controller. The developed optimization method minimizes iron losses and the total motor losses to optimize the efficiency of the IM drive. The scheme has been implemented using both fuzzy logic controller and PI controller. The performance analysis of IM drive is carried out for sudden change in speed and load torque condition and on different speed and different torque conditions. Efficiency of the IM drive system is improved significantly with total losses optimization algorithm as compared to the iron loss optimization and without optimization.

CHAPTER VII

EFFICIENCY OPTIMIZATION IN IFOC IM DRIVE BASED ON SEARCH CONTROL

7.1 GENERAL

Induction motors are commonly used in industries because of their low operational charge and maintenance. So there is a great demand to improve the efficiency of induction motors for different operating conditions to reduce the energy consumption. Efficiency improvement can have major impact on the environment and electricity demand. A new algorithm of searching the flux current component for efficiency optimization of IM drives is described in this chapter. This new algorithm can be considered as an alternative to the search control problems. The online optimization of efficiency of vector controlled induction motor drives through optimal search control (SC) approach is discussed. This approach uses the optimal control of the flux producing current component to reduce the core losses and to minimize the measured dc-link power to the inverter at light load conditions. The proposed drive system is simulated in a MATLAB/ Simulink and the improvement in the efficiency of the drive system is demonstrated.

Efficiency improvement and energy saving in recent years are one of the most important objectives and have been getting a lot of attention by the researchers to maximize the efficiency of electrical motors. Induction motor (IM) operation is very efficient at rated load and rated flux but if IM operates at light loads with rated flux for most of the time during its life span it causes significant core loss and consequently decreases the efficiency of the IM. Optimum efficiency of IM can be obtained by controlling the flux according to the load. A number of the techniques have been proposed in literature for efficiency improvement through flux programming, thereby minimizing the motor losses and maximizing the efficiency. These loss minimization algorithms are divided into two main parts: the loss model control technique (LMC) and the search control technique (SC). The LMC technique is faster than the SC technique but with variation in motor parameters its performance deteriorates. The SC technique iteratively searches the optimal operating point till the considered input power settles to the minimum value. The SC is independent of motor parameters but it is slower in response and bears torque ripples.

Optimal flux level is searched through Rosenbrock method to determine the minimum input power by using fuzzy controller [171]. Efficiency improvement of IM is discussed through optimal control by using loss model control (LMC) and SC that includes artificial neural network, genetic algorithm, fuzzy logic, differential evolution in optimization, expert systems and nature inspired algorithms [175]. In order to minimize the DC link power, three techniques based on the power-flux gradient, reducing the flux current component in a smooth manner and hybrid method of loss model and search control for the optimization of vector controlled IM drives are presented [181]. The optimal rotor flux value is obtained through golden section technique such that the input power of the drive system is minimum [182]. LMC was compared with SC and found that the LMC is more suitable in vector control because the optimal value of flux can be obtained in a small time but in search control the flux oscillates around the optimal value. Optimization of efficiency based on fuzzy logic approach was achieved for induction motor drives [150]. The flux level at the lowest point can be calculated by using the quadratic interpolation method [152]. Relationship between flux-producing current component and ohmic losses power was formulated to get the optimal value [153]. Input power minimization can be investigated through loss model controller (LMC) by using particle swarm optimization (PSO) and search controller to improve the result of the drive system.

In this chapter a novel online efficiency optimization algorithm called deep valley search algorithm has been used to minimize the power input of an induction motor drive. Dc-link power as a controlled variable is used for searching the optimal flux current component. The proposed algorithm is simple and can be realized easily. The results obtained shows good dynamic response without varying the commanded speed. As compared to the ramp search control algorithm [147], where flux reduces from rated value to the flux corresponding to the light load, the proposed algorithm can be applied for load transition from rated value to light load in downward direction as well as from light load to the higher load in upward direction also. If the power input difference between the two successive measurements is small even than the proposed search process continues and does not depend on higher step size for its operation.

7.2 DEEP VALLEY SEARCH ALGORITHM FOR OPTIMIZATION

At light load on IM the power factor and efficiency can be made better by adjusting the flux value in accordance with the speed and load. The proposed algorithm searches optimum flux by measuring the dc link power (input power) of the drive. The torque current command (i_{qs}^*) increases with the decrease of the flux command current (i_{ds}^*) current such that the torque developed remains constant. The copper loss increases with decrease of flux but the iron loss and the total losses (converter and induction motor) decreases which results in reduction of dc link power. The search process is continued till the power reaches at lowest dc-link power point. This is realized easily by utilizing the deep valley search algorithm and can be considered as an online efficiency optimization for an IM drive. The search process starts by decreasing the value of commanded flux current component for light load through a step value and it will go on decreasing till the power changes its direction and optimal flux value is obtained for a particular speed and torque.

The novel deep valley search algorithm mathematically represented as:

$$i_{ds}^{*}(n+1) = i_{ds}^{*}(n) + k\,\delta\,, \quad \left\{ \begin{array}{l} k = -1:\ \text{if}\,\Delta P(n) < 0 \\ k = +1:\ \text{if}\,\Delta P(n)\ > 0 \end{array} \right\}$$

Where δ is the step value which can be varied depending on whether the requirement of convergence is fast or slow and dc link power, $\Delta P(n) = P(n) - P(n-1)$

Fig. 7.1 represents the flowchart of deep valley search control algorithm

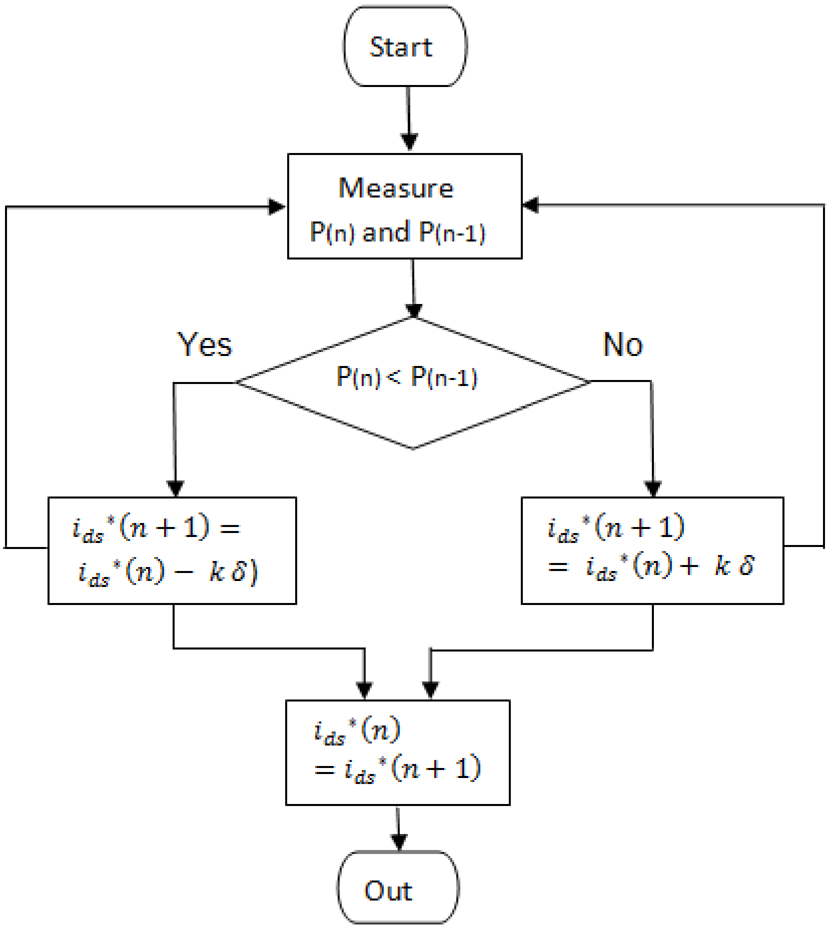

Fig. 7.1 Flow chart of deep valley search control

Table 7.1: Ratings of three phase IM

Rated power	Input voltage	Input current	Input frequency	Rated speed	No. of Pole
2.2kW	430 V ±10%	4.8A	50 Hz	150rad/s	4

7.3 IMPLEMENTATION OF DEEP VALLEY SEARCH ALGORITHM ON AN IVC IM DRIVE

Fig. 7.2 is the block diagram of an indirect vector controlled IM drive which consists of a voltage source inverter (VSI) along with the efficiency optimization control algorithm. The performance of the IM for a 2.2 kW, 430 V, 50 Hz, 1430 rpm IM is simulated in the Matlab/ Simulink. The speed control feedback loop generates torque command current (i^*_{qs}), and the flux command current (i^*_{ds}) is obtained according to the implemented search control algorithm. In order to follow the reference current commands, motor currents are controlled using a hysteresis current controller. The dc-link power P_{dc} is considered as a control variable in order to minimize the overall drive system losses. The dc-link power to the inverter is calculated by the product of the dc link current and dc link voltage. The dc link voltage is considered to be constant and dc link current that flows from source to inverter is responsible for variation in input power. The unit vector is generated from the slip frequency and rotor speed. Rotor speed is sensed and slip is generated in feed forward manner as shown in the block diagram.

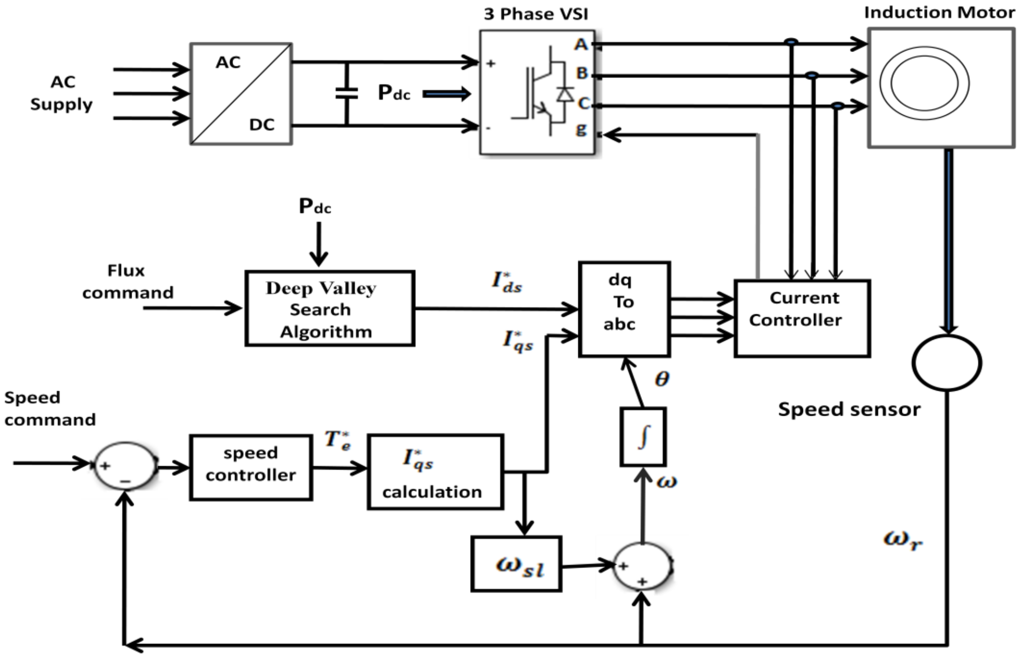

Fig. 7.2 Vector controlled induction motor drives

7.3.1 Evaluation of Deep Valley Search Algorithm on IM Drive

The simulation study of the complete drive system is carried out to evaluate the effectiveness of the proposed optimization algorithm for a 2.2 kW, 430 V, 50 Hz, 1430 rpm induction motor. The proposed algorithm block in simulation is used to measure the dc link power at two different instants P(n), P(n-1) and depending on their comparison, +ve or –ve sign is generated to show whether the power is increasing or decreasing. The simulation result of the algorithm in terms of step value changes in flux command current (i_{ds}^*) as a function of dc-link power is shown in the Fig. 7.3, where an abrupt change of torque from 0.2 pu to 0.6 pu at 7 sec is applied for a speed command of 75 rad/sec. The flux command current (i_{ds}^*) up to 2 sec is kept at rated value to get the fast transient response and after that it is stepped down in terms of cumulative sum until the drive system achieves the optimum value of i_{ds}^*, which is obtained at 6.2 sec for a load torque of 0.2 pu. With the change of load torque of 0.6 pu at 7 sec, it is stepped up in terms of cumulative sum until the drive system achieves the optimum value of i_{ds}^*, which is obtained at 10.5 sec. It is observed that the flux command current oscillates about the optimal point after achieving the optimal value at 6.2 sec for a load torque of 0.2 pu and at 10.5 sec for a load torque of 0.6 pu. The cumulative sum adds the steps value to the flux current to generate the optimal flux command current. It is observed that it takes large time to achieve the optimal value. This time taken can be reduced by increasing the step size but it will increase the pulsation in torque. So it is not recommended for smooth and high performance drive applications. But it is not sensitive to parameter variations and can be used for drives meant for routine task with considerable energy savings.

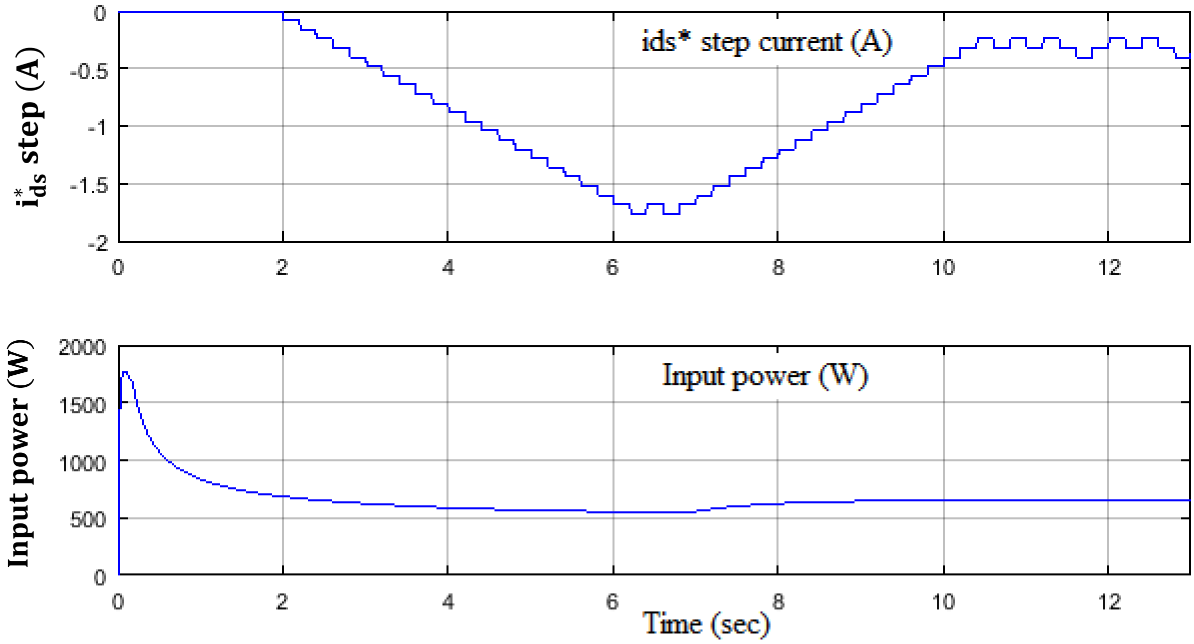

Fig. 7.3 Search algorithm ($k\ \delta$) as a function of input power with sudden change of load torque

7.4 PERFORMANCE ANALYSIS OF IVC IM DRIVE

The simulation results of the indirect vector control IM drive system with deep valley search algorithm is analyzed under different operating conditions.

7.4.1 Performance Study of IM Drive at Rated Speed and Light Load

The performance of IM drive system with the proposed algorithm at rated speed and light load is analyzed. A speed command of 150 rad/sec (rated speed) and a torque of 3 Nm (20% of rated value) is applied at t = 0 sec. Initially the motor draws high power and current to build up the necessary starting torque. The SC algorithm starts at 2 sec and reaches at its optimum value at 6.2 sec. and after that the flux current command oscillates around the optimum value. The response of the dc-link power (input power), speed and torque is shown in Fig. 7.4; whereas the response of flux command current, developed flux current and torque producing current is shown in Fig. 7.5. As the magnetizing current decreases, the torque current increases so that the torque remains constant.

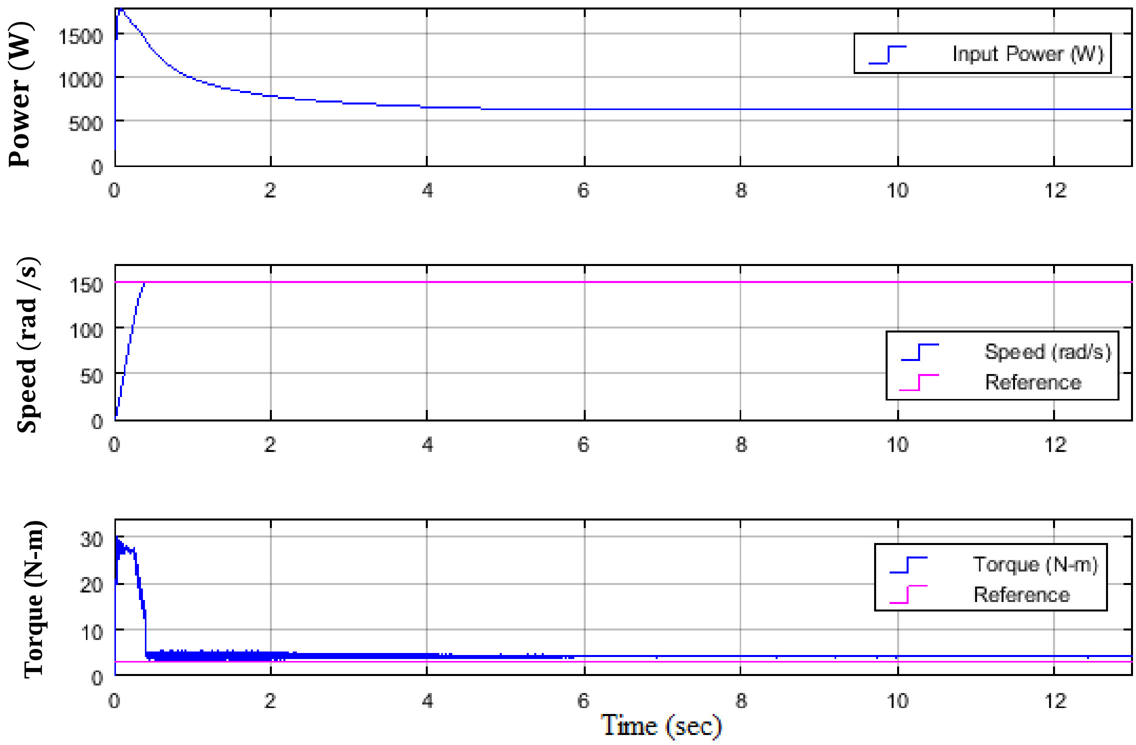

Fig. 7.4 Drive performance for input power, speed and load torque

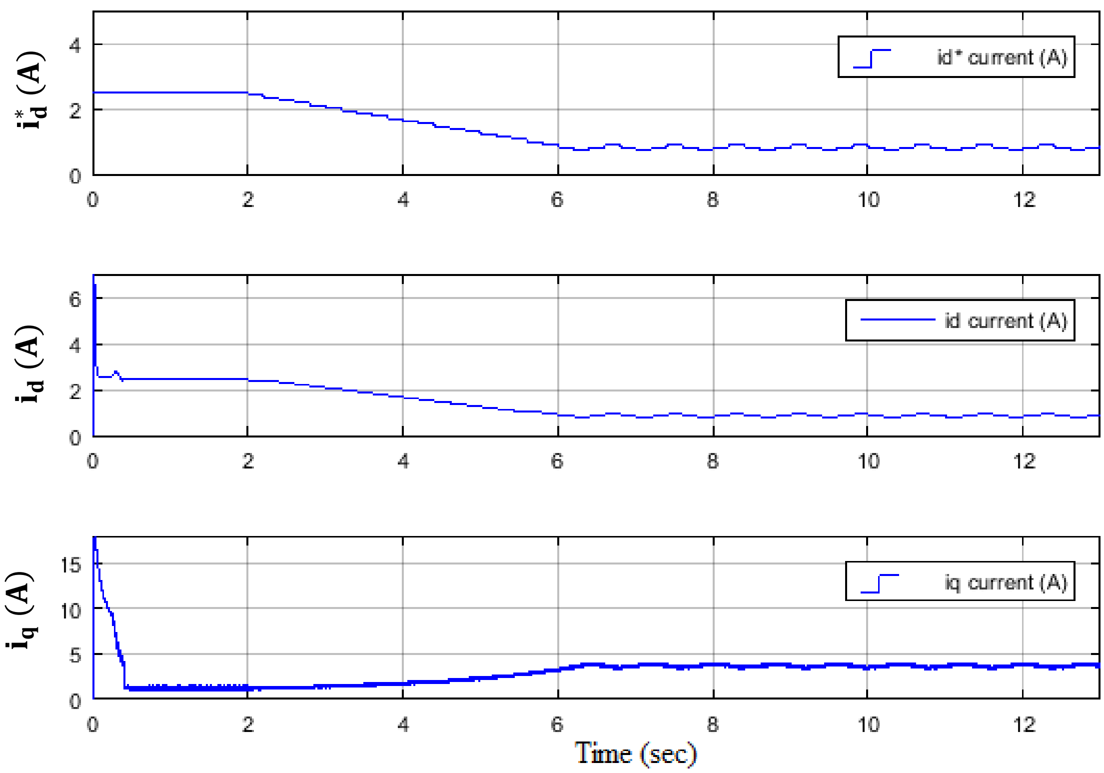

Fig. 7.5 Drive performance for current components i_d^* , i_d and i_q at speed of 75 rad/sec and load torque of 3 Nm

7.4.2 Performance Study of IM Drive with Sudden Change in Speed

The performance of IM drive system with the proposed algorithm for a sudden variation in speed is analyzed. A step change in speed command is applied at t = 7 sec from a speed of 75 rad/sec (50% of rated speed) to 120 rad/sec (80% of rated speed) and forcing the drive system to switch to a dynamic mode. Initially and at the time of speed transition the motor draws high power and current to develop the necessary torque. The SC algorithm starts at 2 sec and reaches at its optimum value at 6.2 sec. and after that the flux current command oscillates at around the optimum value. The response of the dc-link power, speed and torque are shown in Fig. 7.6 whereas the response of flux command current, developed flux current and torque producing current are shown in Fig. 7.7. The motor speed follows the commanded speed and the electromagnetic torque developed tracks the commanded torque by maintaining a balanced value for the current. Small ripples in the flux and developed torque current are seen due to search control.

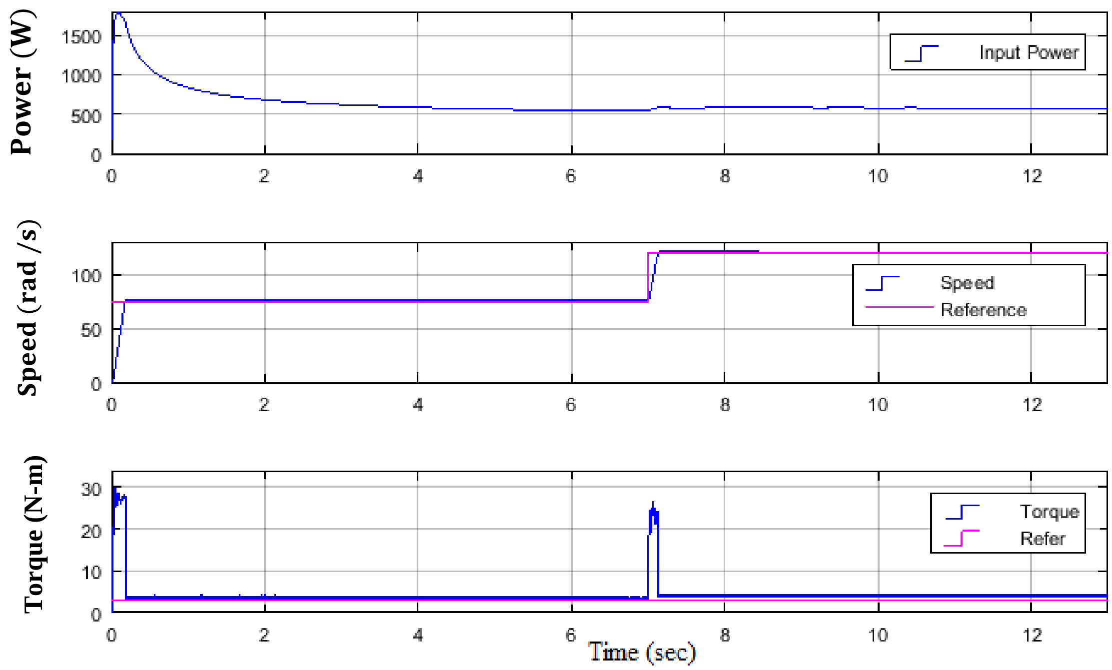

Fig. 7.6 Drive performance for input power, speed and load torque with sudden increase of speed

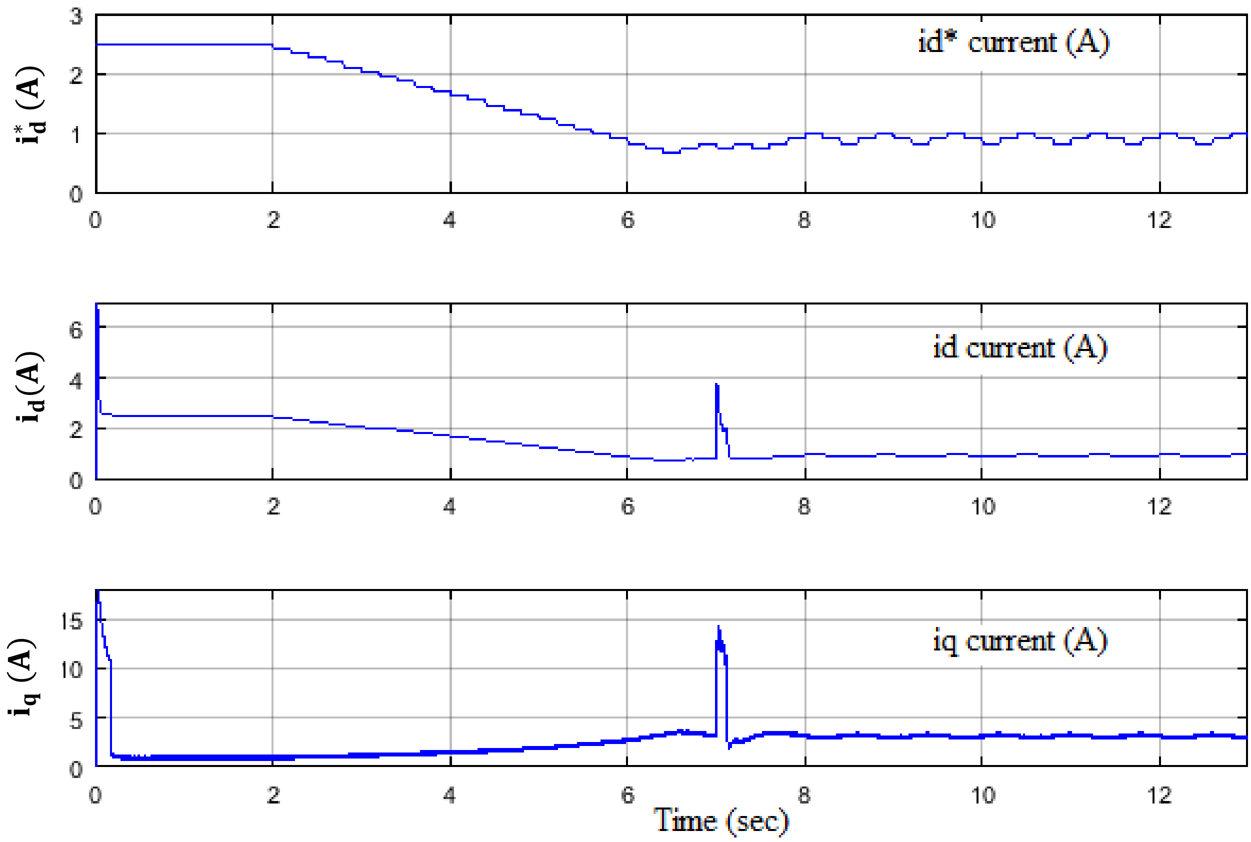

Fig. 7.7 Drive performance for current components i_d^* , i_d and i_q
with sudden increase of speed

7.4.3 Performance Study of IM Drive with Sudden Change in Load Torque

The performance of IM drive system with the proposed algorithm is evaluated for a sudden change in torque at a speed of 75 rad/sec. A step change in load torque command from 3 Nm (20% of rated torque) to 9Nm (60% of rated torque) is applied at t = 7 sec. Initially and at the time of torque transition the motor draws high torque producing current to develop the necessary torque without any change in speed. The SC algorithm starts at 2 sec and reaches at its optimum value at 6.2 sec. for 3 Nm load torque and at 10.5 sec for 9 Nm load torque, after which the flux current command oscillates at around the optimum value. Fig. 7.8 and Fig. 7.9 show the various dynamic responses under changing load conditions. Drive performance for id current and rotor flux are also shown in Fig. 7.10. The motor speed follows the commanded speed and developed torque by the motor follows the commanded torque by maintaining a proportionate value for the current which shows the capability of the proposed control approach to handle with sudden variations in working condition. Some ripples in the torque and flux current are seen because of search control. With the increase of load, dc-link power increases by maintaining a proportionate value for the flux producing current and torque producing current components. When flux current component decreases the torque producing current component increases correspondingly so that the torque developed remains constant.

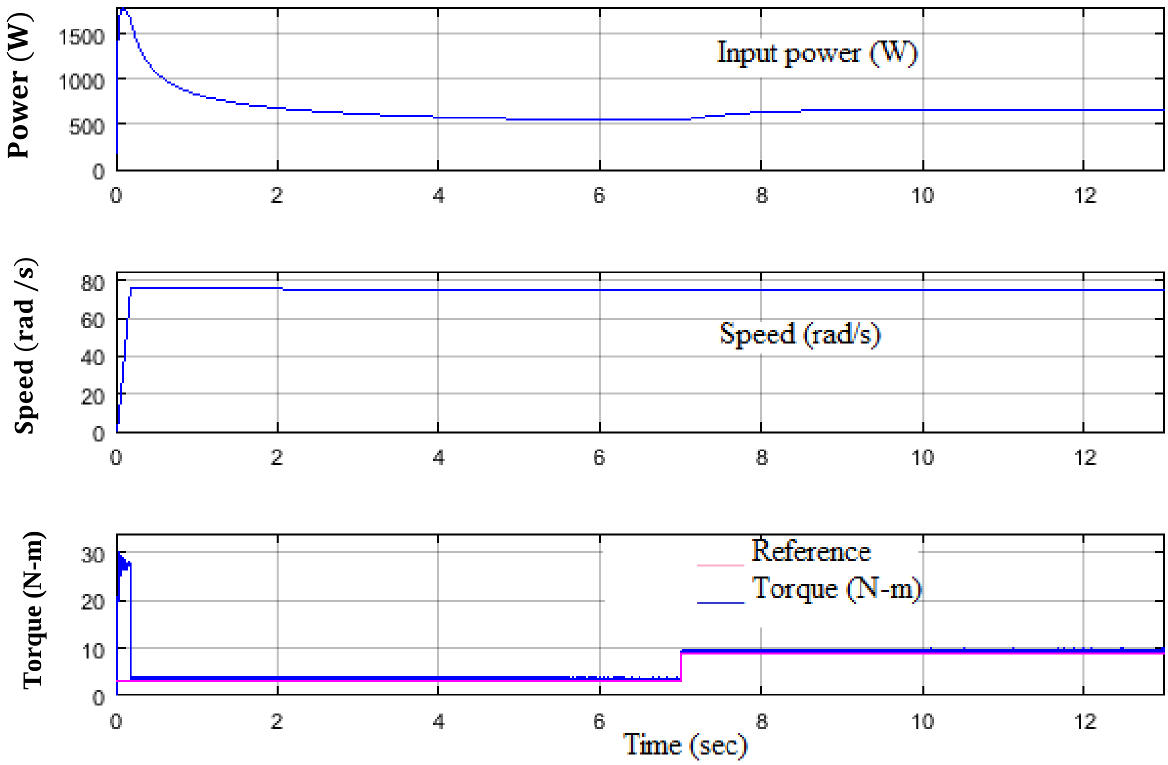

Fig. 7.8 Drive performance for input power, speed and torque with sudden increase of load torque

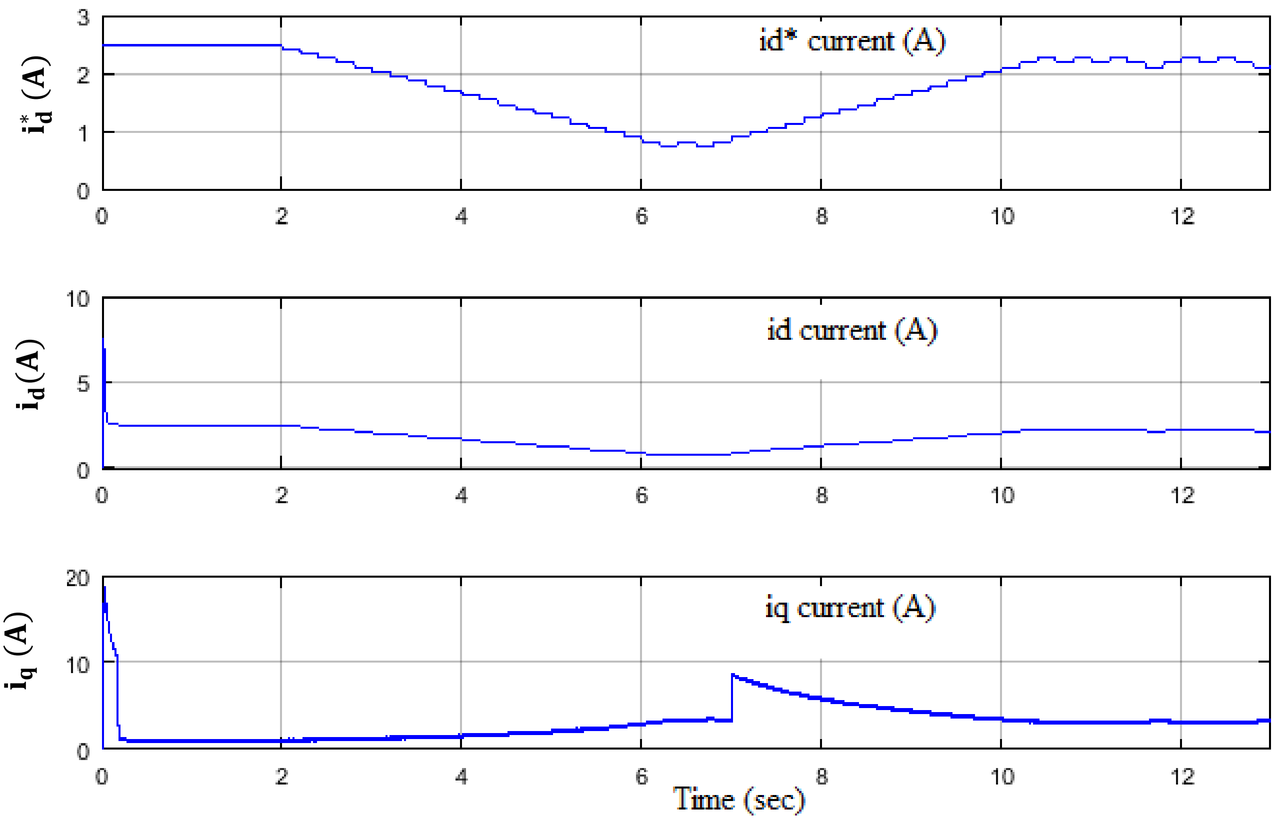

Fig. 7.9 Drive performances for current components i_d^* , i_d and i_q for sudden increase of load torque

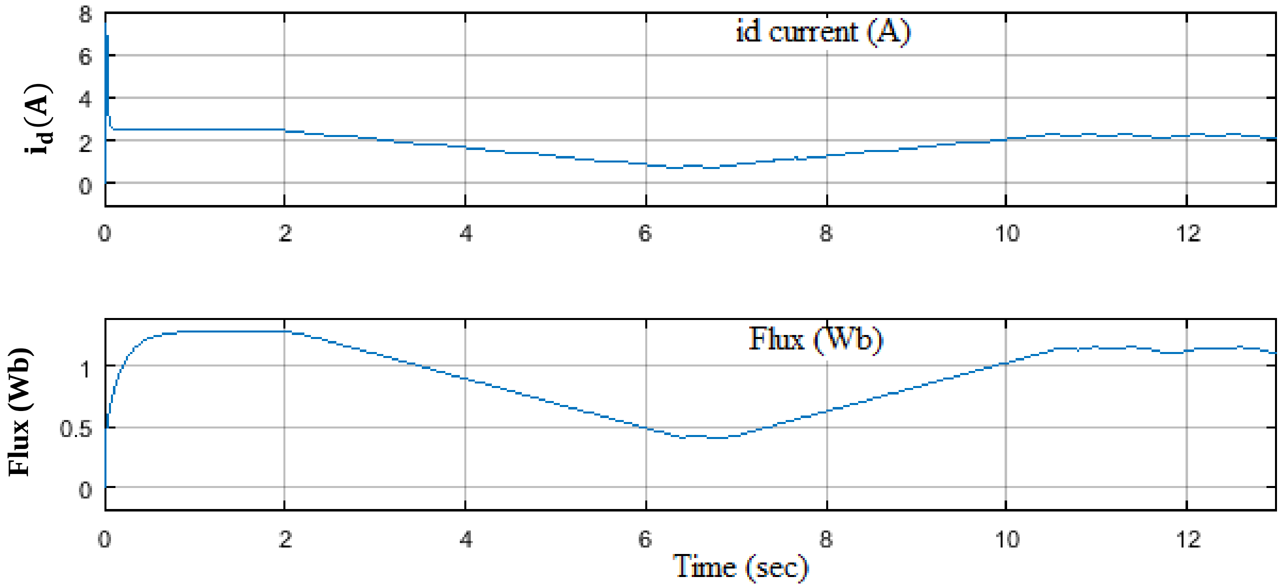

Fig. 7.10 Drive performance for id current and flux for sudden increase of load torque

7.4.4 Analysis of Efficiency for Different Operating Conditions

Fig. 7.11 shows the efficiency of the IM drive system for varying load at a particular speed with and without optimization. The analysis is carried out for four different speeds viz. 1pu, 0.75 pu, 0.50 pu and 0.25 pu at different load torques. Efficiency at without optimization (rated) is compared to efficiency obtained at with optimization. Efficiency improvement in the IM drive is observed with the use of optimum flux and it is also observed that the improvement in the efficiency is more at light load and lower speed. At 10 percent of rated load torque 50 percent improvement in efficiency is observed for 25 percent of rated speed. Similarly 19 percent, 6 percent and 4 percent improvement in efficiency are observed for 50 percent, 75 percent and 100 percent of rated speed respectively at 10 percent of rated load torque.

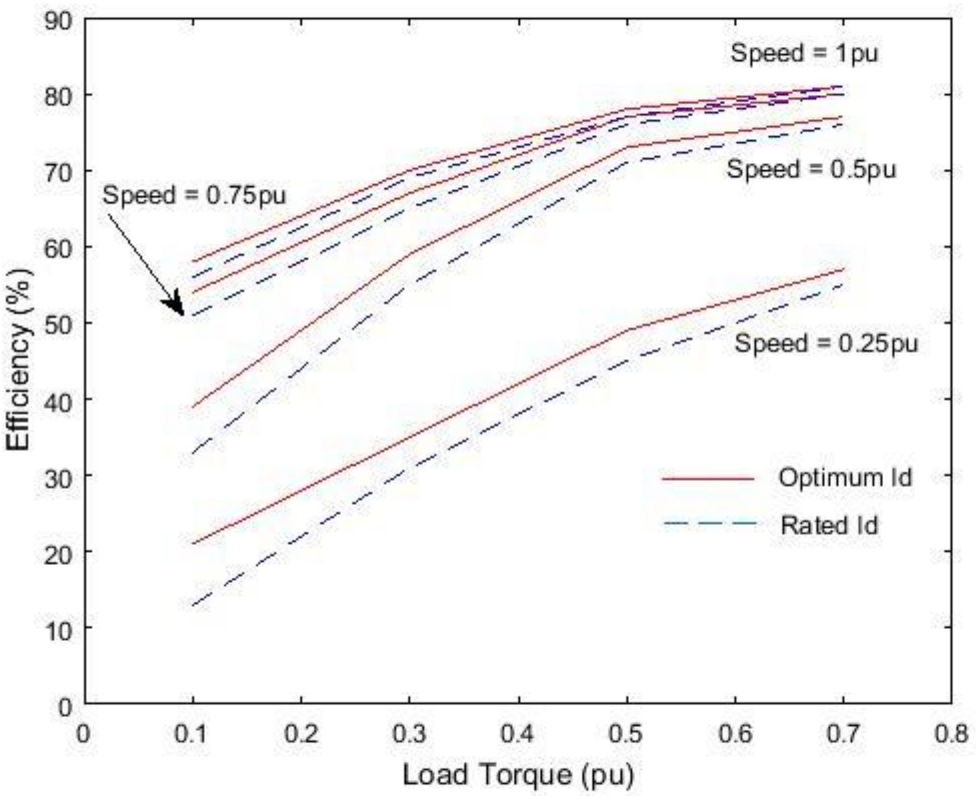

Fig. 7.11 Efficiency with different load torque

7.5 CONCLUSION

Efficiency optimization through a new search algorithm called deep valley search algorithm of indirect vector control of IM drive system is implemented. The proposed algorithm optimizes the flux producing current component by using the dc link power as the controlled variable. Simulation results for sudden change in torque and speed of IM drive was carried out and optimum value of flux is achieved under all operating conditions. It is also observed that the speed has followed the commanded speed during the search process without any objectionable variation in speed. The algorithm can be applied to any conditions and showed good performance at light load and low speed operations. Efficiency improvement of the IM drive for optimal flux operation is significant.

CHAPTER VIII

MAIN CONCLUSIONS AND FUTURE SCOPE OF WORK

8.1 GENERAL

The three phase IMs are commonly used as industrial drives because they are very reliable and economic. The scope of adjustable AC drives is growing extremely with aim of saving energy used in industrial processes. One of the most important aspects of electric drive system is their mechanical and electrical efficiency. The IMs use major part of total power used in industries. Hence, the performance of the improvement in efficiency of IM is a prominent area of research and development. Even a small increase in the motor efficiency will results in a huge amount of saving in energy. Three-phase induction motor efficiency can be increased by proper design and selection of the motor and by selecting a suitable control strategy. For reducing the motor losses and improving the efficiency, loss model and search control method based controller methods are commonly used. In a search control method, the air gap flux is iteratively searched to get the minimum input power for a particular operating condition. Here power input is used as a controlled variable. On the other hand the loss model control method computes the losses based on the machine loss model. Loss model controller provides fast response but it depends on motor parameters. Search controller is independent of the parameters but its response is slow. Both these methods are used for efficiency optimization and can be applied to the scalar control and to the vector control drives.

8.2 MAIN CONCLUSIONS

In this thesis different optimal control techniques of induction motor drives like simple state control, loss model control and search control were studied. The main goal of this research work is to optimize the efficiency of the induction motor through different control strategies.

Search control and loss model control techniques were implemented for improvement in the motor efficiency. Conventional motor speed control schemes like scalar control, vector control including sensorless control and indirect field oriented control are discussed. Scalar control is easy to implement and can create satisfactory performance in variable frequency drives. Scalar control applications are limited to the areas where high precision control of motor is not required because of the inherent torque and flux coupling effect. Due to this coupling effect the response of the drive system becomes slow. Scalar control offers good steady-state performance, but it suffers from poor dynamic performance. These problems can be conquered by using vector control, where response of the drive system is fast and gives good steady-state and dynamic performance. The main drawback of vector control is that it is parameter dependent. So in order to get the satisfactory performance from the vector control, motor parameters must be accurate. Motor parameters change with the operating conditions of the motor and it becomes serious in case of sensorless induction motor drive for low speed applications. These variations in parameters must be compensated by using appropriate parameter estimation techniques so as to avoid the deterioration of the motor performance. Model reference adaptive system is implemented for estimation of the stator resistance and motor speed in a vector controlled sensorless IM drive system for making the speed estimation independent of parameter variation.

The main findings of the present research work are as follows:

- The simulation and analysis of conventional methods of speed control such as constant V/f and IFOC IM drives is carried out using full spectrum simulator (FSS) and MATLAB/Simulink. The FSS simulation also provides real time simulation of the drives.

- The sensitivity analysis of IM performance was achieved based on steady state equivalent circuit of induction motor with and without core loss resistance component.
- A MRAS based motor speed and stator resistance estimator for sensorless induction motor drive is presented. Stator resistance estimator is implemented using ANFIS controller. The stability analysis of IM drive system with a variation of stator resistance is carried out by linearizing the motor equations around the operating point.
- Efficiency implementation in IM drive is implemented by using optimal control of the d-axis current component using a loss model controller. The scheme has been implemented using both PI controller and fuzzy logic controller for optimizing iron losses only and total motor losses separately.
- Efficiency optimization through a new search control algorithm of IFOC IM drive system is implemented, where the flux producing current component is optimized using power at dc link. This algorithm has resulted significant improvement in performance at light load and low speed operations. Higher efficiency of the drive system is observed with optimal flux than the rated flux operation.

8.3 FUTURE SCOPE OF WORK

The defined objectives of the research work are achieved successfully and the research areas can further be extended by using advanced artificial intelligent (AI) and machine learning based control approaches like artificial neural network, particle swarm optimization, genetic algorithm etc. for energy optimization in IM drives.

- The IM efficiency has been improved with the proposed loss model control and search control algorithm. The search control algorithm includes the inverter losses. The efficiency can further be improved if the inverter losses are also incorporated for loss model control algorithm. The developed control algorithms can further be extended to other motor drive systems.

- There is scope to improve the power quality of inverter fed IM drives system so as to enhance the efficiency and performance of the system. Inverter plays a significant role in AC drives. It would be better if the multilevel inverter is used for the drive system to minimize the effect of ripples in speed and torque during load transition in the proposed algorithm.
- Experimental validation of advance control algorithm for speed regulation of the motor may be carried out to verify the behavior of motor obtained through offline simulation using MATLAB/ Simulink.
- The drive parameters are very significant for high precision motor drive system to tune the controllers. The entire estimation of motor parameters may further be improved if the identification of parameters is obtained through soft computing methods of AI and machine learning techniques.

REFERENCES

[1] B.K. Bose, "Modern Power Electronics and AC Drives," Ist edition (India: Pearson Education Asia, Inc., 2003 (LPE)).

[2] P.C. Krause, “Electric Machines,” Prentice Hall, 1985.

[3] R. Krishnan, “Electric Motor Drives – Modeling, Analysis and Control,” Pearson Prentice Hall, 2013.

[4] B. K. Bose, “Power Electronics and Variable Frequency Drives,” IEEE Press, 1997.

[5] S. S. Sivaraju, N. Devarajan, “Novel Design of Three Phase Induction Motor Enhancing Efficiency, Maximizing Power Factor and Minimizing Losses,” *European Journal of Scientific Research*, Vol.58, No.3, pp. 423-432, 2011.

[6] Mehdi Dhaoui, Lassaad Sbita, “A New Method for Losses Minimization in IFOC Induction Motor Drives,” *International Journal of Systems Control* , Vol.1, Issue 2, pp. 93-99, 2010.

[7] J. Rodríguez, J. Pontt, C. Silva, S. Kouro, A. Liendo, J. Rebolledo, “Hysteresis Current Control of a Vector Controlled Induction Motor and DTC: An Assessment,” *International Journal of Electronics*, Vol. 91, No. 11, pp. 639–651, 2004.

[8] J.W. Finch, and D. Giaouris, "Controlled AC Electrical Drives," *IEEE Transactions on Industrial Electronics*, Vol. 55, Issue 2, pp. 481 – 491, 2008.

[9] C. Thanga Raj, S. P. Srivastava and P. Agarwal, “Differential Evolution based Optimal Control of Induction Motor Serving to Textile Industry,” *International Journal of Computer Science*, Vol. 35, No. 2, 2008.

[10] F. J. Ferreira and A. T. de Almeida, "Method for in-field Evaluation of the Stator Winding Connection of Three-Phase Induction Motors to Maximize Efficiency and

Power Factor," *IEEE Transactions on Energy Conversion*, Vol. 21, pp. 370-379, 2006.

[11] Jacek F. Gieras and Izabella A.Gieras, “Recent Development in Motors and Drives,” *United Technologies Research Center*, East Hartford, CT, U.S.A.

[12] F. Abrahamsen, F. Blaabjerg, J.K. Pedersen, P.B. Thoegersen, “Efficiency Optimized Control of Medium Size Induction Motor Drives,” *IEEE Transactions on Industrial Applications*, Vol. 37, No. 4, pp. 1761-1767, 2001.

[13] M. Nasir Uddin, Sang Woo Nam, “New Online Loss-Minimization-Based Control of an Induction Motor Drive,” *IEEE Transactions on Power Electronics*, Vol. 23, No. 2, pp. 926 – 933, March 2008.

[14] N. Tsouvalas, Ioannis Xydis, Ioannis TsakirakisZ.Papazacharopoulos, “Asynchronous Motor Drive Loss Optimization,” Material Processing and Technology, Vol. 181, pp. 301-306, 2007.

[15] A. Kusko, D. Galler, “Control Means for Minimization of Losses in AC and DC Motor Drives,” *IEEE Transactions on Industrial Applications*, Vol. 1, No. 4, pp. 561-570, 1983.

[16] C. Li, A. Rahman, “Three-Phase Induction Motor Design Optimization using the Modified Hooke-Jeeves Method,” *International Journal of Electrical Machines and Power Systems*, Vol. 18, pp. 1-12, 1990.

[17] R. Ramarathnam, B. G. Desai, “Optimization of Poly Phase Induction Motor Design: a Nonlinear Programming Approach,” *IEEE Transactions on Power Apparatus and Systems*, Vol. 90, No. 2, pp. 570-578, 1971.

[18] J. Faiz, M.B.B. Sharifian, “Optimal Design of Three-Phase Induction Motors and Their Comparison with a Typical Industrial Motor,” *Computers and Electrical Engineering*, Vol. 27, pp. 133-144, 2001.

[19] O. Muravlev, Eugenia Vekhter, “Energetic Parameters of Induction Motors as the Basis of Energy Saving in a Variable Speed Drive,” *Electrical Power Quality and Utilization,* Vol. IX, No. 2, 2005.

[20] W. Jazdzynski, “Multi Criterial Optimization of Squirrel-Cage Induction Motor Design,” *IEEE Proceedings*, Vol. 136, Part B, No.6, 1989.

[21] Bhim Singh, B. N. Singh, “Experience in the Design Optimization of a Voltage Source Inverter Fed Squirrel Cage Induction Motor,” *Electric Power Systems Research,* Vol. 26, pp. 155-161, 1993.

[22] J. Faiz and M. Sharifian, "Optimum Design of a Three Phase Squirrel Cage Induction Motor based on Efficiency Maximization," *Computer and Electronics Engg.,* Vol. 21, pp. 367-373, 1995.

[23] D. G. Bharadwaj, K. Venkatesan, R.B. Saxena, “Induction Motor Design Optimization using Constrained Rosenbrock Method (Hill Algoritm),” *Computer and Electrical Engineering,* 6, pp. 41-46, 1979.

[24] J. W. Kim, Byung-Taek Kim, Byung Il Kwon, “Optimal Stator Slot Design of Inverter Fed Induction Motor in Consideration of Harmonic Losses,” *IEEE Transactions on Magnetics,* Vol. 41, No.5, 2005.

[25] A. Boglietti, A. Cavagnino, Lucca Ferraris, M. Lazzari, “No Tooling Cost Process for Induction Motors Energy Efficiency Improvements,” *IEEE Transactions on Industrial Applications*, Vol. 41, No. 3, pp. 808-816, 2005.

[26] S. Padma, R. Bhuvaneswari, S. Subramanian, “Application of Soft Computing Techniques to Induction Motor Design,” *Computation and Mathematics in Electrical and Electronics Engg.*, Vol 26, No. 5, pp. 1324-1345, 2007.

[27] R. H. A. Hamid, A. M. A. Amin, R. S. Ahmed, A. El-Gammal, “New Technique for Maximum Efficiency of Induction Motors based on PSO,” *IEEE Conference Proceedings*, pp. 2176-2181, 2006.

[28] R. H. A. Hamid, A. M. A. Amin, R. S. Ahmed, A. El-Gammal, “Optimal Opearation of Induction Motors using Artificial Neural Network based PSO, ” *IEEE Conference Proceedings*, pp. 2408-2413, 2006.

[29] O.S. El-Laben, “Particle Swarm Optimized Direct Torque Control of Induction Motor,” *IEEE Conference Proceedings*, IECON, pp. 1586-1591, 2006.

[30] C. Cao, B. Zhou, Min Li, Jing Du, “Digital Implementation of DTC based on PSO for Induction Motors,” *IEEE Conference Proceedings for Intelligent Control and Automation*, pp. 6349-6352, 2006.

[31] Jan Pawel Wieczorek, Ozdemir Gol, Z. Michalewicz, “An Evolutionary Algorithm for the Optimal Design of Induction Motors,” *IEEE Transactions on Magnatics*, Vol. 34, No. 6, 1998.

[32] Eric Poirer, Mohsen Ghribi, A. Kaddouri, “Loss Minimization Control of Induction Motor Drives based on Genetic Algorithm,” *IEEE Conference Proceedings, Electrical machines and Drives*, pp. 475-478, 2001.

[33] L.R. Valdenebro, E. Bim, “A Genetic Algorithm Approach for Adaptive Field Oriented Control of Induction Motor Drives,” *IEEE Conference Proceedings, Electrical machines and drives*, IEMD, WA, USA, pp. 643-645, 1999.

[34] M. Cunkas, R. Akkaya, “Design Optimization of Induction Motor by Genetic Algorithm and Comparison with Existing Motor,” *Mathmatical and Computational Applications*, Vol. 11, No. 3, pp. 193-203, 2006.

[35] M. K. Kim, C. G. Lee, H. K. Jung, "Multi Objective Optimal Design of Three-Phase Induction Motor using Improved Evolution Strategy," *IEEE Transactions on Magnetics*, Vol. 34, No.5, pp. 2980-2983, 1998.

[36] Mohamed Yazid Kaikaa, Fatima Babaa, Abdelmalek Khezzar, Mohamed Boucherma, "Analytical Analysis of Rotor Slot Harmonics in the Line Current of Squirrel Cage Induction Motors," *Journal of Electrical Engineering*, Vol. 57, No. 1, pp. 12–19, 2006.

[37] Rateb H. Issa, "Optimal Efficiency Controller of AC Drive System," *International Journal of Computer Applications,* Vol 62, No.12, pp. 40-46, January 2013.

[38] M. Nageswara Rao, A. Rajani, "Speed Control of Induction Motor using Fuzzy Logic Approach," *International Journal of Engineering Research & Technology (IJERT)* , Vol. 2 Issue 8, pp. 1067-70, August 2013.

[39] K. Anitha, G. Santosh, L. Suneel, K. Spandana, E. Ravi Teja, "Simulation and Speed Control of 3-Phase Induction Motor Drives," *International Journal of Engineering Science and Computing,* Vol 6, Issue 4, pp. 4478-4481, 2016.

[40] A. Abbou, T. Nasser, H. Mahmoudi, M. Akherraz, A. Essadki, 'Induction Motor Controls and Implementation Using Dspace," *WSEAS Transactions on Systems and Control*, Vol. 7, Issue 1, pp. 26-35, 2012.

[41] J. R. Pottebaum, "Optimal Characteristics of a Variable Frequency Centrifugal Pump Motor Drive," *IEEE Transactions on Industrial Application*, Vol. IA-20, No.1, pp. 23-31, 1984.

[42] F. Abrahamsen, F. Blaabjerg, J. K. Pedersen, "On the Efficiency Optimized Control of Standard and High Efficiency Induction Motor in CT and HVAC Applications," *IEEE Transactions on Industrial Applications*, Vol. 34, No. 4, pp. 822-831, 1998.

[43] Pabitra Kumar Behera, Manoj Kumar Behera, Amit Kumar Sahoo, “Comparative Analysis of Scalar & Vector Control of Induction Motor Through Modeling & Simulation,” *International Journal of Innovative Research in Electrical, Electronics, Instrumentation and Control Engineering,* Vol. 2, Issue 4, pp. 1340-1344, April 2014.

[44] G. Kohlrusz, D. Fodor, “Comparison of Scalar and Vector Control Strategies of Induction Motors,” *Hungarian Journal of Industrial Chemistry,* pp. 265-270, 2011.

[45] Rahaman Naveed, H.V. Govindraju, “Modelling & Simulation of a 3 Phase Electric Traction Induction Motor using Matlab Simulink,” *International Journal of Electrical, Electronics and Computer Systems* (IJEECS), Vol. 2, Issue-5, pp. 18-25, 2014.

[46] Rutuja S Hiware, Jagdish G Chaudhari, “Indirect Field Oriented Control for IM,” *Fourth International Conference on Emerging Trends in Engineering & Technology* ICETET, pp. 191-194, 2011.

[47] S. Allirani and V. Jagannathan, "High Performance Direct Torque Control of Induction Motor Drives Using Space Vector Modulation," *International Journal of Computer Science,* Vol. 7, Issue 6, pp 178-186, November 2010.

[48] Nikhil Krishna Bajjuri, Amit Kumar Jain, “Torque Ripple Reduction in Double-Inverter Fed Wound Rotor Induction Machine Drives Using PWM Techniques,” *IEEE Transactions on Industrial Electronics*, Vol. 66, Issue: 6, pp. 4250-4261, 2019.

[49] Y. Tang and G. Lin, "Direct Torque Control of Induction Motor Bbased on Self-Adaptive PI Controller," *5th International Conference on Computer Science and Education,* pp. 1230-1234, *2010*.

[50] F. M. Abdel-kader, A. El-Saadawi, A. Kalas, and O. M. EL-baksawi, "Study in Direct Torque Control of Induction Motor by Using Space Vector Modulation," *12th International Middle-East Power System Conference,* pp. 224-229, 2008.

[51] K. Ranjith Kumar, D. Sakthibala, Dr. S. Palaniswami, “Efficiency Optimization of Induction Motor Drive using Soft Computing Techniques,” *International Journal of Computer Applications*, Vol. 3, No.1, pp. 6-12, June 2010.

[52] Han Ho Choia, Jin-Woo Junga, Rae-Young Kimb, “Fuzzy Adaptive Speed Control of a Permanent Magnet Synchronous Motor,” *International Journal of Electronics,* Vol. 99, No. 5, pp.657–672, May2012.

[53] S. Sathi Kumar and J. Vithayathil, “Digital Simulation of Field-Oriented Control of Induction Motor,” *IEEE Transactions on Industrial Electronics*, Vol. IE-31, No. 2, pp. 141–148, 1984.

[54] I. Takahashi and Y. Ohmori, "High-Performance Direct Torque Control of an Induction Motor," *IEEE Transactions on Industry Applications*, Vol. 25, No. 2, pp. 257-264, April 1989.

[55] M. P. Kazmier Kowski and A. B. Kasprowicz, "Improved Direct Torque and Flux Vector Control of PWM Inverter-Fed Induction Motor Drives," *IEEE Transactions on Industrial Electronics*, Vol. 42, No. 4, pp. 344-350, Aug. 1995.

[56] Navneet Kumar, Thanga Raj Chelliah, S.P. Srivastava, “Adaptive Control Schemes for Improving Dynamic Performance of Efficiency Optimized Induction Motor Drives” *ISA Transactions*, Vol. 57, pp. 301-310, 2015.

[57] Jie Li, Fei-Fei Xiao, Shu-Quan Zhang, “Simplified Loss Model Control Efficiency Optimization Algorithm for Vector Control Induction Motor Drives,” *43rd Annual Conference of the IEEE Industrial Electronics Society*, pp. 5178 – 5183, 2017.

[58] Min-Huei Kim, James C. Hung, “Vector Control System for Induction Motor Without Speed Sensor at Very Low Speed,” *21st International Conference on IEEE (IECON*), Vol. 1, pp. 524-529, 1995.

[59] S. Sen, S. N. Yeh, "Optimal Efficiency Analysis of Induction Motors Fed by Variable-Voltage and Variable-Frequency Source," *IEEE Transactions on Energy Conversion*, Vol. 7, No. 3, pp.537-543, 1992.

[60] Sukanta Das, Rakesh Kumar, Abhisek Pal, "MRAS-Based Speed Estimation of Induction Motor Drive Utilizing Machine's d and q Circuit Impedances," *IEEE Transactions on Industrial Electronics*, Vol. 66 , Issue: 6, pp. 4286 – 4295, June 2019.

[61] Shuying Yang, Dawei Ding, Xi Li, Zhen Xie, Xing Zhang, Liuchen Chang, "A Decoupling Estimation Scheme for Rotor Resistance and Mutual Inductance in Indirect Vector Controlled Induction Motor Drives," *IEEE Transactions on Energy Conversion*, Vol. 34, Issue: 2, June 2019.

[62] A. Ba-Razzouk, A. Cheriti & G. Olivier, "Field-Oriented Control of Induction Motors Using Neural-Network Decouplers," *IEEE Transactions on Power Electronics*, Vol. 12, Issue 4, pp. 752 –763, 1997.

[63] B. Pryymak, J. M. Moreno-Eguilaz and J. Peracaula, "Neural Network Flux Optimization Using a Model of Losses in Induction Motor Drives," *8th International Conference on Modeling and Simulation of Electric Machines, Converters and Systems*, Vol. 71, Issues 4–6, pp. 290-298, 2006.

[64] O. E. Ebrahim, M. A. Badr, A. S. Elgendy and P. K. Jain, "ANN-Based Optimal Energy Control of Induction Motor Drives in Pumping Applications," *IEEE Transaction on Energy Conversion*, Vol. 25, No. 3, pp. 652-660, 2010.

[65] Garg Rachna, Mahajan Priya, & Gupta Nikita, "A Comparative Study Between Field Oriented Control and Direct Torque Control of AC Traction Motor," *Recent Advances and Innovations in Engineering,(ICRAIE)*, May 2014.

[66] Sridharan Srikanthan, & Krein Philip, “Minimization of System-Level Losses in VSI-Based Induction Motor Drives: Offline Strategies,” *IEEE Transactions on Industry Applications,* Vol. 53, Issue 2, pp 1096-1105, March-April 2017.

[67] Kumar Rakesh, Das Suanta and Chattopadhyay Ajit Kumar, “Comparative Assessment of Two Different MRAS Schemes for Speed Sensorless Control of Induction Motor Drives,” IET Electrical Power Applications, Vol. 10, Issue 2, pp. 141-154, 2016.

[68] Raichurkar, Priya, Subhash, & Jamadar Asif Liyakat, “V/F Speed Control of 3 Phase Induction Motor Using Space Vector Modulation,” *International Journal of Engineering Research & Technology (IJERT),* Vol. 4, Issue 05, pp. 735-742, 2015.

[69] Liu Yi-Hwa, Chen Chern-Lin, & Tu Rong Jie, “A Novel Space-Vector Current Regulation Scheme for a Field-Oriented- Controlled Induction Motor Drive,” *IEEE Transactions on Industrial Electronics.* Vol. 45, Issue 5, pp 730 – 737, Oct. 1998.

[70] S. Sujitjorn, K. L. Areerak, “Numerical Approach to Loss Minimization in an Induction Motor, ” *Applied Energy,* Vol. 79, pp. 87-96, 2004.

[71] S. S. Sivaraju N. Devarajan, “Novel Design of Three Phase Induction Motor Enhancing Efficiency, Maximizing Power Factor and Minimizing Losses,“ *European Journal of Scientific Research,* Vol.58, No.3, pp. 423-432, 2011.

[72] F. G. G. Buck, P. Gistelinck, and D. Backer, “A Simple but Reliable Loss Model for Inverter Supplied Induction Motors,” *IEEE Transactions on Industrial Applications,* Vol. IA 20, No. 1, pp. 190-201, 1984.

[73] D. H. Kim, “GA-PSO Besed Vector Control of Indirect Three Phase Induction Motor,” *Applied Soft Computing,* Vol. 7, Issue 2, pp. 601-611, March 2007.

[74] W. Deleroi, J. B. Woudstra, A. A. Fahim, “Analysis and Application of Three-Phase Induction Motor Voltage Controller with Improved Transient Performance,” *IEEE Transactions on Applications*, Vol. 25, No. 2, pp. 280-286, 1989.

[75] Nikolaos Jabbour, Christos Mademlis, “Online Parameters Estimation and Auto Tuning of a Discrete-Time Model Predictive Speed Controller for Induction Motor Drives,” *IEEE Transactions on Power Electronics*, Vol. 34, Issue 2, pp. 1548-1559, 2019.

[76] M. Benbouzid, “A Review of Induction Motors Signature Analysis as a Medium for Faults Detection,” *IEEE Transactions on Industrial Electronics*, Vol. 47, No. 5, pp. 984–993, Oct. 2000.

[77] F. Ponci, L. Cristaldi, M. Faifer, and M. Lazzaroni, “Innovative Approach to Early Fault Detection for Induction Motors,” *Proceedings IEEE SDEMPED*, pp. 283–288, 2007.

[78] Khambadkone A. M. and Holtz J., “Vector-Controlled Induction Motor Drive with a Self-Commissioning Scheme,” *IEEE Transactions on Industrial Electronics*, Vol. 38, pp. 322–327, Oct. 1991.

[79] Matsuo T. and Lipo T. A., “A Rotor Parameter Identification Scheme for Vector Controlled Induction Motor Drives,” *IEEE Transactions on Industrial Applications*, Vol. IA-21, pp. 624–632, May/June 1985.

[80] Loron L. and Laliberté G., “Application of the Extended Kalman Filter to Parameters Estimation of Induction Motors,” *Proceedings European Conference Power Electronics Application*, Vol. 5, pp. 85–90. 1993.

[81] Garces L. J., “Parameter Adaption for the Speed-Controlled Static AC Drive with a Squirrel-Cage Induction Motor,” *IEEE Transactions on Industrial Applications*, Vol. IA-16, pp. 173–178, Mar./Apr. 1980.

[82] Demirili K. and Muthukumaran P., “Higher Order Fuzzy System Identification Using Subtractive Clusterin,” *IEEE Journal of Intelligent and Fuzzy System*, pp. 129-158, 2000.

[83] Ballal M. S., Khan Z. J., Suryawanshi H. M., and Sonolikar R. L., “Adaptive Neural Fuzzy Inference System for the Detection of Inter-Turn Insulation and Bearing Wear Faults in Induction Motor,” *IEEE Transactions on Industrial Electronics,* Vol. 54, No. 1, pp. 250–258, Feb. 2007.

[84] Bouzid M. B. K., Champenois G., Bellaaj N. M., Signac L., and Jelassi K., “An Effective Neural Approach for the Automatic Location of Stator Inter Turn Faults in Induction Motor,” *IEEE Transactions on Industrial Electronics,* Vol. 55, No. 12, pp. 4277–4289, Dec. 2008.

[85] I. Sanchez and P. Pillay, "Sensitivity Analysis of Induction Motor Parameters," *IEEE Department of Electrical Engineering University of New Orleans LA 70148*, pp. 50-54, 1994.

[86] Sang-Hoon Lee, Anno Yoo, Hak-Jun Lee, Young-Doo Yoon, and Byung-Moon Han, “Identification of Induction Motor Parameters at Standstill based on Integral Calculation,” *IEEE transactions on industry applications,* Vol. 53, pp. 2130 – 2139, 2017.

[87] Rakesh Kumar, Sukanta Das, “Eigen Value-Based Relative Parameter Sensitivity Analysis for Optimised Performance of Sensorless Induction Motor Drives,” *IET Electric Power Applications,* Vol. 10, pp. 723–734, 2016.

[88] Ganesh P. Prajapat, N. Senroy, I. N. Kar, “Eigen Value Sensitivity Analysis Based Optimized Control of Wind Energy Conversion Systems,” *IEEE Innovative Smart Grid Technologies - Asia (ISGT-Asia)* , pp. 647 – 652, 2016.

[89] Krishnan and A. S. Bharadwaj, "A Review of Parameter Sensitivity and Adaptation in Indirect Vector Controlled Induction Motor Drive Systems," *21st Annual IEEE Conference on Power Electronics Specialists*, San Antonio, TX, USA, pp. 560-566, 1990.

[90] C.S. Indular and K. Ramalingam, “Sensitivity Analysis of Induction Motor Performance,” https://www.researchgate.net/.242751687, 2007.

[91] Mini Sreejeth, Madhusudan Singh, and P. Kumar, “Sensitivity Analysis of Induction Motor Using Fourth Order Slip Estimator”, *International Journal of Power and Energy Systems*, Vol. 33, No. 2, pp. 1-10, 2013.

[92] Attila Fodor, Roland Bálint, Attila Magyar and Gábor Szederkényi, “Stability and Parameter Sensitivity Analyses of an Induction Motor,” *Hungarian Journal of Industry and Chemistry Veszprém*, Vol. 42(2), pp. 109–113, 2014.

[93] Jiahao Chen, Jin Huang, "Stable Simultaneous Stator and Rotor Resistances Identification for Speed Sensorless Induction Motor Drives: Review & New Results”, *IEEE Transaction on Power Electronics*, Vol. 33, Issue 10, pp. 8695 – 8709, Oct. 2018.

[94] Rakesh Kumar, Suanta Das and Ajit Kumar Chattopadhyay, “Comparative Assessment of Two Different MRAS Schemes for Speed Sensorless Control of Induction Motor Drives”, *IET Electric Power Applications*, Vol. 10, Issue 2, pp. 141-154, 2016.

[95] R. J. Kerkman, B. J. Seibel, T. M. Rowan, D. Schlegel, “A New Flux and Stator Resistance Identifier for AC Drive Systems”, *IEEE Transactions on Industrial Applications*, Vol. 32, pp. 585–593, 1996.

[96] M. Cirrincione, M. Pucci, G. Cirrincione, G. A. Capolino, “A New Adaptive Integration Methodology for Estimating Flux in Induction Machine Drives,” *IEEE Transactions on Power Electronics*, Vol. 19, No.1, pp. 25–34, 2004.

[97] Jiahao Chen, Jin Huang, “Stable Simultaneous Stator and Rotor Resistances Identification for Speed Sensorless Induction Motor Drives: Review and New Results,” *IEEE Transactions on Power Electronics,* Vol. 33, Issue 10, pp. 8695 – 8709, 2018.

[98] J. Guzinski and H. Abu-Rub, "Speed Sensorless Induction Motor Drive with Predictive Current Controller," *IEEE Transactions on Industrial Electronics*, Vol. 60, No. 2, pp. 699-709, Feb. 2013.

[99] A. V. Ravi Teja, Vimlesh Verma, and Chandan Chakraborty, “A New Formulation of Reactive-Power-Based Model Reference Adaptive System for Sensorless Induction Motor Drive,” *IEEE Transactions on Industrial Electronics,* Vol. 62, No. 11, pp. 6797 – 6808, 2015.

[100] S. Davari Alireza, Fengxiang Wang, M. Kennel Ralph, "Robust Deadbeat Control of an Induction Motor by Stable MRAS Speed and Stator Estimation,” *IEEE Transaction on Industrial Informatics*, Vol. 14, Issue 1, pp. 200 – 209, 2018.

[101] Vimlesh Verma, Chandan Chakraborty, “New Series of MRAS for Speed Estimation of Vector Controlled Induction Motor Drive,” *IECON*, pp. 755-761, 2014.

[102] S. Mohan Krishna, J. L. Febin Daya, “Dynamic Performance Analysis of MRAS Based Speed Estimators for Speed Sensorless Induction Motor Drives,” *International Conference on Advances in Electronics, Computers and Communications,* pp. 1-6, 2014.

[103] S. Alireza Davari, Fengxiang Wang, Ralph M. Kennel, "Robust Deadbeat Control of an Induction Motor by Stable MRAS Speed and Stator Estimation," *IEEE Transactions on Industrial Informatics*, Vol. 14, Issue 1, pp. 200 – 209, 2018.

[104] K. Sedhuraman, S. Himavathi, A. Muthuramalingam, "Neural Learning Adaptive System Using Simplified Reactive Power Reference Model Based Speed Estimation in Sensorless Indirect Vector Controlled Induction Motor Drives," *Archives of Electrical Engineering*, Vol.62(1), pp. 25-41, 2013.

[105] Cao-Minh Tay, Toshiyuki Uchida, Yoichi Hori, "MRAS-Based Speed Sensorless Control For Induction Motor Drives Using Instantaneous Reactive Power," *27th Annual Conference of the IEEE Industrial Electronics Society*, Vol. 2, pp. 1417-1422, 2001.

[106] Veran Vasic, N. Slobodan, Vukosavic & Levi Emil, "A Stator Resistance Estimation Scheme for Speed Sensorless Rotor Flux Oriented Induction Motor Drives," *IEEE Transactions on Energy Conversion.*, Vol.18, No. 4, pp. 476-483, 2003.

[107] Hussain Shoeb and Bazaz Abid Mohammad, "ANFIS Implementation on a Three Phase Vector Controlled Induction Motor with Efficiency Optimization," *IEEE International Conference on Circuits, Systems, Communication and Information Technology Applications (CSCITA)*, pp. 391-396, 2014.

[108] Aisha Jilani, Sadia Murawwat and Syed Omar Jilani, "Controlling Speed of DC Motor with Fuzzy Controller in Comparison with ANFIS Controller," *Intelligent Control & Automation*, Vol. 6, pp. 64-74, 2015.

[109] Mokhtar Zerikat, Soufyane Chekroun, Abdelkader Mechernene, "A Robust MRAS Sensorless Scheme Based Rotor and Stator Resistances Estimation of a Direct Vector Controlled Induction Motor Drive," *16th International Conference of IEEE*, pp. 151-156, 2011.

[110] Saji Chackol, Chandrashekhar N. Bhende, Shailendra Jain, R. K. Nema, “A Novel on Line Rotor Resistance Estimation Technique Using EA Tuned Fuzzy Controller for Vector Controlled Induction Motor Drive,” *IEEE International Conference on Electrical, Computer and Communication Technologies (ICECCT),* pp. 1-11, 2015.

[111] A.V Ravi Teja, Chandan Chakraborty, Suman Maiti, Yoichi Hori, “A New Model Reference Adaptive Controller for Four Quadrant Vector Controlled Induction Motor Drives,” *IEEE Transaction on Industrial Electronics,* Vol.59, No.10, pp. 3757 – 3767, 2012.

[112] Chandan Chakraborty, A.V Ravi Teja, Suman Maiti, Yoichi Hori, “A New V x I Based Adaptive Speed Sensorless Four Quadrant Vector Controlled Induction Motor Drive,” *International Power Electronics Conference (IPEC),* pp. 3041-3048, 2010.

[113] Aswathy Vijay and Binoj Kumar, “Speed and Stator Resistance Estimation of Four Quadrant Vector Controlled IM Drives,” *International Journal of Advvance Research in Electrical, Electronics and Instrial Engg*., Vol.3, No.5, pp. 329-337, 2014.

[114] Mini Sreejeth and Avinash Mehra, “Estimation of Stator Resistance in Sensor-Less Induction Motor Drive Using MRAS,” *IEEE 1st International Conference on Power Electronics, Intelligent Control and Energy Systems (ICPEICES),* pp. 1-6, 2016.

[115] Shirazul Islam, Farhad I Bakhs, AtifIqbal, Mohammad Saleh, Akhtar Kalam, “Stability Analysis of a Series-Connected Five-Phase Induction Motor Drive System Using Flux-Linkage Model,” *8th Conference of IEEE (ICIEA),* pp. 445-450, 2013.

[116] M. Bashir Uddin, Md. Nuruzzaman Pramanik, Sheikh Abu Reza, “Low Frequency Stability Study of a Three-Phase Induction Motor,” *The 7th International Conference on Power Electronics / EXCO, Daegu, Korea,* pp. 1115-1120, 2007.

[117] Weili Li, Purui Wang, Dong Li, “Multi Physical Field Collaborative Optimization of Premium Induction Motor Based on GA,” *IEEE Transactions on Industrial Electronics*, Vol. 65, Issue 2, pp. 1704 – 1710, Feb. 2018.

[118] M. Cacciato, A. Consoli, G. Scarcella, G. Scelba and A. Testa, “Efficiency Optimization Techniques via Constant Optimal Slip Control of Induction Motor Drives”, *IEEE Conference, SPEEDAM*, 2006.

[119] Z. Rouabah, F. Zidani, B. Abdelhadi, “Efficiency Optimization of Induction Motor Drive using Fuzzy Logic and Genetic Algorithms”, *IEEE International Symposium on Industrial Electronics*, pp. 737-742, 2008.

[120] Yiqi Liu, Ali M. Bazzi, “A Comprehensive Analytical Power Loss Model of Motor Drive System with Loss Minimization Control,” *IEEE (IEMDC)*, pp. 1638-1643, 2015.

[121] Mini Sreejeth, Madhusudan Singh, Parmod Kumar, “Efficiency Optimization of Vector Controlled Induction Motor Drive”, *The 38th Annual Conference of the IEEE Industrial Electronics Society, IECON*, Canada, pp. 1758 – 1763, 2012.

[122] P. K. Choudhary, Dr. S. P. Dubey, V. K. Gupta, “Efficiency Optimization of Induction Motor Drive at Steady-State Condition”, *IEEE conference (ICCICCT)*, pp. 470-475, 2015.

[123] S. Chen and S. N. Yeh, “Optimal Efficiency Analysis of Induction Motors Fed by Variable-Voltage and Variable-Frequency Source,” *IEEE Transactions on Energy Conversion*, Vol. 7, No. 3, 1992.

[124] G. Dong and O. Ojo, "Efficiency Optimizing Control of Induction Motor Using Natural Variables," *IEEE transaction on industrial electronics*, Vol. 53, No. 6, pp. 1791-1798, 2006.

[125] A. E. Fadili, F. Giri, A. E. Margi, R. Lajouad and F. Z. Chaoui, "Towards a Global Control Strategy for Induction Motor: Speed Regulation, Flux Optimization And Power Factor Correction," I*nternational Journal of Electrical Power and Energy System*, Vol. 43, pp. 230- 244, 2012.

[126] J. Liu, L. Fei, S. Hu and T. Q. Zheng, "Optimal Efficiency Control of Linear Induction Motor for Linear Metro," *Conference on Industrial Electronics and Applications*, Harbin, pp. 673 – 677, 2008.

[127] P. Famouri and J. J. Cathey , "Loss Minimization Control of an Induction Motor Drive," *IEEE Transactions on Industry Applications*, Vol. 27, No. 1, pp. 32-37, 1991.

[128] S. Kaboli, M. R. Zolghadri and E. Vahdati Khajeh, "A Fast Flux Search Controller for DTC-Based Induction Motor Drives," *IEEE transactions on Industrial electronics*, Vol. 54, No. 5, pp. 2407-2416, 2007.

[129] M. C. Ta, C. Chakravorty and Y. Hori, "Efficiency Maximization of Induction Motor Drives for Electric Vehicles Based on Actual Measurement of Input Power," *IEEE conference IECON'O*, Vol. 3, pp. 1692-1697, 2001.

[130] J. G. Cleland, V. E. Mccormick and M. W. Turner, "Design of an Efficinecy Optimization Controller for Inverter-Fed AC Induction Motors," *Conference Record of the 1995 IEEE Industry Applications Conference, Thirtieth IAS Annual Meeting*, 1995.

[131] Ankit Chourasia, Sharad Salunke, Vivek Saxena, “Efficiency Optimization of Three Phase Induction Motor by Slip Compensation: a Review”, *International Journal of Electronics and Electrical Engineering*, Vol. 1, No. 4, pp. 308-314, December 2013.

[132] M.E.H. Benbouzid, N.S. Nait, “An Efficiency-Optimization Controller for Induction Motor Drives,” *IEEE Power Engineering Review*, Vol. 18, Issue 5, pp. 63-64, May 1998.

[133] Hussein Sarhan, “Energy Efficient Control of Three-Phase Induction Motor Drive”, *Energy and Power Engineering*, Vol. 3, pp. 107-112, 2011.

[134] S. Vaez-Zadeh and F. Hendi, “A Continuous Optimization Controller for Induction Motor Drives,” *Energy Conversion and Management*, Vol. 46, pp. 701-713, 2005.

[135] T. M. Rowan, T. A. Lipo, “A Quantitative Analysis of Induction Motor performance Improvement by SCR Voltage Control,” *IEEE Transactions on Power Apparatus and Systems*, Vol. IAS-19, No. 4, July/Aug. 1983.

[136] H. R. Andersen, J. K. Pedersen, “low Cost Energy Optimised Control Strategy for a Variable Speed Three Phase Induction Motor,” *Power Electronics Specialists Conference, 27th Annual IEEE*, 1996.

[137] L. D. Jones, D. Blackwell, “Energy Saver Power Factor Controller for Synchronous Motors”, *IEEE Transactions on Power Apparatus and Systems*, Vol. PAS-102, No. 5, May 1983.

[138] Ali Mamizadeh, Ires Iskender, “Designing of Induction Motor Efficiency Monitoring System Without Using Torque Meter and Speed Sensor,” *International Conference on Optimization of Electrical and Electronic Equipment*, pp. 330-335, 2017.

[139] Rouabah Zineb, Zidani Fatiha, Abdelhadi Bachir, “Fuzzy Efficiency Enhancement of Induction Motor Drive,” *4th International Conference on IEEE (PEEED)*, pp. 175-180, 2013.

[140] Nejatian Samad, Omidvar Rohollah, Mohamadi Hadayat, Baghbani Arash Eskandar, Rezaie Vahideh, Parvin Hamid, “An Optimization Algorithm Based on Behaviour of See-See Partridge Chicks,” *Journal of Intelligent & Fuzzy Systems*, Vol. 33, No. 6, pp. 3227-3240, 2017.

[141] P. Famouri and J. J. Cathey, “Loss Minimization Control of an Induction Motor Drive,” *IEEE Transactions on Industry Applications*, Vol. 27, No.1, pp. 32-37, 1991.

[142] J. Li, L. Xu, and Z, Zhang, “A New Efficiency Method on Vector Control of Induction Motor,” *IEEE Conference on Electrical Machines and Drives*, pp. 1995-2001, 2005.

[143] F. C. Lin and Sheng-Ming Yang, “On-line Tuning of an Efficiency-Optimized Vector Controlled induction Motor Drive,” *Tam Kang Journal of Science and Engineering*, Vol. 6, No. 2, pp. 103-110, 2003.

[144] Iordanis Kioskeridis and Nikos Margaris, “Loss Minimization in Induction Motor Adjustable Speed Drives,” *IEEE Transactions on Industrial Electronics*, Vol. 43, No. 1, pp. 226 – 231, February 1996.

[145] S. Lim, K. Nam., “Loss Minimization Control Scheme for Induction Motors,” *IEEE proceedings on Electrical Power applications*, Vol. 151, No. 4, pp. 385-397, 2004.

[146] Felipe C. F. Azevedo, M. Nasir Uddin, “Recent Advances in Loss Minimization Algorithms for IPMSM Drives”, *IEEE Industry Application Society Annual Meeting,* pp. 1-9, 2014.

[147] Chandan Chakraborty, Yoichi Hori, “Fast Efficiency Optimization Techniques for the Indirect Vector-Controlled Induction Motor Drives,” *IEEE Transactions On Industry Applications*, Vol. 39, No. 4, pp. 1070 – 1076, July/August 2003.

[148] S. N. Vukosavic and E. Levi, "Robust DSP-Based Efficiency Optimization of a Variable Speed Induction Motor Drive," *IEEE transaction on Industrial Electronics,* Vol. 50, No. 3, pp. 560-570, 2003.

[149] D. D. S. Almeida, W. C. P. D. A. Filho and G. C. D. Sausa, "Adaptive Fuzzy Controller for Efficiency Optimization of Induction Motors,” *IEEE transaction on Industrial motors,* Vol. 54, No. 4, pp. 2157-2164, 2007.

[150] Juan Moreno, Miguel Cipolla, Juan Peracaula, Paul J. da Costa Branco, “Fuzzy Logic based Improvements in Efficiency Optimization of Induction Motor Drives,”

Proceedings of 6th international fuzzy systems conference, Vol. 1, pp. 219 – 224, 1997.

[151] Gilbert C. D. Sousa, Bimal K. Bose, “Fuzzy Logic Based On-Line Efficiency Optimization Control of an Indirect Vector-Controlled Induction Motor Drive”, *IEEE Transactions On Industrial Electronics*, Vol. 42, No. 2, pp. 192-198, April 1995.

[152] Myoung-Ho Shin, “A Study on Fast Maximum Efficiency Control of Stator-Flux-oriented Induction Motor Drives”, *Journal of Electrical Engineering & Technology,* Vol. 6, No. 5, pp. 626-633, 2011.

[153] Alex Borisevich, “Numerical Method for Power Losses Minimization of Vector-Controlled Induction Motor,” *International Journal of Power Electronics and Drive System (IJPEDS),* Vol. 6, No. 3, pp. 486-497, September 2015.

[154] C. Thanga Raj, S. P. Srivastava, and Pramod Agarwal, “Particle Swarm and Fuzzy Logic Based Optimal Energy Control of Induction Motor for a Mine Hoist Load Diagram”, *IAENG International Journal of Computer Science,* Vol. 36(1), 2009.

[155] Jiahao Chen, Jin Huang, Yan Sun, “Resistances and Speed Estimation in Sensorless Induction Motor Drives Using a Model with Known Regressors,” *IEEE Transactions on Industrial Electronics*, Vol. 66, Issue 4, pp. 2659-2667, 2019.

[156] S. K. Sul, M. H. Park, “A Novel Technique for Optimal Efficiency Control of a Current Source Inverter-Fed Induction Motor,” *IEEE Transactions on Power Electronics,* Vol. 3, No. 2, pp. 192-199, 1988.

[157] S .B. Bodkhe and M. V. Aware, “Speed-Sensorless, Adjustable-Speed Induction Motor Drive Based on DC Link Measurement,” *International Journal of Physical Sciences,* Vol.4 (4), pp. 221-232, April 2009.

[158] Mokhtar Zerikat, Soufyane Chekroun and Abdelkader Mechernene, “A Robust MRAS-Sensorless Scheme Based Rotor and Stator Resistances Estimation of a Direct

Vector Controlled Induction Motor Drive,” *16th International Conference on Methods & Models in Automation & Robotics,* pp. 151-156, 2011.

[159] F. F. Bernal, A. G. Cerrada, “Model-Based Minimization for DC and AC Vector-Controlled Motors Including Core Saturation,” *IEEE Transactions on Industrial Applications*, Vol. 36, No.3, pp. 755-763, 2000.

[160] G. O. Garcia, “An Efficient Controller for an Adjustable Speed Induction Motor Drive,” *IEEE Transactions on Industrial Electronics,* Vol. 41, No. 5, pp. 533-539, 1994.

[161] Z. Rouabah, F. Zidani, B. Abdelhadi, “Efficiency Optimization of Induction Motor Drive using Fuzzy Logic and Genetic Algorithms,” *IEEE International Symposium on Industrial Electronics*, 2008.

[162] C. M. Vega, J. R. Arribas and D. Ramirez, "Optimal Regulation of Electric Drives with Constant Load Torque," *IEEE transaction on Industrial Electronics,* Vol. 53, No. 6, pp. 1762-1769, 2006.

[163] Hossein Abootorabi Zarchi, Hamidreza Mosaddegh Hesar, Mojtaba Ayaz Khoshhava, “Online Maximum Torque Per Power Losses Strategy for Indirect Rotor Flux-Oriented Control-Based Induction Motor Drives,” *IET Electric Power Applications*, Vol. 13, Issue 2, pp. 259 – 265, 2019.

[164] Kirschen, N.W. Novotny, T. A. Lipo, “Optimal Efficiency Control of an Induction Motor Drive,” *IEEE Transactions on Energy Conversion*, Vol. EC-2, No.1, pp. 561-570, 1983.

[165] C. Thanga Raj, S. P. Srivastava, Pramod Agarwal, “Energy Efficient Control of Three-Phase Induction Motor - a Review,” *International Journal of Computer and Electrical Engineering,* Vol. 1, No. 1, pp. 61-70, April 2009.

[166] J.C. marino, T.A. Lipo, V. B. Blasco, "Simple Efficiency Maximize for an Adjustable Frequency Induction Motor Drive," *IEEE Transactions on Industrial Applications*, Vol. 27, No. 5, pp. 940-946, 1991.

[167] G. S. Kim, I. J. Ha, M. S. Ko, H. K. Bae, "Control of Induction Motors for Both High Dynamic Performance and High Power Efficiency," *IEEE Transactions on Industrial Electronics,* Vol. 39, pp. 323-333, 1992.

[168] F. Farhani, Chiheb Ben Regaya, Abderrahmen Zaafouri, Abdelkader Chaari, "Real Time PI-Back Stepping Induction Machine Drive with Efficiency Optimization", *ISA Transactions*, Vol. 70, pp. 348-356, 2017.

[169] D. S. Kirschen, Donald W. Novotny, Thomas A. Lipo, "On-line Efficiency Optimization of a Variable Frequency Induction Motor Drive," *IEEE Transactions on Industrial Applications,* Vol. 1A-21, No. 4, pp. 610-616, 1985.

[170] Kioskesidis, N. Margaris, "Loss Minimization in Scalar Controlled Induction Motor Drives with Search Controller," *IEEE Transactions on Power Electronics*, Vol. 11, No. 2, pp. 213-220, 1996.

[171] Durval de Almeida Souza, Wilson C. P. de Aragão Filho, and Gilberto Costa Drumond Sousa, "Adaptive Fuzzy Controller for Efficiency Optimization of Induction Motors," *IEEE transactions on industrial electronics*, Vol. 54, No. 4, pp. 2157-2164, August 2007.

[172] V. K. Gupta, B. Tiwari, B. Dewangan, "Efficiency Optimization of Induction Motor Drive: A Review," *International Journal of Innovative Science, Engineering & Technology,* Vol. 2, Issue 12, pp. 650-665, December 2015.

[173] Zarko Cucej, Dusan Borojevic, "Input Power Minimization at Inverter Fed Induction Motor Drive System with FOC by Field Weakening," *IEEE Annual Power Electronics Specialists Conference,* Vol. 2, pp. 1493 – 1499, 1997.

[174] C. Thanga Raj, S. P. Srivastava, and Pramod Agarwal, “Energy Efficient Control of Three-Phase Induction Motor - A Review,” *International Journal of Computer and Electrical Engineering,* Vol. 1, No. 1, pp. 61-70, April 2009.

[175] D. H. Kim, “GA-PSO Based Vector Control of Indirect Three Phase Induction Motor”, *Applied Soft Computing,* Vol. 7, No. 2, pp. 601-611, 2007.

[176] Eric Poirer, Mohsen Ghribi and A. Kaddouri, “Loss Minimization Control of Induction Motor Drives Based on Genetic Algorithm,” *IEEE Conference Proceedings Electrical machines and Drives,* IEMDC, pp. 475-478, 2001.

[177] L. R. Valdenebro and E. Bim, "A Genetic Algorithm Approach for Adaptive Field Oriented Control of Induction Motor Drives," *IEEE International Conference Electric Machines and Drives,* pp. 643-645, 1999.

[178] Ali M. Bazzi , Philip T. Krein, “Input Power Minimization of an IM Operating From an Electronic Drive Under Ripple Correlation Control,”, *IEEE Annual Power Electronics Specialists Conference,* DOI: 10.1109/PESC.2008.4592705, 2008.

[179] S. Ghozzi, K. Jelassi, X. Roboam, “Energy Optimization of Induction Motor Drives,” *IEEE International Conference on Industrial Technology,* DOI: 10.1109/ICIT.2004.1490143, 2004.

[180] Chandan Chakraborty, Minh C. Ta, Toshiyuki Uchida and Yoichi Hori, “Fast Search Controllers for Efficiency Maximization of Induction Motor Drives Based on DC Link Power Measurement,” *Proceedings of the power conversion conference - Osaka,* Vol. 2, pp. 402-408, 2002.

[181] Cao-Minh Ta, Yoichi Hori, “Convergence Improvement of Efficiency-Optimization Control of Induction Motor Drives,” *IEEE Transactions On Industry Applications,* Vol. 37, No. 6, pp. 1746-1753, November/December 2001.

[182] H. Rehman and X. Longya, "Alternative Energy Vehicles Drive System: Control, Flux, Torque Estimation, and Efficinecy Optimization," *IEEE transactions on Vehicularte Chnology*, Vol. 60, No. 8, pp. 3625-3634, 2011.

[183] S. N. Vulosavic, E. Levi, “Robust DSP-Based Efficiency Optimization of a Variable Speed Induction Motor Drive,” *IEEE Transactions on Industrial Electronics*, Vol. 50, No. 3, pp. 560-570, 2003.

[184] M. K. Yoon, C. S. Jeon, and S. Ken Kauh, “Efficiency Increase of an Induction Motor by Improving Cooling Performance,” *IEEE Transactions on Energy Conversion*, Vol. 17, No. 1, March 2002.

PUBLICATIONS

[1] Rajinder, Mini Sreejeth, Madhusudan Singh, "Efficiency Optimization of PI and Fuzzy Controller based Induction Motor Drive", *Journal of Intelligent & Fuzzy Systems*, SCI indexed, Volume. 35, No. 5, pp. 5159-5167, 2018.

[2] Rajinder, Mini Sreejeth, Madhusudan Singh, “FSS Based Control of Induction Motor Drive”, *International Journal of Innovative Technology and Exploring Engineering*, SCOPUS indexed, Volume-8 Issue-6, pp. 1435-1440, April 2019.

[3] Rajinder, Mini Sreejeth, Madhusudan Singh, “Speed and Stator Resistance Estimation of Speed Sensorless IM Drive”, *International Journal of Engineering and Technology*, SCOPUS indexed (ISSN: 2227-524X), (accepted).

[4] Rajinder, Mini Sreejeth, Madhusudan Singh, “Sensitivity Analysis of Induction Motor Performance Variables”, *IEEE International Conference on Power Electronics, Intelligent Control & Energy Systems* (ICPEICES-2016), DOI: 10.1109/ICPEICES.2016.7853609

[5] Rajinder, Mini Sreejeth, Madhusudan Singh, “Induction motor efficiency optimization based on a new search control” *ISA Transactions*, Elsevier, SCI Expanded indexed (under review).